



HAL
open science

Études biochimiques et analytiques de la biodégradation des hydrocarbures par des isolats bactériens.

Kevin Ehiosun

► **To cite this version:**

Kevin Ehiosun. Études biochimiques et analytiques de la biodégradation des hydrocarbures par des isolats bactériens.. Chimie analytique. Université de Pau et des Pays de l'Adour, 2022. Français. NNT : 2022PAUU3012 . tel-03975595

HAL Id: tel-03975595

<https://theses.hal.science/tel-03975595>

Submitted on 6 Feb 2023

HAL is a multi-disciplinary open access archive for the deposit and dissemination of scientific research documents, whether they are published or not. The documents may come from teaching and research institutions in France or abroad, or from public or private research centers.

L'archive ouverte pluridisciplinaire **HAL**, est destinée au dépôt et à la diffusion de documents scientifiques de niveau recherche, publiés ou non, émanant des établissements d'enseignement et de recherche français ou étrangers, des laboratoires publics ou privés.

THÈSE

UNIVERSITE DE PAU ET DES PAYS DE L'ADOUR

École doctorale des Sciences Exactes et de leurs Applications (ED 211)

Présentée et soutenue le 19/09/2022

par **Kevin Iyere EHIOSUN**

pour obtenir le grade de docteur
de l'Université de Pau et des Pays de l'Adour

Spécialité : Chimie analytique

BIOCHEMICAL AND ANALYTICAL STUDIES OF HYDROCARBON BIODEGRADATION BY SELECTED BACTERIAL ISOLATES

MEMBRES DU JURY

RAPPORTEURS

- Pierre GIUSTI Ingénieur (HDR) / TotalEnergies, Gonfreville
- Christophe MERLIN Maître de conférences (HDR) / Université de Lorraine, Nancy

PRÉSIDENT DU JURY

- Beatrice LAUGA Professeure / Université de Pau et des Pays de l'Adour, Pau

EXAMINATEURS

- Claudine BARAQUET Maître de conférences / Université de Toulon, Toulon
- Beatrice LAUGA Professeure / Université de Pau et des Pays de l'Adour, Pau
- Zofia KOWALEWSKA Professeure / Polytechnique de Varsovie, Płock, Pologne

DIRECTEURS

- Ryszard LOBINSKI Directeur de recherche / CNRS, Pau
- Régis GRIMAUD Professeur / Université de Pau et des Pays de l'Adour, Pau



Acknowledgements

This thesis work was carried out within the Environmental Chemistry and Microbiology Team, which is part of the Institute of Analytical and Physical Chemistry for Environment and Materials (IPREM), UMR 5254, Université de Pau et des Pays de l'Adour, Pau, France. The thesis was funded by the Petroleum Technology Development Fund, Nigeria (PTDF ID: 18/GFC/PHD/024).

I give glory to the Almighty God for the gift of life and good health.

I wish to express my deepest gratitude to my supervisors, Prof. Ryszard Lobinski and Prof. Régis Grimaud, for their acceptance, professional guidance, comments, constructive criticism, and patience.

I am also greatly indebted to Prof. Brice Bouyssiere, Dr. Sophie Nolivos, Prof. Rémy Guyoneaud, Prof. Zofia Kowalewska, Dr. Laurent Urios, Prof. Pierre Sivadon and Prof. Jerome Gury, whose worthwhile advice, excellent suggestions and motivation were valuable.

My thanks are also due to Simon Godin, Hugues Preud'homme, Hélène Laplassotte and Dr. Cristiana Cravo-Laureau for their technical assistance with HPLC and GC-MS and GC-FID analyses. Likewise, I appreciate Vicmary Vargas and Génesis González for helping with SARA fractionation. Patrick Bouriat, thanks for putting me through on how to use the Tensiometer. I wish to express my honest gratitude to Joanna Szpunar, Florene Hakil, Claire Gassie, Alice Baldy, Ange Angaits and Marion Guignard for making sure I don't run out of supply of the various consumables.

I am also grateful to my wife, Chioma Star, Elvis, Elora, and Elyon for their candid support during this work. My immense gratitude goes to my parents, Mr. and Mrs. Ediale and in-laws (The Ezeorjikas) for every moral, financial and spiritual support. I equally acknowledge my loving and supportive siblings, Marvel, Lydia, Daniel, and Victor.

My gratitude to Jonathan Lapleau, Kilian Ducos, Zeina Bourhane, Joyce Alvarez Barragan, Diva Scuvée, Eva Sandoval Quintana, Ivan Gonzalez Alvarez, Samia Haddadi, Camille Maziere, Guillaume Cazaudehore, Sophie Barrouilhet, Elise Chatillon, Etienne Richy, Emmanuel Duval, Isaura Del Carmen Caceres, and all other students I met in IBEAS.

I am grateful to Campus France, the International office (UPPA), Doctoral school (ED 211) for their warm welcome, hosting, and companionship. Thanks to Joëlle Buron and H  l  ne Josse for helping me with administrative procedures.

Finally, I wish to extend my sincere thanks to everybody who I have not mentioned by name.

Table of contents

Acknowledgements	iii
Table of contents.....	v
List of figures	ix
List of tables	xi
Abbreviations.....	xii
Abstract.....	xv
Résumé	xvii
General introduction and thesis objectives	1
Chapter one.....	7
1. Literature review	9
1.1 Crude oil	9
1.2 Bioremediation of petroleum hydrocarbon pollution	10
<i>1.2.1 In situ techniques</i>	10
<i>1.2.2 Ex situ techniques</i>	10
1.3 Bacterial metabolism and degradation of petroleum hydrocarbons	11
<i>1.3.1 Bacterial strategies for accessing hydrocarbons as carbon and energy sources</i>	13
<i>1.3.1.1 The hydrophobicity of hydrocarbons</i>	13
<i>1.3.1.2 Biosurfactant production</i>	14
<i>1.3.1.3 Biofilm formation</i>	16
<i>1.3.2 Aerobic and anaerobic biodegradation</i>	19
<i>1.3.2.1 Biodegradation of saturated hydrocarbons</i>	20
<i>1.3.2.2 Biodegradation of aromatic hydrocarbons</i>	20
1.4 Carboxylic acids as analytical targets of hydrocarbon biodegradation	21
1.5 Mass spectrometric techniques for the analysis of carboxylic acids	23
<i>1.5.1 Sample pre-treatment</i>	25
<i>1.5.1.1 Blanks and controls</i>	25
<i>1.5.1.2. Extraction of carboxylic acids</i>	26
<i>1.5.1.3. Derivatization</i>	27
<i>1.5.2 Direct analysis by Fourier Transform Ion Cyclotron Resonance - mass spectrometry (FT – ICR MS)</i>	27

1.5.3 Gas chromatography - mass spectrometry (GC - MS)	28
1.5.4 Liquid chromatography – mass spectrometry (LC - MS)	30
1.6 Applications of mass spectrometry for the monitoring of carboxylic acids after hydrocarbon biodegradation	31
1.6.1 Model systems: saturated hydrocarbons (alkanes and cycloalkanes).....	31
1.6.2 Model systems: aromatic hydrocarbons.....	32
1.6.3 Crude oil.....	33
Chapter two	37
2. Materials and methods	39
2.1 Crude oil-polluted soil sampling site	39
2.2 Sampling crude oil-polluted soil	39
2.3 Isolation of bacterial strains by enrichment on crude oil	40
2.3.1 Media composition	40
2.3.2 Enrichment conditions.....	40
2.3.3 Isolation of bacteria	40
2.4 Molecular biology analysis	41
2.4.1 Genomic DNA extraction and Illumina sequencing	41
2.4.2 Pacbio Sequel for bacterial identification.....	42
2.5 Biodegradation studies	42
2.5.1 Biodegradation of n-hexadecane.....	42
2.5.2 Biodegradation of saturate fraction of crude oil.....	44
2.5.3 Determination of protein concentration in culture.....	45
2.5.4 GC-FID for residual hexadecane analysis	45
2.5.5 GC-MS for residual saturate hydrocarbon analysis	45
2.5.6 Sampling extracellular and intracellular metabolites	45
2.5.7 LC-MS/MS for untargeted screening of metabolites	46
2.5.8 LC-MS ³ for structural elucidation of metabolites	46
2.5.9 Quantification of hydroxyhexadecanoic acid isomers.....	46
2.6 Biofilm assays	46
2.6.1 Biofilm formation on liquid hydrophobic substrates	46
2.6.2 Biofilm formation as a mechanism to utilize n-hexadecane	47
2.6.3 Biofilm formation on solid hydrophobic substrates	47

2.6.4 Microbial adhesion to hydrocarbon (MATH) assay.....	48
2.6.5 Optical sectioning microscopy (ApoTome) of biofilm.....	48
2.6.6 Screening for biosurfactant production.....	48
Chapter three.....	49
3. Degradation of long-chain alkanes through biofilm formation by bacteria isolated from oil-polluted soil.....	51
3.1 Introduction.....	51
3.2 Materials and methods.....	53
3.2.1 Sampling crude oil-polluted soil.....	53
3.2.2 Isolation of bacterial strains by enrichment on crude oil.....	53
3.2.2.1 Media composition.....	53
3.2.2.2 Enrichment conditions.....	54
3.2.2.3 Isolation of bacteria.....	54
3.2.2.4 Screening of isolates on hydrocarbons.....	54
3.2.3 Molecular biology analysis.....	55
3.2.3.1 Genomic DNA extraction and Illumina sequencing.....	55
3.2.3.2 Pacbio Sequel for bacterial identification.....	55
3.2.4 Biodegradation of n-hexadecane.....	56
3.2.4.1 Determination of protein concentration in culture.....	56
3.2.4.2 GC-FID for residual hexadecane analysis.....	56
3.2.4.3 Sampling extracellular metabolites.....	56
3.2.4.4 LC-MS/MS for untargeted screening of extracellular metabolites.....	57
3.2.4.5 LC-MS ³ for structural elucidation of extracellular metabolites.....	57
3.2.4.6 Quantification of extracellular metabolites.....	58
3.2.5 Biofilm assays.....	58
3.2.5.1 Biofilm formation on liquid alkanes.....	58
3.2.5.2 Biofilm formation on solid alkanes and lipids.....	58
3.2.5.3 Microbial adhesion to hydrocarbon (MATH) assay.....	59
3.2.5.5 Optical sectioning microscopy (ApoTome) of biofilm.....	59
3.2.5.6 Screening for biosurfactant production.....	59
3.3 Results.....	60
3.3.1 Isolation and taxonomic identity of selected strains.....	60
3.3.2 Biodegradation of n-hexadecane.....	62
3.3.3 Biofilm formation on hydrocarbons and lipids.....	64
3.3.4. Screening for extracellular metabolites by untargeted HPLC-MS/MS.....	71

3.3.5 Structural elucidation of metabolites by targeted HPLC-MS ² and MS ³	72
3.4 Discussion	77
3.5 Conclusion	81
Chapter four	83
4. Biodegradation of saturated fraction of crude oil and signature carboxylic acids production	85
4.1 Introduction	85
4.2 Materials and methods	87
4.2.1 Bacteria strains	87
4.2.2 Biodegradation of saturate fraction of Congo Bilondo crude oil.....	87
4.2.2.1 SARA fractionation of Congo Bilondo crude oil.....	87
4.2.2.2 Biodegradation of the saturated fraction.....	87
4.2.2.3 Sampling extracellular metabolites	87
4.2.3 Analytical analysis and identification of extracellular metabolites	87
4.2.3.1 GC-MS for residual saturate hydrocarbon analysis.....	87
4.2.3.2 Evaluating biodegradation efficiency	88
4.2.3.4 LC-MS ³ for structural elucidation of metabolites.....	89
4.3 Results and discussion	89
4.3.1 SARA fractionation of Congo Bilondo crude oil	89
4.3.2 Characterization of the saturate fraction by GC-MS	90
4.3.3 Biodegradation of the saturated fraction	96
4.3.4 Identification of carboxylic acids metabolites and elucidation of degradation pathway.....	97
4.4 Conclusion	106
Chapter five	109
5. Conclusions and perspectives	111
Scientific publications and communications	113
References	1135

List of figures

Figure 1.1: Schematic diagram showing culture-dependent and independent strategies for bioremediation [66].	13
Figure 1.2: Schematic of hydrocarbon solubilization by rhamnolipid (RL) biosurfactants.	16
Figure 1.3: Stages of biofilm formation.	17
Figure 1.4: GC×GC–MS total ion current chromatogram of methylated acidic extract of crude oil incubated under sulfate reducing condition for 686 days.	29
Figure 1.5: HPLC separation of position isomers of toluic acids.	31
Figure 2.1: Geographical location of Bodo (https://www.bbc.com/news/world-africa-14398659).	39
Figure 2.2: Bacteria enrichment and isolation workflow.	43
Figure 2.3: SARA fractionation scheme	44
Figure 3.1: Workflow tree of untargeted screening of <i>n</i> -hexadecane metabolites using Compound Discoverer 2.1™. T	57
Figure 3.2: Krona chart showing the bacterial diversity in the crude oil contaminated soil sample.	60
Figure 3.3: Relative abundance of bacterial phyla during soil enrichment carried out using four media with or without 1 % (v/v) filter-sterilized Congo Bilondo crude oil.	61
Figure 3.4: Phylogenetic tree, based on 16S rRNA gene sequences, showing the relationships between the isolated strain and closely related representative strains. T	62
Figure 3.5: (a) Pictures of colonies of the isolated strains.	63
Figure 3.6: Residual <i>n</i> -hexadecane and protein concentration in culture media of (a) <i>Novosphingobium</i> sp. S1, (b) <i>Gordonia amicalis</i> S2 and (c) <i>Gordonia terrae</i> S5.	63
Figure 3.7: Images of oleolytic biofilm formed by (a) <i>Novosphingobium</i> sp S1, (b) <i>Gordonia amicalis</i> S2 and (c) <i>Gordonia terrae</i> S3 on <i>n</i> -hexadecane by day 3.	63
Figure 3.8: Calibration curve establishing the relationship between crystal violet colouration at 595 nm and OD _{600nm} for (a) <i>Novosphingobium</i> sp S1, (b) <i>Gordonia amicalis</i> S2 and (c) <i>Gordonia terrae</i> S3.	65
Figure 3.9: Planktonic growth versus biofilm formation on (A) <i>n</i> -hexadecane, (B) <i>n</i> -octadecane (C) paraffin, (D) hexadecyl hexadecanoate and (E) tristearin by <i>Novosphingobium</i> sp. S1, <i>Gordonia amicalis</i> S2 and <i>Gordonia terrae</i> S5.	66
Figure 3.10: Comparative growth profile of <i>Novosphingobium</i> sp. S1, <i>Gordonia amicalis</i> S2 and <i>Gordonia terrae</i> S5 in culture insert and well compartment separated by a membrane filter.	67

Figure 3.11: Maximum Intensity Projection (X:Y:Z plane) of biofilm formed by <i>Gordonia terrae</i> S5 on paraffin wax after (a) 24 h and (b) 40 h and hexadecyl hexadecanoate after (c) 24 h and (d) 40 h. Scale bar = 20 μ m. Biofilms were stained with 0.1 % SYTO 9 (green).	68
Figure 3.12: Microscopic images of the surface of Hexadecyl hexadecanoate and paraffin (a) before and (b) after biofilm formation by <i>Gordonia terrae</i> S5.....	69
Figure 3.13: Adhesion of <i>Novosphingobium</i> sp. S1, <i>Gordonia amicalis</i> S2 and <i>Gordonia terrae</i> S5 to hexadecane grown on (a) propionate and (b) <i>n</i> -hexadecane. Insert: images of <i>Novosphingobium</i> sp. (left), <i>Gordonia amicalis</i> (middle) and <i>Gordonia terrae</i> (right) adhering to <i>n</i> -hexadecane.....	70
Figure 3.14: Extracted chromatogram of (a) 8-hydroxyhexadecanedioic acid (m/z 301.2021) at RT 9.67 min and (b) hydroxyhexadecanoic acid (m/z 271.2280) at RT 12.22 and 12.45 min. Specific signals for the two isomers were extracted with specific fragments m/z 127.112.	72
Figure 3.15: Structural elucidation of 8-hydroxyhexadecanedioic acid by MS ³ fragmentation. Insert: MS ³ mass spectrum showing the product fragments from m/z 241.1802 and m/z 283.1916. Peaks of m/z 178 and m/z 148 are regarded as artefacts.	74
Figure 3.16: Structural elucidation of 8-hydroxyhexadecanoic acid and 7-hydroxyhexadecanoic acid by MS ² fragmentation. Insert: MS ² mass spectrum showing the product fragments from each isomer. Peaks of m/z 178 and m/z 148 are regarded as artefacts.	75
Figure 3.17: Evolution of (a) 8-hydroxyhexadecanedioic acid abundance in culture during <i>n</i> -hexadecane degradation by <i>Novosphingobium</i> sp. S1 and <i>Gordonia amicalis</i> S2 and (b) 8-hydroxyhexadecanoic acid and 7-hydroxyhexadecanoic by <i>Gordonia terrae</i> S5.	76
Figure 3.18: Standard curve of 16-hydroxyhexadecanoic used for the quantification of 7-hydroxyhexadecanoic acid and 8-hydroxyhexadecanoic acid.....	78
Figure 4.1: Picture of the fractions obtained from the SARA procedure of Congo Bilondo crude oil.	90
Figure 4.2: Chromatographic profiles of hydrocarbons in the saturated fraction of Congo Bilondo crude oil with deuterated dodecane as internal standard.	90
Figure 4.3: Ion chromatogram typical for <i>n</i> -alkanes and isoprenoid alkanes (m/z 43, m/z 57, m/z 71 and m/z 85).....	93
Figure 4.4: Chromatogram showing the relative changes in the distribution and abundance of alkanes on (a) day 3 and (b) day 5 of biodegradation study	98
Figure 4.5: Optimization of the LC separation and detection of standard metabolites (1) 50 ppb benzoic acid, (2) 200 ppb hexadecanoic acid and (3) 0.5 ppb 16-hydroxyhexadecanoic acid. Benzoic acid, in particular, was spiked into the mobile phase, water and culture medium to evaluate matrix effect.....	101
Figure 4.6: Proposed alkane degradation pathway for the bacteria strains. monocarboxylic acids either enter β -oxidation or be oxygenated further by the ω -fatty acid monooxygenases to form dicarboxylic acid.....	102
Figure 4.7: Levels of carboxylic acids in culture medium of (a) <i>Novosphingobium</i> sp. S1 (b) <i>Gordonia amicalis</i> S2 and (c) <i>Gordonia terrae</i> S5 on day 3 and 5	107

List of tables

Table 1.1: Some hydrocarbon-degrading bacteria.....	12
Table 1.2: Classification of biosurfactants produced by bacteria during hydrocarbon degradation	15
Table 1.3: Field and model studies using carboxylic acids as biomarkers for hydrocarbon biodegradation	24
Table 1.4: Carboxylic acids from the biodegradation of saturated hydrocarbons	32
Table 1.5: Characterization of carboxylic acids from the biodegradation of BTEX and polyaromatic hydrocarbons	35
Table 1.6: Carboxylic acids detected during crude oil biodegradation	36
Table 3.1: Volumetric and topological characterization of biofilms by <i>Gordonia terrae</i> S5 on paraffin and hexadecyl hexacanoate. Values are means and standard deviation of data from 5 image stacks.....	69
Table 3.2: Screening for biosurfactant production by bacteria. Key: + = positive, - = negative and ND = not determined.	71
Table 3.3: Metabolites detected and elucidated by HPLC-MS ² and MS ³ (ESI-) during biodegradation of <i>n</i> -hexadecane.	76
Table 3.4: Concentrations of 7-hydroxyhexadecanoic acid and 8-hydroxyhexadecanoic acid in culture of <i>Gordonia terrae</i> S5.	77
Table 4.1: Calculated weight distribution of the different fractions of Congo Bilondo crude oil.....	89
Table 4.2: Hydrocarbons detected by GC-MS in the saturated fractions of Congo Bilondo crude oil	94
Table 4.3: Relative biodegradation efficiency for each alkane on day 3 and day 5 of biodegradation.....	99
Table 4.4: Extracellular metabolites produced by <i>Novosphingobium</i> sp. S1, <i>Gordonia amicalis</i> S2 and <i>Gordonia terrae</i> S5	103
Table 4.5: Annotation and fragmentation pattern of detected extracellular metabolites. Most of the carboxylic acids were found on database search and a fragmentation pattern characteristic of dehydration, decarboxylation and dealkylation was commonly observed.	104

Abbreviations

APPI: Atmospheric pressure photoionization
BSA: Bovine Serum Albumin
BSTFA: Bis(trimethylsilyl)trifluoroacetamide
BTEX: Benzene, Toluene, Ethylene, and Xylene
CCS: Circular Consensus Sequence
CID: Collision-Induced Dissociation
CMC: Critical Micelle Concentration
CMM: Complete Mineral Medium
DBE: Double Bond Equivalent
DNA: Deoxyribonucleic acid
E₂₄: Emulsification index
EPS: Extracellular Polymeric Substances
ESI: Electrospray ionization
FISh: Fragment Ion Search
FT-ICR: Fourier Transform Ion Cyclotron Resonance
FWD: Forward
GC: Gas Chromatography
HCD: Higher-energy C-trap Dissociation
IFT: Interfacial Tension
IMM: Incomplete Mineral Medium
LB: Lysogeny Broth
LC: Liquid Chromatography
MRM: Multiple Reaction Monitoring
MS: Mass Spectrometry
NAs: Naphthenic acids
NCBI: National Center for Biotechnology Information
NIST: National Institute of Standards and Technology
NSO: Nitrogen-Sulphur-Oxygen
OD: Optical Density
OTUs: Operational Taxonomic Units
Pacbio: Pacific biosciences

PAHs: Polyaromatic hydrocarbons
RCM: Rich Complete Medium
RDP: Ribosomal Database Project
REV: Reverse
RIM: Rich Incomplete Medium
SARA: Saturates, Aromatics, Resins and Asphaltenes
SDS: Sodium dodecyl sulphate
SEM: Scanning Electron Microscopy
SPE: Solid Phase Extraction
SRM: Selected Reaction Monitoring
TCA: Tricarboxylic Acid
TEM: Transmission Electron Microscopy
TMS: Trimethylsilylation
TOF: Time of Flight

Abstract

Decades of research have demonstrated that microbial degradation remains the major strategy used for bioremediation of hydrocarbons. However, in recent times, focus has shifted to improving the efficiency of the degradation process. This interest has further driven the search for strains with versatile metabolic capability to access, assimilate and degrade a wide range of hydrocarbons. Furthermore, understanding hydrocarbon biodegradation mechanisms and pathways has become crucial to designing more efficient bioremediation strategies. This can be achieved through the characterization of signature metabolites, particularly carboxylic acids, produced during the degradation process. This interest has been reinforced by the extensive and robust developments in chromatographic and mass spectrometric methods.

Three bacteria, *Novosphingobium* sp. S1, *Gordonia amicalis* S2 and *Gordonia terrae* S5 isolated from a crude oil polluted soil, were studied to understand the mechanism by which they circumvent the very low bioavailability of long-chain alkanes in aqueous medium and utilize them. Results showed none of the strains produced biosurfactant, but growth occurred only when the cells had access to the alkane-water interface through biofilm formation. This interfacial access to alkanes was also supported by the ability of the strains to adhere to hydrocarbons and was an important property of these strains to form a biofilm and utilize hydrocarbons as carbon and energy source.

Furthermore, the capability as well as understanding the pathway to degrading a wide range of hydrocarbons in the saturated fraction of Congo Bilondo crude oil by the three bacteria was examined. The study combined the efficiency of GC-MS and LC-MS for characterizing the hydrocarbons and comprehensive screening of carboxylic acid metabolites, respectively. Results showed that the strains can efficiently use as carbon and energy source the *n*-alkanes (C₁₀ - C₂₈) as well as methyl-substituted alkanes (C₁₁ - C₂₆). The series of mono-, hydroxy- and dicarboxylic acids found in this study confirmed the active biodegradation of the alkanes and suggest that their degradation was via the bi-terminal oxidation pathway. The results highlight the potential application of the strains in bioremediation of crude oil contaminated sites. Biofilm-mediated bioremediation is a promising approach to efficient cleanup of hydrocarbons.

Keywords: Biofilm, Biodegradation, *Gordonia*, *Novosphingobium*, Carboxylic acids, SARA

Résumé

Des décennies de recherche ont démontré que la dégradation microbienne reste la principale stratégie utilisée pour la bioremédiation des hydrocarbures. Cependant, ces derniers temps, l'attention s'est portée sur l'amélioration de l'efficacité du processus de dégradation. Cet intérêt a encore poussé la recherche de souches ayant une capacité métabolique polyvalente pour accéder, assimiler et dégrader une large gamme d'hydrocarbures. De plus, comprendre les mécanismes et les voies de biodégradation des hydrocarbures est devenu crucial pour concevoir des stratégies de bioremédiation plus efficaces. Ceci peut être réalisé grâce à la caractérisation des métabolites signatures, en particulier les acides carboxyliques, produits au cours du processus de dégradation. Cet intérêt a été renforcé par les développements importants et robustes des méthodes chromatographiques et spectrométriques de masse.

Trois bactéries, *Novosphingobium* sp. S1, *Gordonia amicalis* S2 et *Gordonia terrae* S5 ont été isolées d'un sol pollué par du pétrole brut et étudiées pour comprendre le mécanisme par lequel elles contournent la très faible biodisponibilité des alcanes à longue chaîne en milieu aqueux et les utilisent. Les résultats ont montré qu'aucune des souches ne produisait de biosurfactant, mais la croissance ne se produisait que lorsque les cellules avaient accès à l'interface alcane-eau par la formation de biofilm. Cet accès interfacial aux alcanes était également soutenu par la capacité des souches à adhérer aux hydrocarbures et était une propriété importante de ces souches pour former un biofilm et utiliser les hydrocarbures comme source de carbone et d'énergie.

La capacité ainsi que la compréhension de la voie de dégradation d'un large éventail d'hydrocarbures dans la fraction saturée du pétrole brut Congo Bilondo par les trois bactéries ont été examinées. L'étude a combiné l'efficacité de la GC-MS et la LC-MS pour respectivement caractériser les hydrocarbures et identifier des acides carboxyliques métaboliques. Les résultats ont montré que les souches peuvent utiliser efficacement comme source de carbone et d'énergie les *n*-alcanes (C₁₀ - C₂₈) ainsi que les alcanes méthyl-substitués (C₁₁ - C₂₆). La série d'acides mono-, hydroxy- et dicarboxyliques trouvée dans cette étude a confirmé la biodégradation active des alcanes et suggère que leur dégradation se faisait par la voie d'oxydation bi-terminale. Ces résultats mettent en évidence l'application potentielle des souches dans la bioremédiation des sites contaminés par le pétrole brut. La bioremédiation par biofilm est une approche prometteuse pour un nettoyage efficace des hydrocarbures.

Mots clé : Biofilm, Biodégradation, *Gordonia*, *Novosphingobium*, Acides carboxyliques, SARA

General introduction and thesis objectives

Crude oil is an important resource with enormous energy and economic benefits. As population and modernization of society continue to grow, crude oil is predicted to remain a primary source of energy and feedstock for industries in decades [1]. However, crude oil pollution remains inevitable during exploration, production, refining, transportation, and storage. Crude oil pollution causes serious environmental and health problems especially in oil producing countries. Soil contamination leads to limited use of ground water and decreased agricultural productivity due to the alteration in the physicochemical properties and biological activities in the soil [2]. Contamination of water bodies threatens aquatic life because of reduced light and oxygen penetration [3]. Genetic damage, impaired visual function and decrease in both growth and fecundity have also been reported in fish [4,5]. Toxicity in other animals includes liver damage, cancer, genotoxicity and oxidative stress [6]. Microbial communities are also negatively affected resulting in reduction of species richness, evenness and phylogenetic diversity [7]. Consequently, there is the need for improved, less expensive, and more eco-friendly techniques to clean up hydrocarbon spills.

Bioremediation remains increasingly a popular technique for the cleanup of petroleum hydrocarbon pollution because it's less expensive, non-invasive, and more eco-friendly. Bioremediation essentially depends on microorganisms to degrade petroleum hydrocarbons to CO₂ and H₂O, through intermediate degradation products. As such, the metabolic potential and genetic machinery of microorganisms are assets in bioremediation. Reports have shown that bacteria can effectively degrade hydrocarbons to less toxic metabolites [8] through diverse metabolic pathways that involve intra- and extra-cellular enzymes [9]. However, in recent times, focus has shifted to improving the efficiency of the process. It is of common knowledge that the inherent low water solubility of hydrocarbons limits their accessibility and availability to the degrading bacteria. Enhancing the bioavailability of and bioaccessibility of hydrocarbons, which would subsequently increase the rate of bioassimilation and biodegradation has become a focal point for optimization of hydrocarbon biodegradation. To overcome the hydrophobicity of hydrocarbons during biodegradation, bacteria adopt two known specific mechanisms; biosurfactant production and biofilm formation. Thus, the need to overcome this caveat is further driving the search for strains with efficient biosurfactant production and/or biofilm formation capabilities to optimize bioremediation.

Furthermore, characterization of the metabolites produced during the degradation process, which are considered as signatures of the effectiveness of the bacterial transformations, is gaining in importance. It gives an insight into the microbial processes within and outside the cell during the biodegradation process. Such insights are important for the elucidation of hydrocarbon degradation mechanisms and pathways which is useful for designing more efficient bioremediation strategies.

This interest has been accompanied by the extensive and robust developments in analytical platforms, with particular surge in chromatographic and mass spectrometric methods [10]. Suitable signature metabolites are produced during active biodegradation and are specific to the parent hydrocarbon and/or to the biological process [11]. They include various alcohols, aldehydes, ketones, esters and, especially, carboxylic acids. The latter are produced in significant amounts during both aerobic and anaerobic biodegradation processes, and often occur at the convergence of several degradation pathways. Hence, over the years, carboxylic acids have served as useful metabolites and indicators of hydrocarbon biodegradation in both field and model studies. However, carboxylic acids occur at low concentration in complex matrices and could be transient, which represents a considerable challenge to the analyst. Nonetheless, chromatography with mass spectrometric detection has been established as reference technique, with the continuous and on-going improvement of the chromatographic and mass spectrometric resolution and accuracy.

This thesis aims at studying the mechanism of hydrocarbon degradation by soil bacteria for bioremediation application. The objectives include:

- Enrichment, isolation, and identification of bacteria strains that degrade hydrocarbons from crude oil polluted soil
- Physiological characterization of the strategies for accessing hydrocarbons as carbon and energy source during degradation by selected bacteria strains
- Analytical characterization of extracellular metabolites produced during hydrocarbon biodegradation by selected bacteria strains

The manuscript is organized as follows:

- Chapter 1: « Literature review » focuses on the mechanism of bacterial metabolism and degradation of hydrocarbons and carboxylic acids as analytical targets of hydrocarbon biodegradation.
- Chapter 2: « Materials and methods » presents the crude oil-polluted soil sampling site, bacteria enrichment and isolation workflow, molecular biology analysis and methods used for the biodegradation studies of model hydrocarbons and saturated fraction of Congo Bilondo crude oil.
- Chapter 3: presents the degradation of long-chain alkanes through biofilm formation by selected bacteria isolated from crude oil-polluted soil.

- Chapter 4: focuses on biodegradation of saturated fraction of Congo Bilondo crude oil and elucidation of the degradation pathway through analytical determination of signature carboxylic acids.
- Chapter 5: the thesis manuscript ends with a general conclusion and perspectives.

Chapter one

Literature review

1. Literature review

1.1 Crude oil

Crude oil is a natural complex mixture composed of hydrocarbons and other organic and inorganic compounds found in geologic formations. The non-hydrocarbons compounds include heteroatoms (nitrogen (N), sulphur (S), and oxygen (O))-containing analogues of hydrocarbons, inorganics such as sulphur and trace elements (nickel (Ni), vanadium (V), iron (Fe), copper (Cu), etc.) [12]. The molecular composition of crude oil varies with location, age, and depth of the oil reservoir. Consequently, the physical properties of crude oil such as volatility, specific gravity, viscosity, and colour also vary.

Crude oil is categorized into four fractions based on solubility, polarity, and adsorption affinity of the components.

- (i) Saturates are hydrocarbons having their carbon atoms linked by single bonds. They represent the highest portion of crude oil composition [8]. The carbon chains could be aliphatic or branched such as in alkanes. Cycloalkanes also contain one or more saturated rings.
- (ii) Unsaturated or aromatic hydrocarbons contain one or more fused aromatic rings. Accordingly, aromatic hydrocarbons can be monoaromatic such as benzene, toluene and xylene or polycyclic aromatic hydrocarbons (PAHs) such as naphthalene (two-ringed), phenanthrene (three-ringed) and chrysenes (four-ringed) etc. Aromatic hydrocarbons could also be substituted with linear, branched, or cyclic alkyl groups.
- (iii) Resins are high molecular weight non-hydrocarbon containing numerous polar functional groups formed with heteroatoms (N, S, and O) and trace metals (Ni, V, Fe, Cu). Resins can contain several aromatic rings or naphthenic acids and are abundant in heavy and non-conventional crude oils, such as bitumen [8]. Resins are precursors and peptizing agents for asphaltene.
- (iv) Asphaltenes are viscous, high molecular weight and the most water insoluble fraction in crude oil. This fraction also contains compounds with metals, predominately Ni and V, in porphyrin and other structures [12].

The rapid global economic development and urbanization have driven the high demand of crude oil as source of energy and industrial feedstocks. Inevitably, this has led to crude oil being a major source of petroleum hydrocarbon pollution. Crude oil pollution is a widespread and persistent problem that poses serious threats to human health and the environment. Therefore, contamination

by oil spills often requires cleaning up of the affected site. Conventional methods involving mechanical and chemical techniques (such as the use of booms, skimmers, absorbents, chemical dispersants and burning) for the remediation of hydrocarbon-polluted environment are often expensive, invasive, technologically complex, and not environmentally friendly and sustainable. Because of these shortcomings, bioremediation has remained the viable, imperative, efficient, green, and economical alternative to cleaning up crude oil spill.

1.2 Bioremediation of petroleum hydrocarbon pollution

Bioremediation involves the use of biological agents and process to degrade or clean-up hydrocarbons present in crude oil [13,14]. It was developed in the 1940s but became popular after the Exxon Valdez oil spill in 1980s [15]. Microbial degradation remains the major strategy used for the bioremediation of hydrocarbons. Thus, the availability of microorganism with the appropriate metabolic capabilities is essential [16–18]. Soil bioremediation can be carried on site (*in situ*), or away from the contaminated site (*ex situ*).

1.2.1 In situ techniques

There are three basic methods of *in situ* bioremediation: natural attenuation, biostimulation, and bioaugmentation [19,20]. Natural attenuation is a passive approach that depends essentially on natural mechanisms such as microbial degradation, volatilization, dispersion, sorption and dilution to clean-up hydrocarbons [21]. Microbial degradation is the most important and preferred attenuation mechanism. Natural attenuation relies on the degradation activities of indigenous microorganisms. However, longer treatment duration is required. Over time, enhanced natural attenuation, such as biostimulation and bioaugmentation have become increasingly accepted strategies to clean up contaminated sites. These techniques aim at enhancing microbial metabolic activities that accelerates the biodegradation of hydrocarbons. Biostimulation involves altering the physical and chemical parameters of the soil by addition of nutrients or electron acceptors (phosphorus, nitrogen, oxygen, carbon) to boost the activities of the indigenous degrading microorganisms [22]. In contrast, bioaugmentation is the introduction of specific exogenous microorganisms with the desired metabolic/catalytic capabilities into the contaminated environment [23].

1.2.2 Ex situ techniques

This method involves excavation of the contaminated soil and subsequent transfer to a processing location. Although additional cost and risk are involved with the transportation of the contaminated

soil, *ex situ* methods allow more efficient removal of pollutants, by controlling the physico-chemical condition of the biodegradation process, resulting in the shortening of the total time of reclamation [22]. The contaminated soil is treated through one of these *ex situ* methods; slurry bioreactors, land farming, composting and biopiles [24].

1.3 Bacterial metabolism and degradation of petroleum hydrocarbons

Bacteria are considered as nature's ultimate scavenger due to their ability to acquire carbon and energy from numerous compounds [25]. Bacteria are considered the first responder and most active in crude oil degradation having developed various mechanisms for degrading hydrocarbons. Thus, the isolation, characterization and study of bacteria involved in crude oil degradation have been widely reported (Table 1.1).

A petroleum polluted environment provides ideal repository for isolating bacteria with capabilities to degrade hydrocarbons [26–28]. This is because the presence of hydrocarbons in an environment influences the diversity of the bacterial community [29–31]. Characterizing bacteria in such environments requires both culture-dependent and culture-independent techniques (Figure 1.1). Culture-independent techniques, including metagenomics, proteomics, and transcriptomics are applied to analyse the richness, composition, structure and functional profile of the intrinsic bacterial community [32–34] within a hydrocarbon-contaminated environment. In addition, predictive functional and genetic biomarker analysis are useful tools in providing assessment of biodegradation process. Indeed, the recent and ongoing advances in molecular tools had enabled evaluation of non-culturable microorganisms from contaminated environments [35]. Alternatively, culture-dependent technique involves the enrichment and isolation of hydrocarbon-degrading bacteria, their production and subsequent application in biodegradation [36]. Although culture-dependent methods do recover fewer microbial populations, it is a critical component of bioremediation development and research [26,37]. Furthermore, it allows *in vitro* assessments and characterization of isolates' physiology, hydrocarbon degradation pathways and mechanisms, and efficiency [38]. Additionally, bioaugmentation relies on the introduction of specific exogenous bacteria with desired metabolic/catalytic capabilities, obtained by culture-dependent techniques, into a contaminated environment [23,36]. Complementarily, the environmental and ecological factors that shape microbial abundance, as observed from culture-independent techniques would be invaluable in developing culturing methods [37]. Therefore, improving enrichment and isolation of microbes are important to design and optimize bioremediation processes [2,32,37,39].

Table 1.1: Some hydrocarbon-degrading bacteria

Hydrocarbon	Bacterial species	Reference
Saturates	<i>Acinetobacter pittii</i>	[40]
	<i>Pseudomonas</i> , <i>Bacillus</i> , and <i>Burkholderia</i>	[41]
	<i>Corynebacterium aurimucosum</i> , <i>Acinetobacter baumannii</i> and <i>Microbacterium hydrocarbonoxydan</i>	[42]
	<i>Bacillus pumilus</i>	[43]
	<i>Enterobacter</i> , <i>Pandoraea</i> and <i>Burkholderia</i>	[27]
	<i>Gordonia amicalis</i> HS-11	[44]
	<i>Aeribacillus pallidus</i> SL-1	[45]
	<i>Pseudomonas aeruginosa</i> XJ16, <i>Bacillus cereus</i> XJ20, and <i>Acinetobacter lwoffii</i> XJ19	[46]
	<i>Bacillus subtilis</i> BL-27	[47]
	<i>Rhodococcus</i> sp. JZX-01	[48]
	<i>Rhodococcus</i> sp. T1	[49]
	<i>Bacillus amyloliquefaciens</i> , <i>Staphylococcus epidermidis</i> , <i>Micrococcus luteus</i> , <i>Nitratireductor aquimarinus</i> , and <i>Bacillus pumilus</i>	[50]
	<i>Geobacillus thermoparaffinivorans</i> IR2, <i>Geobacillus stearothermophilus</i> IR4 and <i>Bacillus licheniformis</i> MN6	[51]
	<i>Gordonia rubripertincta</i> CWB2 and <i>Rhodococcus erythropolis</i> S43	[52]
	Aromatics	<i>Haererehalobacter</i> sp. <i>Oceanobacillus</i> sp., <i>Pseudoalteromonas</i> sp.
<i>Pseudomonas</i> sp.		[54]
<i>Streptomyces</i> sp.		[55]
<i>Chryseobacterium</i> sp., <i>Bacillus</i> sp. and <i>Pseudomonas</i> sp.		[56]
<i>Aeribacillus pallidus</i> , <i>Bacillus axarquiensis</i> , <i>Bacillus siamensis</i> and <i>Bacillus subtilis</i>		[57]
<i>Microbacterium hydrocarbonoxydan</i>		
<i>Aeribacillus pallidus</i> UCPS2, <i>Bacillus axarquiensis</i> UCPD1, <i>Bacillus siamensis</i> GHP76 and <i>Bacillus subtilis</i> U277		[42]
<i>Sphingobacterium</i> sp. RTSB		[58]
<i>Novosphingobium pentaromativorans</i> US6-1		[59]
<i>Pseudomonas aeruginosa</i> RS1		[60]
<i>Aeribacillus pallidus</i> SL-1		[45]
<i>Sphingomonas</i> sp.		[61]
<i>Rhodococcus</i> sp. T1		[49]
<i>Bacillus amyloliquefaciens</i> subsp. <i>plantarum</i> W1		[62]
Asphaltenes	<i>Pseudomonas aeruginosa</i>	[63]
	<i>Staphylococcus saprophyticus</i> and <i>Bacillus cereus</i>	[64]
Heteroatomic compounds	<i>Pseudomonas aeruginosa</i> and <i>Acinetobacter iwoffii</i>	[65]

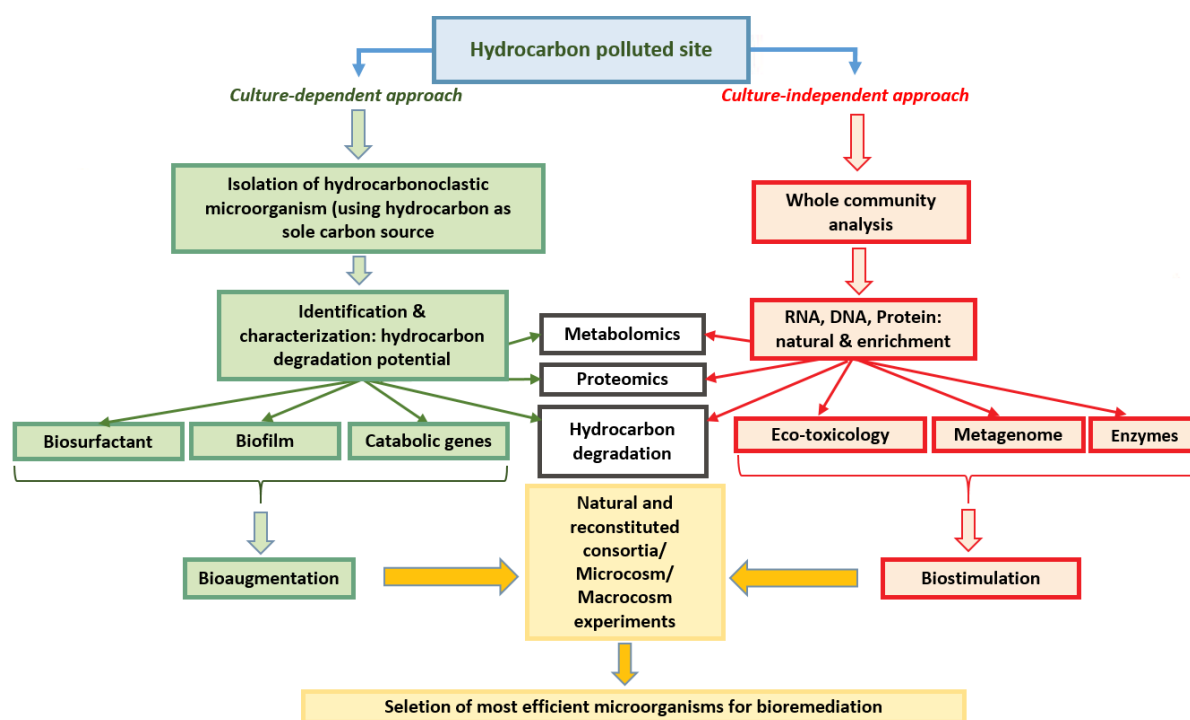


Figure 1.1: Schematic diagram showing culture-dependent and independent strategies for bioremediation [66]. Whole community-level studies rely on culture-independent methods based on the direct analysis of DNA/RNA and proteins without any culturing step. In contrast, bacterial culturing, bioassays with hydrocarbons as sole carbon source, and hydrocarbon degradation profiling are applied in culture-dependent analysis to characterize the hydrocarbon degradation potential of isolates.

1.3.1 Bacterial strategies for accessing hydrocarbons as carbon and energy sources

1.3.1.1 The hydrophobicity of hydrocarbons

Biodegradation requires that microorganisms grow in the presence of hydrocarbons [67] but this depends on the ability of the degrading bacteria to access the hydrocarbons, which are inherently unavailable in aqueous media. The hydrophobicity of hydrocarbons is thus often an indicator of its bioavailability and bioaccessibility. In this context, bioavailability is referred to the degree of interaction of hydrocarbons with the bacteria. It is often expressed as the fraction of hydrocarbons that can be readily taken up or degraded by bacteria [68]. This depends on the physical state and characteristics and spatial distribution of the hydrocarbons relative to the catabolically active bacteria. The differentiation of immediate bioavailability (hydrocarbons being taken up) from potential bioavailability (hydrocarbons that may become bioavailable by dissolution, desorption, diffusion etc.) is called bioaccessibility. Thus, the bioaccessible fraction comprises the amount that can reach the bacteria within a predefined time frame [69]. The hydrophobicity of hydrocarbons increases with molecular mass and the degree of saturation. Long-chain alkanes are more

hydrophobic than short-chains, saturated aliphatics are more hydrophobic than unsaturated aliphatics and aromatics of the same molecular mass, and PAHs consisting of a higher number of rings are more hydrophobic than those of low molecular mass [69]. To circumvent the challenge of hydrophobicity during biodegradation, bacteria adopt two known specific assimilation mechanisms: biosurfactant production and biofilm formation. The need to overcome this caveat is driving the search for strains with efficient biosurfactant production and/or biofilm formation capabilities.

1.3.1.2 Biosurfactant production

Bacteria produce surface-active compounds known as biosurfactants to enhance the solubility of hydrocarbons through emulsification, thereby facilitating hydrocarbons bioavailability, uptake and degradation [70]. Biosurfactants are amphipathic molecules, containing both hydrophilic and hydrophobic ends, that allows interaction at the interface between aqueous and non-aqueous systems. They constitute heterogeneous group of biomolecules such as glycolipids, lipoproteins complexes and lipopolysaccharide-protein complexes (Table 1.2). Low molecular weight biosurfactants are primarily used for decreasing interfacial tension at the oil-water interface while the high molecular weight biosurfactants are quite effective in acting as emulsifying agents [71]. The diversity of biosurfactants supports their potential application in degrading different class of hydrocarbons. Likewise, biosurfactants are preferred to synthetic surfactants because of their unique properties: higher biodegradability, lower toxicity, and effectiveness at extremes of temperature, pH, and salinity [72].

Due to the amphiphilic structure, biosurfactants can increase hydrophobic substance surface area, as well as change the cell surface property of bacteria [70]. Bacteria produce biosurfactant into the surrounding media to decrease interfacial tension at the hydrocarbon-water interface and enhance the pseudo-solubilization of hydrocarbons via micelle or vesicle formation. The critical micelle concentration (CMC) is the lowest concentration of surfactant molecules associating micelles, which is a crucial parameter to the biosurfactant [73]. Above the CMC, the biosurfactant molecules aggregate to form supra-molecular structures like spherical micelles, bilayers, and vesicles that reduce the surface tension and increase solubility (Figure 1.2). Then, the pseudo-solubilized hydrocarbons form highly dispersed emulsions and droplets that enhance bioavailability, rate of assimilation and subsequent biodegradation. The uptake and accumulation of pseudo-solubilized *n*-hexadecane by *P. aeruginosa* PU1 as intracellular inclusion bodies was monitored by SEM and TEM analysis [74]. Furthermore, biosurfactants enhance the cell surface hydrophobicity for easy adsorption to hydrocarbons thereby increase the permeability of the membrane. Such modifications

in the cell membrane could include change in proteins composition or the reduction of lipopolysaccharides [75].

Recent studies have shown how biosurfactants promote hydrocarbon emulsification and solubility during biodegradation [76–80].

Table 1.2: Classification of biosurfactants produced by bacteria during hydrocarbon degradation

Group	Sub-group	Class	Microorganism	Reference
Low-molecular weight biosurfactants	Glycolipids	Rhamnolipids Sophorolipids Trehalolipids Cellobiolipids	<i>Bacillus pumilus</i> 2A <i>Corynebacterium aurimucosum</i> , <i>Microbacterium hydrocarbonoxydans</i> and <i>Pseudomonas aeruginosa</i> <i>Micrococcus luteus</i> BN56 <i>Gordonia amicalis</i> HS-11 <i>Pseudomonas</i> sp. CQ2 <i>Gordonia</i> sp. BS29 <i>Achromobacter</i> sp. PS1 and <i>Bacillus</i> sp. SLDB1 <i>Bacillus algicola</i> 003-Phe1, <i>Rhodococcus soli</i> 102-Na5, <i>Isoptericola chiayiensis</i> 103-Na4, and <i>Pseudoalteromonas agarivorans</i> (SDRB-Py1) <i>Pseudomonas aeruginosa</i> san ai	[76] [42] [81] [44] [73] [82] [80] [79] [83]
	Lipopeptides Lipoproteins	Surfactin Viscosin	<i>Bacillus subtilis</i> BSS <i>Azotobacter chroococcum</i> <i>Rhodococcus</i> sp. TW53 <i>Pseudomonas aeruginosa</i> <i>Bacillus subtilis</i> A1 <i>Planomicrobium</i> sp., <i>Aneurinibacillus</i> sp. And <i>Pseudomonas</i> sp. <i>Pseudomonas stutzeri</i> NA3 and <i>Acinetobacter baumannii</i> MN3 <i>Aeribacillus pallidus</i> UCPS2, <i>Bacillus axarquiensis</i> UCPD1, <i>Bacillus siamensis</i> GHP76 and <i>Bacillus subtilis</i> subsp. <i>inaquosorum</i> U277	[84] [85] [86] [78] [87] [77] [88] [57]
High-molecular weight biosurfactants	Polymeric biosurfactants	Emulsan Biodispersan Alasan Liposan mannoprotein	<i>Acinetobacter calcoaceticus</i> PTCC1318 <i>Acinetobacter venetianus</i> RAG-1	[89] [90]
	Particulate biosurfactants	Vesicles fimbriae Whole cells	<i>Acinetobacter</i> sp. <i>Acinetobacter calcoaceticus</i> RAG-1	[91]

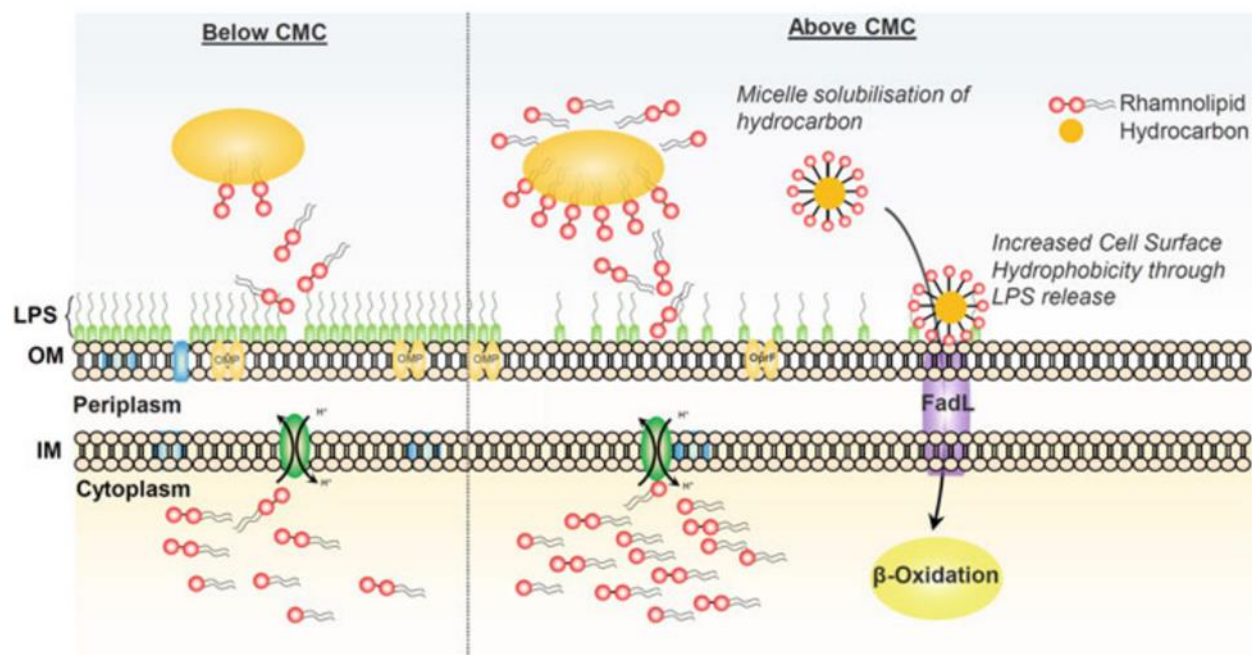


Figure 1.2: Schematic of hydrocarbon solubilization by rhamnolipid (RL) biosurfactants. At concentrations below the critical micelle concentration (CMC) monolayers of RL accumulate at the aqueous-hydrocarbon interface. When RL concentrations are above the CMC the hydrocarbon readily partitions into the hydrophobic core of the micelle thus increasing hydrocarbon bioavailability through solubilisation. RLs also induce cell surface changes that increase cell hydrophobicity via the release of cell associated lipopolysaccharides (LPS) [92].

1.3.1.3 Biofilm formation

A biofilm is defined as microbial aggregates that are often embedded in a self-produced matrix of extracellular polymeric substances (EPS) and adhere to each other and/or to a surface [93]. Biofilm formation during hydrocarbon degradation is an adaptation strategy and it is typically characterized by attachment of cells to hydrocarbons at the hydrocarbon-water interface [94–96]. When compared with artificial cell immobilization, biofilm is endowed with naturally immobilized cells with self-generation of cofactors and enzymes [97]. Dasgupta *et al.* [94] reported that biofilm-forming *Pseudomonas* strains degraded crude oil more readily and extensively than planktonic strains. Similarly, biofilm of *Stenotrophomonas acidaminihila* NCW-702 was able to degrade PAHs more efficiently than planktonic cells [98]. Recently, the effectiveness of bioaugmentation with biofilm-forming bacteria was reported [99].

Moreover, biofilm-forming bacteria revolves between planktonic growth and biofilm formation through some unique consecutive phases (Figure 1.3). Biofilm formation and planktonic-biofilm transition are complex and highly regulated processes [100,101].

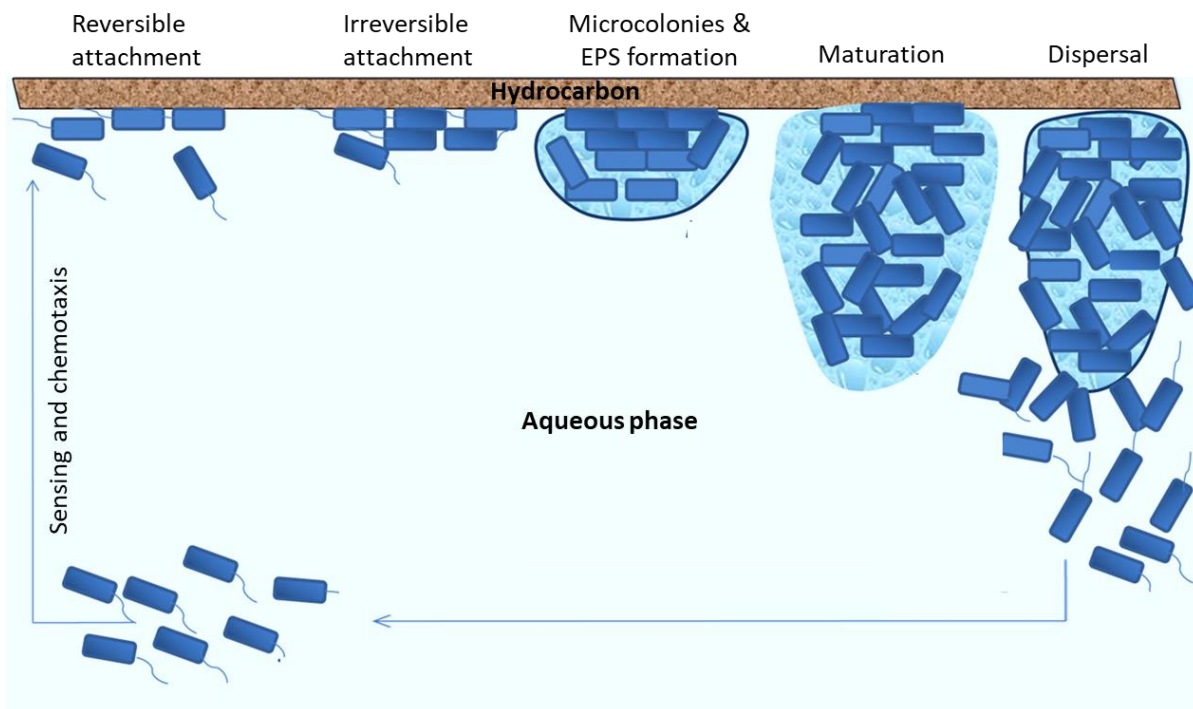


Figure 1.3: Stages of biofilm formation [102].

a) Nutrient sensing and chemotaxis

Bacteria initiate biofilm development in response to specific physico-chemical signals, such as nutrient availability. Sensing a nutritive surface requires that bacteria know they are in contact with a surface and recognize the nutritive character of the surface [96]. Nutrient surface sensing can be achieved either through appendages such as flagella, pilli, fibrils, or curli, or through body contact [103]. Chemotaxis, in this context, is the directed movement of bacterial cells toward a nutrient source along a concentration gradient [104]. Chemotaxis is important for biofilm formation by guiding cells towards nutrient sources. Bacterial cells with chemotactic capabilities can sense hydrocarbon gradient and move toward it, thereby overcoming the mass-transfer limitations in the biodegradation process [105]. The ability to attach to hydrocarbons stems mostly from bacteria inter-surface positioning and motility. Consequently, active movement is required for bacteria to move toward the hydrocarbon-water interface and establish contact. Furthermore, in fluid, motion characterized by sedimentation, diffusion, and convection is the primary mechanism of bacterial and mass transport along a surface [103]. The role of fluid dynamics in biofilm formation encompasses both motile and non-motile cells. If a bacterium is motile, its motility is facilitated by flagella. In contrast, non-motile cells can achieve inter-surface proximity via medium flow mechanisms such as convection, or vortex currents. These are most effective at low flow velocities

allowing circulation of nutrients and cells, with no disruption to the hydrocarbon-water interface. The differences in biofilm formation at the hydrocarbon-water interface under diffusion-limited conditions and diffusion caused by stirring have been reported [106].

b) Bacterial attachment

Following the hydrocarbon-water interface positioning activity, the biofilm formation process continues with the initial adhesion of the bacteria to the hydrocarbons. At this phase, adhesion is reversible, bacteria remain in a two dimensional Brownian motion and can be easily detached from the interface by either bacterial mobility or shearing effects of the medium flow [107]. The forces involved at this phase are hydrophobic, electrostatic and van der Waals interactions. Afterward, irreversible attachment is attained through the effects of short-range interactions such as dipole-dipole interactions, hydrogen, ionic and covalent bonding, and hydrophobic interactions with involvement of bacterial structural adhesions [104].

The adhesion of bacteria to the hydrocarbon-water interface effectively enhances the rate of hydrocarbon assimilation by reducing the distance for mass transfer [108]. Attachment to hydrocarbons relies on bacterial cell surface properties such as hydrophobicity, charge, roughness and extracellular appendages [96]. Hydrophobic cellular surface facilitates adhesion to and uptake of hydrocarbons and is a characteristic of hydrocarbon-degrading microorganisms. The uptake of medium and long-chain *n*-alkanes such as *n*-hexadecane by *Rhodococcus* species was shown to occur exclusively in cells adhering to the hydrocarbon-water interface [109,110]. Although, adhesion to hydrocarbons does not automatically predict utilization or degradation of the hydrocarbons by the adhered cells [108,111]. Additionally, it was suggested that the process of bacterial adsorption and biofilm formation at oil-water interfaces is not solely based on hydrophobicity; it is also likely promoted by metabolic factors and biosurfactants secreted by the bacteria to modify the interface [112–114]. Cell-bound surface active compounds and glycosylated peptidolipid (Gordonin) were shown to be responsible for enhanced cell hydrophobicity in *Gordonia* sp. BS29 and *Gordonia hydrophobica*, respectively, [115,116]. Other factors such as concentration of the carbon source, ionic strength, pH, and surfactant concentration affects adhesion of bacteria at the interface [117]. An increase in nutrient concentration is correlated with an increase in the number of attached bacterial cells [118]. Adhesion to hydrocarbons can also vary according to growth phase. *Gordonia* sp. cells demonstrated increased adhesion to hydrocarbons in early growth phase than the late growth phase [116].

Thereafter, the attachment progresses through microcolonies formation and into the production of EPS and an organized structure entrapped in the EPS matrix [104].

c) Microcolony formation and maturation of biofilm

After irreversible attachment, the bacteria start growing and developing into microcolonies over the interface. Microcolonies are clusters of aggregated bacterial cells, that eventually develop into larger cellular aggregates encircled by the EPS matrix to give a mature biofilm architecture [119]. EPS is produced to serve as building material for the three-dimensional architecture of the biofilm, as well as, anchoring material for attachment to surfaces [120]. EPS is composed of total carbon (50 - 90%), proteins, glycoproteins and nucleic materials [121]. The cells and secreted solubilisation factors such as biosurfactants and exoenzymes that play important roles in hydrocarbon assimilation are retained and accumulated within the EPS matrix [96,122]. This retentive property of the matrix localizes and stabilizes solubilisation and enzymatic activities within the matrix and thus increase mass transfer of hydrocarbons toward the cell for degradation. Furthermore, the EPS regulate various metabolic and behavioural activities such as colonization, cell recognition, surface attachment, signalling, cell protection against environmental stress, and exchange of genetic materials [119].

d) Dispersal or detachment of bacterial biofilms

Biofilm detachment or dispersal is the final process of biofilm development. When biofilm formation at the hydrocarbon-water interface becomes fully matured, cells begin to strategically detach from the biofilm in order to colonize new hydrocarbon surfaces [108]. The detachment process of bacterial cells from surfaces is mainly governed by a signal transduction mechanism, natural signal molecules, and effectors [123].

1.3.2 Aerobic and anaerobic biodegradation

Biodegradation frequently takes place under aerobic conditions, but it also does under anaerobic conditions. In aerobic degradation, oxygen is used as electron acceptor and as co-substrate for hydroxylation and ring cleavage. Anaerobic biodegradation commonly occurs where the availability of oxygen is limited, i.e. in subsurface environments (soils, sediments, aquifers and reservoirs), and is different from aerobic biodegradation in terms of the degradation pathways and generated metabolites [124]. Anaerobes also use alternate electron acceptors, such as nitrate (NO_3), sulfate (SO_4^{3-}) or ferric ions (Fe^{2+}). Subsurface environments were also found to support microaerobic growth and degradation [125]. In any case, oil reservoirs are considered habitats for bacteria

utilizing hydrocarbons as the sole source of carbon and energy under strictly anaerobic conditions [126].

1.3.2.1 Biodegradation of saturated hydrocarbons

Alkanes are the oil components most susceptible to undergo aerobic biodegradation. They are generally activated by enzymatic incorporation of molecular oxygen or, in rare cases, peroxides [127] through terminal or sub-terminal oxidation to yield the corresponding primary or secondary alcohols. The primary alcohols are oxidized to aldehydes, which are further converted into fatty acids. In some cases, fatty acids can be converted into dicarboxylic acids by ω -hydroxylation. Ketones are generated from oxidation of the secondary alcohols and are converted into esters, which, on their turn, are hydrolysed to fatty acids. Fatty acids are converted into acetyl-CoA through the β -oxidation pathway and metabolized in the tricarboxylic acid cycle (TCA) to generate CO₂ and reducing equivalents that are channelled into the respiratory chain to produce energy under the form of ATP. H₂O is produced by reduction of O₂ that is the final electron acceptor in aerobic respiration [127]. Fumarate addition is the most well-characterized activation mechanism of alkane degradation under anaerobic conditions [128]. It proceeds via terminal or sub-terminal addition of fumarate to alkanes, yielding alkyl succinate. Furthermore, alkyl succinate is degraded via carbon skeleton rearrangement and β -oxidation. An alternative pathway of anaerobic alkane degradation, though not well understood, involves subterminal carboxylation of alkanes at C-3 with removal of the two subterminal carbon atoms from the alkane chain terminus. This mechanism produces odd numbered fatty acids from even numbered *n*-alkanes, and vice versa [129].

1.3.2.2 Biodegradation of aromatic hydrocarbons

The biodegradability of aromatic hydrocarbons decreases with the increasing number of aromatic rings and alkylation [25]. The aerobic degradation of aromatics begins by the hydroxylation via a dioxygenase to form a *cis*-dihydrodiol, which gets rearomatized to a diol intermediate by dehydrogenase. A subsequent *ortho*- or *meta*-cleavage mediated by a multicomponent enzyme system produces intermediates, such as benzoic, phthalic or salicylic acids, that are ultimately converted into the TCA cycle intermediates [25]. The *n*-alkyl side chains of alkylated PAHs are also converted by β -oxidation into carboxylic acid derivatives. During anaerobic degradation, aromatic hydrocarbons are believed to be activated by: (i) the addition of fumarate to yield aromatic-substituted succinates, (ii) direct carboxylation, (iii) methylation of unsubstituted aromatics, or (iv) hydroxylation of an alkyl group. Further degradation generates alkyl aromatic acids that are

converted into long-chain volatile fatty acids via ring cleavage. The fatty acids produced are subsequently metabolized to methane (CH₄) and CO₂ [8].

1.4 Carboxylic acids as analytical targets of hydrocarbon biodegradation

Monitoring biodegradation of hydrocarbons involves the use of specific microbiological and chemical markers. Microbiological markers allows to characterize the richness, composition, structure and functional profile of the bacterial community [32–34] during hydrocarbon biodegradation. In addition, functional and genetic analysis of the community provides assessment of the biodegradation process. On the other hand, microbial activities are revealed by chemical analysis. Typically, the relative decrease in hydrocarbon concentrations is commonly used to demonstrate the occurrence of microbial degradation, and to estimate the level of biodegradation. However, this analysis is not sufficient to demonstrate unambiguously the occurrence of intrinsic or enhanced biodegradation. The relative decrease in hydrocarbon concentrations could be influenced by abiotic factors such as volatilization, dispersion sorption or dilution [21]. Likewise, the decrease in hydrocarbon concentrations cannot provide information on the biodegradation process, for example aerobic and anaerobic, and the biochemical pathway(s) adopted by the bacteria, which is essential for evaluation, design and development of efficient remediation biotechnologies [130,131]. Therefore, the profiling of intermediate metabolites characteristic of bacterial transformations has recently become popular for assessing biodegradation [132]. It allows an insight into the microbial processes within and outside the cell during the biodegradation process. Such insights are important for the elucidation of hydrocarbon degradation mechanisms and pathways that is useful for designing more efficient bioremediation strategies. Useful metabolic biomarkers are produced during active biodegradation and are specific to the parent hydrocarbon and/or to the biological process [11]. They include various alcohols, aldehydes, ketones, esters and, especially, carboxylic acids. The latter are produced in significant amounts during both aerobic and anaerobic biodegradation processes, and often occur at the convergence of several degradation pathways. Mohler *et al.* [133] reported that carboxylic acids were the most frequent class of polar metabolites identified with high confidence in hydrocarbon contaminated groundwater. Consequently, carboxylic acids are common targets in field and model studies, and their characterization is considered an appropriate approach to study the biodegradation of hydrocarbons (Table 1.3).

The terminal degradation pathway for *n*-alkanes and branched chain alkanes produces monocarboxylic acids and dicarboxylic acids as intermediates. Aromatic hydrocarbons undergo aerobic biodegradation to form key metabolites, such as benzoic acid, phthalic, and salicylic acid

naphthoic acid. These signature metabolites were demonstrated as a valuable tool for tracing microbial activity [83,126,134–136]. Fumarate addition is the most characterized activation mechanism of hydrocarbon degradation under anaerobic conditions [128], which now represents a central paradigm in anaerobic hydrocarbon degradation. Fumarate addition to alkanes proceeds via terminal or sub-terminal addition, yielding alkyl succinates. The addition of fumarate to aromatic hydrocarbons yields aromatic-substituted succinates. Thus, alkylsuccinic and 2- or 4-methylalkanoic acids, as well as benzylsuccinic and methylbenzylsuccinic acids are unique metabolites indicative of *in situ* anaerobic biodegradation of alkanes and aromatic hydrocarbons, respectively [137,138]. Succinates are reported as metabolites from biodegradation of hydrocarbons in oil field water [126] and aquifers or ground water [139–141]. These metabolites are considered ideal biodegradation indicators because they are not known to be present in hydrocarbon mixtures, reasonably stable, transient metabolites and have an unambiguous relationship to their parent hydrocarbon [137]. Alternative pathway of anaerobic alkane degradation involves subterminal carboxylation of alkanes at C-3 with removal of the two subterminal carbon atoms from the alkane chain terminus. This mechanism produces odd numbered fatty acids from even numbered *n*-alkanes, and vice versa [129]. Likewise, aromatic hydrocarbons are also activated by either direct carboxylation, methylation of unsubstituted aromatics or hydroxylation of an alkyl group to generate alkyl aromatic acids that are converted into long-chain volatile fatty acids. Direct carboxylation of PAHs generates 2-naphthoic acid as a central metabolite [142]. The pathways illustrate that, though no same metabolic mechanism is exclusively present in all bacteria and/or environments, the production of carboxylic acids is common.

Naphthenic acids (NAs) are complex mixture of alkyl-substituted acyclic and cycloaliphatic carboxylic acids, with the general chemical formula, $C_nH_{2n+Z}O_2$, where *n* is the carbon number and *Z* the number of rings. They occur naturally in crude oil and oil sands bitumen because either the deposit has not undergone enough catagenesis or biodegradation. NAs are widely used to indicate oil biodegradation or oil source maturation especially in oil reservoirs. NAs, such as 5,6,7,8-tetrahydro-2-naphthoic acid and decahydro-2-naphthoic acids, are indicative of anaerobic degradation of crude oil [143]. Also, the ratio of acyclic fatty acids to cyclic naphthenic acids (A/C) was proposed to indicate the extent of in-reservoir biodegradation of crude oil [144]. Moreover, NAs are toxic and environmentally persistent components in refinery wastewaters and in oil sands extraction waters. The accumulation of NAs indicates partial degradation rather than complete degradation of hydrocarbons. Hence, NAs are designated emerging contaminant, and studies are focusing on their biodegradation. Biodegradation of NAs was reported to produce 1-

cyclohexenecarboxylic acid, cyclohexylidene acetic acid and 8-hydroxyheptanoic acid under aerobic and anaerobic conditions [145].

The molecular characterization of hydrocarbon and their metabolites in environmental matrices is challenging. Carboxylic acids occur at low concentration in complex matrices and could be transient, although carboxylic acids were reported to accumulate as end products of PAHs metabolism [146]. Carboxylic acids characterization requires rigorous sample pre-treatment, involving extraction and dedicated cleanup procedures. In recent years, petroleomics and metabolomics have driven extensive advances in analytical platforms, with a particular surge in mass spectrometric techniques [10]. Mass spectrometry (MS) facilitates metabolite detection, identification, and quantification due to its high specificity and sensitivity, and speed of analysis. Indeed, MS gradually enabled the characterization of complex matrices previously considered to be too challenging [147]. The advent of a variety of high-resolution mass analyzers, such as time-of-flight (TOF), Orbitrap and Fourier transform ion cyclotron resonance (FT-ICR), has significantly expanded the capabilities of MS for structural elucidation and quantification [148]. Moreover, the potential of MS for the analysis of carboxylic acids could be enhanced by combining it with advanced chromatographic techniques such as gas chromatography (GC) or liquid chromatography (LC) [149].

1.5 Mass spectrometric techniques for the analysis of carboxylic acids

The direct determination of carboxylic acids by mass spectrometry is the ultimate goal but still difficult to attain because of several reasons. The major concerns include the production of ions from carboxylic acids in complex mixtures, their separation from other ions of similar mass, and the identity assignment. The simultaneous analysis of abundant and easily ionized compounds suppresses the analyte's signal and renders quantification difficult [150]. Therefore, it is necessary to develop suitable procedures to isolate and pre-concentrate the target metabolites, reducing ionization suppression.

The complexity of crude oil can be simplified by separation into four fractions (saturates, aromatics, resins, and asphaltenes, SARA) based on solubility and polarity [151]. The fractionation could be time-consuming and laborious, and there is a risk of loss of more volatile compounds during sample processing and solvent removal. The use of a chromatographic separation preceding MS, such as GC and LC, is typically required to simplify the matrix and alleviate ionization suppression and

discrimination. Chromatographic separation also provides another dimension of information (retention time) [152].

Table 1.3: Field and model studies using carboxylic acids as biomarkers for hydrocarbon biodegradation.

Hydrocarbon	Carboxylic acids	Remark	Reference
Hydrocarbon contaminated groundwater	Benzylsuccinic acids	Benzylsuccinic acid and methylbenzylsuccinic acid isomers were proposed as distinctive indicators of anaerobic toluene and xylene metabolism in fuel- contaminated aquifers.	[139]
Hydrocarbon contaminated aquifers	Alkylsuccinic acids and naphthoic acids	These anaerobic metabolites of alkane and naphthalene signified in situ biodegradation.	[140]
Hydrocarbon contaminated groundwater	2-Methylbenzylsuccinate and naphthoic acids	These biomarkers were detected in areas with active biodegradation.	[141]
Hydrocarbon contaminated groundwater	Naphthoic acids	Naphthoic acids was found to be a biomarker of anaerobic hydrocarbon biodegradation and of natural attenuation	[153]
Formation water	Alkanoic acids, aromatic acids, dicarboxylic acids and polyalkylated succinic acids	these signature metabolites were demonstrated as a valuable tool for tracing microbial activity in oilfields	[126]
Crude oil	Fatty and naphthenic acids	the abundance of carboxylic acids increased as the degree of biodegradation increased	[154]
Crude oil	Aliphatic and alicyclic acids	Medium molecular weight (C ₁₀ –C ₂₀) carboxylic acids were rapidly produced while after extensive biodegradation higher (>C ₂₀) molecular weight branched and cyclic carboxylic acids appeared	[155]
Perdeuterated pentadecane and ¹³ C-labelled hexadecane	Fatty Acids	Alkanes were oxidized to fatty acids	[135]
Crude oil	Aliphatic and aromatic acids	Oxidation of hydrocarbons to carboxylic acids was shown during the aerobic biodegradation of petroleum.	[136]
<i>n</i> -Octacosane	Dicarboxylic acids	A range of dicarboxylic acids offered an insight into how anaerobic communities may access waxes as growth substrates in anoxic environments.	[156]

BTEX (benzene, toluene, ethylbenzene, xylene)	Benzyl succinic acid, toluic acid and benzoate	2-(2-methylbenzyl)-succinic acid was found to be an important marker of anaerobic microbial degradation.	[157]
Crude oil	naphthenic acids Organic acids	Organic acids indicate evidence of microbial degradation, and 1-2 ring naphthenic acids are indicators for active, ongoing biodegradation in oil reservoirs.	[158]
Hydrocarbon contaminated aquitard	acetate, propionate, and butyrate	Accumulation of the short-chain fatty acids was linked to anaerobic biodegradation.	[159]
Hydrocarbon contaminated groundwater	Several carboxylic acids	Acids were the most frequently identified class of oxygenated metabolites.	[133]
Alkylbenzenes, naphthalene and alkyl-naphthalenes	Toluic acid, 2-methylsuccinic acid and 2-naphthoic acid	Metabolites indicated active anaerobic degradation pathway.	[160]
Pyrene	Phenanthrene-4-carboxylic acid, Phthalic acid and dicarboxylic acids	6,6'-dihydroxy-2,2'- biphenyl dicarboxylic acid indicated a new branch in the degradation pathway of pyrene.	[161]
Groundwater contaminated with toluene, ethylbenzene, and xylene	Benzylsuccinic acid and methylbenzylsuccinic acid	Benzylsuccinic acids are useful as qualitative indicators of <i>in situ</i> biodegradation.	[162]
Benzo[a]pyrene	Phthalic acid	The bacterium uses the <i>meta</i> pathway for biodegrading Benzo[a]pyrene.	[163]
Heavy crude oil	<i>n</i> -fatty acids and naphthenic acids	<i>n</i> -fatty acids and naphthenic acids accumulated over time	[164]

The high complexity of matrix generates spectral overlaps with ions of interest and requires high resolution. A resolution of 1 M at m/z 500 is considered as a reference value for acceptable specificity [165]. Even then, the presence of isomers can perturb the analytical result. The high resolution must be accompanied by high mass accuracy (<1 ppm) for the determination of empiric formula and metabolite identification.

1.5.1 Sample pre-treatment

1.5.1.1 Blanks and controls

Running blanks and control experiments is mandatory in studies of carboxylic acid metabolites. Instrumental blanks are necessary to avoid carry-over contamination. Hexadecanoic acid and octadecanoic acids are common contaminants from plastic labware, hands of the analyst etc. and

were reportedly detected in alkane-free controls [166]. Control experiments are mandatory in order to avoid the ambiguity about the source of detected carboxylic acids [134]. For instance, some carboxylic acids are not unique biodegradation products nor are exclusively related to their parent hydrocarbon. Fatty acids are natural constituents of bacterial cells. Therefore, It is essential to link the loss of the parent hydrocarbons to the appearance of carboxylic acids [167]. Also, biodegradation can be studied using stable isotope-labeled hydrocarbon substrates, such as ^2D - and/or ^{13}C -labelled hydrocarbons [135]. Upon biodegradation, detection of the labelled carboxylic acids would distinguish those produced from other sources.

1.5.1.2. Extraction of carboxylic acids

Because carboxylic acids are often present at low concentrations and the matrices of interest are very complex, isolation and pre-concentration is important to increase the selectivity and the detection limits for identification and quantitative analysis. Solvent-based and adsorbent-based extractions are common extraction strategy [168] as shown in Figure 1. Aliquot samples obtained after biodegradation (free of bacterial cells and insoluble impurities) are acidified to $\text{pH} < 2$ for the preservation and protonation of carboxylic acids prior to their extraction with an organic solvent and GC separation. The extraction efficiency depends on the solvent, the number of extraction steps and the pre- and post-processing of the sample [168]. The typical extraction solvents used have been ethylacetate [83], dichloromethane [169] and diethyl ether [134]; several solvents can be used in a series [156]. The obtained extract is dried by means of anhydrous Na_2SO_4 and the organic phase is concentrated by evaporation.

An alternative to solvent-based extraction is solid phase extraction (SPE) using membranes or disposable syringe-type columns or cartridges filled with sorbents [170]. The nature of the latter determines the interactions with the analytes. Schemeth *et al.* [170] discussed strategies for the fractionation of complex, oil-polluted environmental samples into a neutral fraction and several acid-class fractions. Mixed-mode anion exchangers based on a non-polar polymeric backbone demonstrated the best performance for a broad range of acidic oil degradation products.

One advantage of SPE over liquid-liquid extraction is the elution of samples with small volumes of solvent limiting the need for evaporation. The molecular composition of water-soluble petroleum compounds formed through biodegradation showed that more polar compounds were extracted by SPE than the solvent-based extraction [158]. The ease of coupling with LC is another advantage of SPE. SPE acts as a pre-concentration step allowing the detection of carboxylic acids at concentrations down to $0.01 \mu\text{g/L}$ by LC-MS [137].

1.5.1.3. Derivatization

Carboxylic acids are polar and thus not sufficiently volatile to be amenable by GC. Therefore, they must be derivatized by methylation or silylation of the –COOH group. Furthermore, derivatization improves the thermal stability of the carboxylic acids in the hot GC injector. Derivatization is time consuming, laborious, and increases the risk of sample contamination. In addition, steric hindrance can lead to partially derivatized analytes.

Trimethylsilylation (TMS) has been a prevalent method for the volatilization and stabilization of carboxylic acids during GC separation. TMS forms trimethylsilyl ethers by replacing active hydrogen atom of the carboxylic acids by a trimethylsilyl group. *N,O*-bis(trimethylsilyl)trifluoroacetamide (BSTFA) is a commonly used trimethylsilylation reagent showing signature fragments $[M]^+$, $[M-15]^+$ and $[M-89]^+$. TMS derivatization is faster and offers higher peak resolutions than methylation by diazomethane [134] or BF_3 -methanol [171], the latter reagents suffering from instability and toxicity. In some cases, trimethylchlorosilane (TMCS) is added as a catalyst to BSTFA to increase reactivity [83].

Esterification with alcoholic solution of sulfuric acid or hydrochloric acid (10% *v/v*) at 80 °C takes longer (ca. 1-8 h) [136]. Using this method, non-volatile organic acids were derivatized with ethanol and volatile organic acids with *n*-butanol [138]. Likewise, Ji *et al.* [166] reported using ethanol-hydrochloric acid (refluxed at 80 °C for 8 h) after saponification at 100 °C for 8 h.

1.5.2 Direct analysis by Fourier Transform Ion Cyclotron Resonance - mass spectrometry (FT – ICR MS)

A direct MS analysis of carboxylic acids from complex matrices, such as crude oil, requires ultrahigh resolving power and high mass accuracy. FT-ICR offers a sub-ppm mass accuracy in mass range of m/z 100–1000 with resolution readily achieving 1,000,000 at m/z 500 [172]. This has made FT-ICR an established technique for the characterization of polar and less volatile hetero-atomic species in crude oil that are not resolved by GC [173] [174]. However, limited dynamic range, high cost, required technical expertise and dependence on higher field magnets remain major FT-ICR limitations.

Ions have usually been produced by electrospray ionization (ESI). Carboxylic acids are more efficiently ionized by ESI in the negative mode, with peaks corresponding to deprotonated molecules $[M-H]^-$ observed. However, the selective ionization of highly acidic carboxylic acids in the negative mode limits the detection of weakly acidic species [175]. Alternatively, the introduction of atmospheric pressure photoionization (APPI), can limit fragmentation and promoting high sensitivity [56].

The mass analyser resolves ions with different masses, and determine the latter with sufficient accuracy to calculate the elemental composition of the ion [176]. The ultrahigh mass resolution and mass accuracy of FT-ICR enables distinctive assignment of elemental composition of crude oil and classification considering the heteroatomic compositions (C, H, O,N and S), isotopic pattern, double bond equivalent (DBE) values, and the ratios H/C and N/C [177]. Oxygen-containing species, such as O₂ (monocarboxylic acid), O₃ (hydroxycarboxylic acid), O₄ (dicarboxylic acids) etc. are commonly used to denote the various class of carboxylic acids. The changes DBE are another indicator for estimating the degree of biodegradation. DBE represents the degree of unsaturation and/or aromaticity. Biodegradation of hydrocarbon increases DBE by one for each addition of an organic acid group and reduces DBE by one when an aromatic ring is cleaved [178]. Thus, O₂ acids with DBE lower than 5 are saturated chains and/or saturated rings, and aromatic acids exhibit DBE equal or higher than 5 [154].

FT-ICR MS analysis produces thousands of elemental compositions within a single mass spectrum. Optimized data acquisition system and data processing methods such as Kendrick mass defect analysis, van Krevelen analysis and DBE distribution plots are available for automated processing, quantitation, visualization and interpretation of the multidimensional and multi-sample FT-ICR MS data [179].

1.5.3 Gas chromatography - mass spectrometry (GC - MS)

1.5.3.1 Separation

The methylated and silylated derivatives can be readily separated using non-polar columns. However, complex mixtures of similar compounds do not efficiently separate in one dimension, requiring two-dimensional gas chromatography (GC×GC). GC×GC separations are performed by two columns that are coupled by a modulator. The modulator traps, concentrates and focuses fractions from the first dimension (¹D) column (generally nonpolar) and then, systematically, re-introduces the collected fractions into the second dimension (²D) column (generally polar) as a narrow pulse facilitating comprehensive separations. This improves signal-to-noise ratio, causing very narrow bands of analytes with superior peak resolution and provides extension of metabolic coverage in comparison with GC [180]. Another important feature is the peaks are ordered in a two-dimensional plane where compounds and isomers appear as distinct groups in the chromatogram as a result of their physicochemical properties and interaction with ²D phase [181] as shown in Figure 1.4. This high degree of separation orthogonality facilitates peak identification and quantification. In recent years, numerous instrumental advances and optimization regarding

column properties and configuration, and modulation have been made to achieve higher efficiency and selectivity [180,182].

Generally, GC-based techniques are limited to compounds with volatility below $\sim 400\text{ }^{\circ}\text{C}$ to prevent column degradation [183].

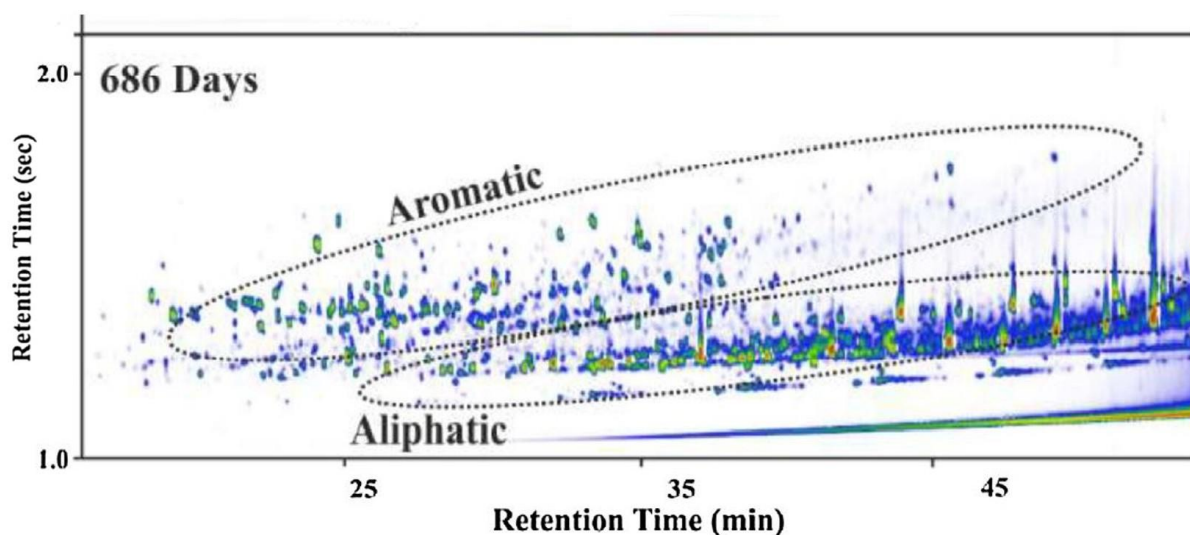


Figure 1.4: GC×GC-MS total ion current chromatogram of methylated acidic extract of crude oil incubated under sulfate reducing condition for 686 days. The expanded peak capacity of GC×GC-MS produced good resolution of aromatic acids from aliphatic acids (indicated by the ellipses), due to the ^2D column (Y-axis) [171].

1.5.3.2 Mass spectrometry

Ionization of the GC effluents has traditionally been achieved by a high-energy electron impact (EI). The generated fragmentation patterns are highly reproducible [184]. Characteristic fragments are useful for fragmentation pathway prediction and structural identification of carboxylic acids [185]. Identification is based on the comparison with standards [169] or by matching spectral libraries [134]. However, the effectiveness of EI decreases significantly for high molecular weight compounds. Furthermore, fragmentation can be too extensive resulting in less specific fragment ions and reduced sensitivity. The absence of diagnostic molecular ion often hinders the identification of co-eluting low abundance molecules [186].

GC-MS or GC×GC-MS are able to provide quantitative information on non-polar compounds that are not effectively measured by FT-ICR MS [41,174]. GC coupled to FT-ICR MS improved the characterization of oil sands process water and groundwater samples [187] though GC separation is limited by the slow acquisition rate of FT-ICR MS ($<1\text{ Hz}$) [188]. Non-targeted carboxylic acid analysis can be achieved by TOF-MS which provides an optimum combination of speed and sensitivity, which preserves high chromatographic resolution. Tandem Q-TOF MS is also an

excellent tool for structural identification of unknown carboxylic acids [189]. Data visualization in GC×GC is usually a 2D plot defined by retention times in both dimensions. Carboxylic acids are semi-quantified using the integration of the GC×GC–TOF MS base peaks ions and comparison with the base peak ion of an internal standard, assuming a response factor of 1 [171].

1.5.4 Liquid chromatography – mass spectrometry (LC – MS)

1.5.4.1 LC separation conditions

In contrast to GC, carboxylic acids can be separated without prior derivatization by using LC. Reversed phase LC is usually used, after addition of a weak acid or a base to the mobile phase. Weak acids, such as acetic, formic or trifluoroacetic acid, keep carboxylic acids in their protonated state while bases, such as ammonium acetate, ammonium hydroxide and tetramethylammonium hydroxide, deprotonate acids and allow their retention on the column for separation [190]. The vast number of mobile phase combinations and acid modifiers have been used to provide suitable separations and ionization. The addition of formic acid, at a concentration of 0.01%, was reported to result in signal suppression not observed with acetic acid. Split peaks were observed at <0.2% acetic acid due to the pH of the mobile phase above and/or close to the pKa of the analytes. The concentration of 0.2% acetic acid allowed narrower peaks that did not split; however, it extended the retention times of the analytes [157]. Ultra-high-performance LC (UPLC) systems have been developed to achieve faster separation with high resolution and separation efficiency. UPLC uses smaller amounts of solvents required for sample elution and produces narrower and more concentrated bands [191]. A good example of the LC separation power can be the separation of 11 BTEX metabolites in one run [157]. Their separation depended on the type and length of the column used, and the concentration of the acid modifier.

1.5.4.2 Mass spectrometry

The prior separation by LC simplifies mass spectrometric analysis and alleviates the negative impact of competitive ionization [175]. The application of high resolution mass analyzers such as TOF [178] or Orbitrap [192] constituted a major advancement towards the structural elucidation of unknown species by proposing chemical formulas that match a given exact mass. The coupling of LC to FT-ICR was also reported for untargeted analysis of metabolites from water-soluble fraction of crude oil [193].

The LC coupling to tandem MS generates molecular fragmentation with higher specificity and reproducibility and increases the confidence of *de novo* identification [194]. MS/MS based fragmentation reactions are also useful for accurate determination using selected reaction

monitoring (SRM) or multiple reaction monitoring (MRM) modes. They are based on a selection of unambiguous representative fragmentation products with particular m/z value for a higher specificity and sensitivity. However, the strength of this technique depends on the separation power of the chromatographic system and a good understanding of the fragmentation of the carboxylic acids of interest. For example, position isomers, such as toluic acids or methylbenzyl-succinic acids fragmented by losing a carboxyl group and produce non-specific transitions in MRM mode with relatively high background noise [157]. Hence, their separation depends critically on the elution conditions (Figure 1.5).

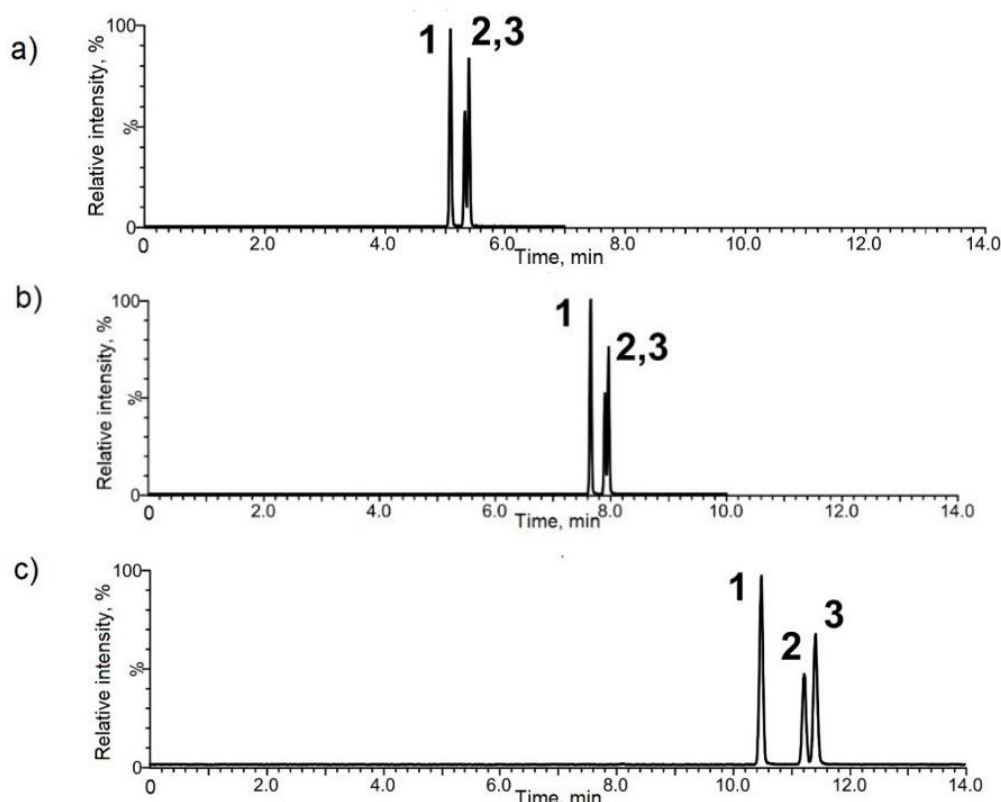


Figure 1.5: HPLC separation of position isomers of toluic acids: (1) *o*-toluic acid (2) *m*-toluic acid (3) *p*-toluic acid using BEH C18 column ($50 \times 2.1 \text{ mm} \times 1.7 \mu\text{m}$). Acetic acid concentration in the mobile phase: (a) 0.05%, (b) 0.1%, and (c) 0.2%. An increase in acetic acid concentration resulted in narrower peaks and extended retention time [157].

1.6 Applications of mass spectrometry for the monitoring of carboxylic acids after hydrocarbon biodegradation

1.6.1 Model systems: saturated hydrocarbons (alkanes and cycloalkanes)

GC-MS has been the primary technique for the degradation studies of saturated hydrocarbons (Table 1.4). Alkylsuccinates generated from fumarate addition were described as the main products of

anaerobic degradation of C₉-C₁₂ *n*-alkanes [166]. Signature fragments at *m/z* 128, 174, [M-45]⁺ and [M-87]⁺ were reported to be distinctive for alkylsuccinates [166,185]. A model waxy alkane, *n*-octacosane, was biodegraded under methanogenic conditions to produce long-chain fatty acids [156]. Additionally, dicarboxylic acids (α , ω) were also detected in concentrations ranging from 3 to 160 μ M. These dicarboxylic acids were speculated to be cell-associated or secreted by cells to act as biosurfactants.

Sulfate-reducing bacteria degraded cyclohexane to cyclohexylsuccinic acid under anoxic conditions. Other metabolites detected include 3-cyclohexylpropionic acid and cyclohexanecarboxylic acid. This indicates that the anaerobic degradation pathway of cyclohexane is similar to that of *n*-alkanes [169].

Table 1.4: Carboxylic acids from the biodegradation of saturated hydrocarbons

Hydrocarbon	Mass spectrometry	Carboxylic acids			Reference
		(Alkyl)Alkanoic/cycloalkanoic acid	Dicarboxylic acid	Alkylsuccinate	
Nonane, decane, undecane and dodecane	GC-MS	Tetradecanoic acid Pentadecanoic acid Hexadecanoic acid* Heptadecanoic acid Octadecanoic acid* Eicosanoic acid Docosanoic acid	Butanedioic acid Pentanedioic acid Hexanedioic acid Octanedioic acid Nonanedioic acid	1-Methyloctylsuccinate 1-Methylnonylsuccinate 1-Methyldecylsuccinate 1-Methylundecylsuccinate	[166]
<i>n</i> -Octacosane	GC-MS		Hexanedioic acid Heptanedioic acid Octanedioic acid Decanedioic acid Dodecanedioic acid		[156]
Cyclohexane	GC-MS	Cyclohexane carboxylic acid 3-Cyclohexylpropionic acid		Cyclohexylsuccinic acid	[169]
Hexadecane	GC-MS	Hexadecanoic acid Propanoic acid Dodecanoic acid Pentanoic acid Butanoic acid			[195]

*also detected in the alkane-free controls

1.6.2 Model systems: aromatic hydrocarbons

GC-MS has also been the primary method used for the analysis of carboxylic acids associated with the biodegradation of polyaromatic hydrocarbons (Table 1.5). Benzoic acid, salicylic acid, protocatechuic acid, phthalic acid and naphthoic acid are principal degradation products [25].

Benzoic and 1,2,3-benzenetricarboxylic acids were revealed as common metabolites during the degradation of phenanthrene and fluorene under saline condition [195]. Pyrene degradation by *Bacillus megaterium* produced phenanthrenecarboxylic acid and phthalic acid [196].

GC×GC-MS demonstrated that phthalate and salicylate degradation pathways played jointly a role in fluorene degradation by *Pseudomonas aeruginosa* [83]. The peak ratio of phthalic to salicylic acid was 1:3, implying an accumulation of salicylic acid over time.

LC-MS/MS has been a viable alternative to GC-MS. While muconic acid was detected as a product from the ring cleavage of benzene, benzoic and *p*-toluic acids were reported for aerobic degradation of toluene by *Bacillus amyloliquefaciens* [62]. Interestingly, the detection of *o*-, *m*-, *p*-toluic acids showed the degradation of all isomers of xylene. Toluic, salicylic, benzoic, benzyl, and phenyl succinic acids were detected above 0.1 ng/mL as BTEX metabolites in a water sample of a deep aquifer hosting natural gas storage [157].

GC-MS and LC-MS were demonstrated to complement each other for the identification of carboxylic acids from phenanthrene biodegradation [54]. GC-MS analysis tentatively identified 4-[1-hydroxy(2-naphthyl)]-2-oxobut-3-enoic acid and salicylic acid, while LC-MS allowed the identification of 1-hydroxy-2-naphthoic acid.

1.6.3 Crude oil

As it was shown in Table 1.6, GC-MS can handle the analysis of metabolites from samples of higher complexity, such as crude oil. GC-MS copes readily with the viscosity of crude oil and profits from the availability of rich mass spectral databases. In addition, GC-MS permits the concomitant monitoring of the residual hydrocarbons.

The parallel determination of the residual hydrocarbons enables their linking with the corresponding carboxylic acids formed. Forty-four carboxylic acids were identified after degradation of 1 % crude oil by *Gordonia rubripertincta* and *Rhodococcus* sp. [134]. Four monoethyl-substituted and two methyl-substituted alkanolic acids were detected from alkane biotransformation. Additionally, cyclohexylalkanoic and cyclopentyl-alkanoic acids as well as phenyl-, naphthyl-, and biphenyl alkanolic acids were identified as metabolites of alkylcyclohexanes and alkylcyclopentanes and alkyl-substituted benzenes, naphthalenes and biphenyls, respectively. In another study, fatty acids, aromatic carboxylic acids, and unsaturated acids were recovered by esterification, confirming that the oxidation of hydrocarbons yields carboxylic acids, and is an important process in the aerobic biodegradation of petroleum [136].

The complexity of biodegraded crude oil leaves some carboxylic acids unresolved and unidentified by GC-MS [197]. FT-ICR MS and GC×GC-MS are potent techniques for carboxylic acids analysis in such complex samples. Aromatic acid metabolites, that were characteristic of the fumarate addition mechanism, were distinguished from aliphatic acids, on the basis of the high phenyl content of the ²D column [171]. This allowed the acquisition of EI mass spectra, relatively free of ions from co-eluting compounds. Likewise, more than 760 unique polar compounds, including carboxylic acids and their esters, were tentatively identified in 22 groundwater samples from fuel release sites by non-targeted GC×GC-MS [133].

FT-ICR MS showed that *n*-alkanes in crude oil were progressively biodegraded to *n*-fatty acids through β -oxidation, or to hydroxycarboxylic acids and dicarboxylic acids through ω -oxidation [41]. The relative concentration of the *n*-fatty acids increased with biodegradation, suggesting that carboxylic acids are the main biodegradation products of crude oils under aerobic conditions. Lui *et al.* [193] examined the evolution of carboxylic acids signatures in microbial treated PAHs of the water-soluble fraction of crude oil. The relative abundance of O3 compounds indicated the production of 3- and 4-methylsalicylic acids, which are key metabolites from PAHs degradation. Interestingly, these compounds decreased substantially with time suggesting they are transient, with production, accumulation, and degradation occurring simultaneously. Similarly, detection of salicylic acids and gentistic acid in archived field samples suggested that these carboxylic acids are viable markers for PAHs degradation.

No single technique is for the moment sufficient for the holistic profiling of metabolite produced during bacterial degradation of hydrocarbons. Bias to specific chemical classes and identification of previously unreported carboxylic acids, especially in complex matrices, remains a challenge for comprehensive analysis. The limited availability of authentic standards still presents a bottleneck for *de novo* identification. Efficient data mining and combination techniques from different methods, including advanced sample pre-treatment and pre-concentration procedures, are essential for effective analysis and data interpretation.

Table 1.5: Characterization of carboxylic acids from the biodegradation of BTEX and polyaromatic hydrocarbons

Hydrocarbon	Mass spectrometry	Carboxylic acids			Reference
		(Alkyl)Benzoic acid	Hydroxy carboxylic acid	Dicarboxylic acid	
Benzene	LC-MS/MS		2-Hydroxy-2,4-pentadienoate, 4-hydroxy-2-oxovalerate	Muconic acid	[62]
Toluene		Benzoic acid, <i>p</i> -toluic acid	2-Hydroxy-2,4-pentadienoate	Maleylacetate 3-oxoadipate	
Ethylbenzene			2-Hydroxy-2,4-pentadienoate, 2-hydroxy-6-oxo-octa-2,4-dienoate		
Xylene		<i>o</i> -Toluic acid, <i>m</i> -toluic acid, <i>p</i> -toluic acid			
Benzene*, toluene, ethylbenzene and xylene	LC-MS/MS	Benzoic acid		Benzylic succinic acid Phenyl succinic acid 2-(1-Phenylethyl)-succinic acid 2-(2-Methylbenzyl)-succinic acid 2-(3-Methylbenzyl)-succinic acid 2-(4-Methylbenzyl)-succinic acid	[157]
		(Alkyl)Benzoic acid	(Alkyl)Polyaromatic acid	Dicarboxylic acid	
Phenanthrene	GC-MS LC-MS	Salicylic acid	1-Hydroxy-2-naphthoic acid 4-[1-Hydroxy(2-naphthyl)]-2-oxobut-3-enoic acid		[54]
Acenaphthene	GC-MS QTOF-MS	Salicylic acid 3-Formyl salicylic acid	1-Naphthoic acid	Naphthalene-1,8-dicarboxylic acid	[58]
Fluorene	GC×GC-MS	Protocatechuic acid Salicylic acid		Adipic acid Succinic acid Phthalic acid	[83]
Phenanthrene	GC-MS	Benzoic acid	1-Hydroxynaphthalene-2-carboxylic acid		[195]
Fluorene		Benzoic acid			
Pyrene		Benzoic acid	4-Phenantroic acid 3,4, Dihydro-phenanthrene-4-carboxylic acid	Phthalic acid	
Naphthalene, Phenanthrene and Fluoranthene	LC-MS	3,4-Dihydroxy-1,5-cyclohexadienoic acid Protocatechuic acid	2-(Hydroxymethyl)-acenaphthylene-1-carboxylic acid 2-(Methoxymethyl)-acenaphthylene-1-carboxylic acid 9-Fluorenone-1-carboxylic acid cis-1,9a-Dihydroxy-1-hydro-1-fluorene-9-one-8-carboxylic acid 4-Hydroxy-6-oxo-6H-benzo[c]chromene-7-carboxylic acid 2-(Hydroxy)-acenaphthene-1-carboxylic acid 2-Formylacenaphthylene-1-carboxylic acid 2-Formylacenaphthene-1-carboxylic acid	Phthalic acid Acenaphthene-1,2-dicarboxylic acid	[198]

*Only benzene was not degraded

Table 1.6: Carboxylic acids detected during crude oil biodegradation

Mass spectrometry	Carboxylic acids				Reference
	(Alkyl)Alkanoic/cycloalkanoic acid	(Aky)aromatic acid	(Alkyl)Polyaromatic acid	Dicarboxylic acid	
GC-MS	Heptanoic acid 2,3-Dimethyl-butanoic acid 2-Ethyl-pentanoic acid 2-Methyl-hexanoic acid 2-Ethyl-heptanoic acid 2-Ethyl-octanoic acid Cyclopentane carboxylic acid Cyclohexane carboxylic acid 3-Methylcyclopentane carboxylic acid Cyclohexylpropanoic acid Cyclohexylacetic acid 4-Methylcyclohexane carboxylic acid	Benzoic acid 2-Hydroxybenzoic acid 3,4-Dihydroxybenzoic acid 4-Biphenylcarboxylic acid Methylbenzoic acid 3-Methylbenzoic acid 4-Ethylbenzoic acid 2,4-Dimethylbenzoic acid 2,3-Dimethylbenzoic acid 2,4,5-Trimethylbenzoic acid Phenylpropanoic acid Phenylacetic acid β -Methylphenylacetic acid γ -Methyl- γ -phenylpropanoic acid	21-Naphthalene carboxylic acid 1-Naphthylpropanoic acid 1-Naphthylbutyric acid 1-Naphthylacetic acid 2-Naphthylacetic acid, Methylnaphthalene carboxylic acid	4,4-Biphenyl-dicarboxylic acid	[134]
GC-MS	Dodecanoic acid Pentadecanoic acid Hexadecanoic acid 3-Hydroxydodecanoic acid 3-Hydroxytridecanoic acid 4-Oxopentanoic acid 17-Methyloctadecanoic acid	4-Methylbenzoic acid <i>m</i> -Methylbenzoic acid <i>m</i> -Tolylacetic acid	1-Naphthalene carboxylic acid 2-Naphthalene carboxylic acid	Butanedioic acid Phthalic acid 1,3-Benzenedicarboxylic acid	[136]
GC×GC-TOFMS		Alkyl-benzoic acids Phenylalkanoic 2-Biphenyl carboxylic acids 3-Biphenyl carboxylic acids 4-Biphenyl carboxylic acids Benzylsuccinate Methylbenzylsuccinates	1-Naphthoic acid 2-Naphthoic acid Phenanthrene-2-Carboxylic acid Methylphenanthryl carboxylic acid Benzothiophene carboxylic acid Dibenzothiophene carboxylic acids Naphthyl-2-methylsuccinic acid Alkyl-naphthyl-2-Methylsuccinic acids		[171]
FT-ICR MS	<i>n</i> -Fatty acids (O2 compound)		Hydroxycarboxylic acid (O3 compound)	Dicarboxylic acids (O4 compound)	[41]
LC-FT-ICR MS		Salicylic acids 3- and 4-Methylsalicylic acids Genticic acid			[193]

Chapter two

Materials and methods

2. Materials and methods

All chemicals used in this study were analytical grade and purchased from Merck (www.sigmaaldrich.com). Water produced from a MilliQ Purification System (ELGA[®], UK) was used throughout.

2.1 Crude oil-polluted soil sampling site

Soil sample was collected from Bodo West crude oil contaminated site ($4^{\circ} 37' 18.1''$ N, $7^{\circ} 15' 53.4''$ E). Bodo is located at the southern coastal end of Ogoniland and east of the Niger Delta, Nigeria (Figure 2.1). It is bounded seaward to the south by the Atlantic Ocean. Bodo has over five decades of immense crude oil pollution affecting coastal and terrestrial environment. Incidents of crude oil spills in this area are compounded by pipelines leaks, sabotage, and artisanal oil refining [30,199].



Figure 2.1: Geographical location of Bodo (<https://www.bbc.com/news/world-africa-14398659>).

2.2 Sampling crude oil-polluted soil

The soil sample was collected using a soil auger at 15 cm depth and stored in a clean plastic container. Soil pH was measured by suspending the soil in water (1:5 w/v). The slurry was vortexed for 1 min and let to settle down. pH was read with a pH meter (Cyberscan 510, EUTECH Instruments, Singapore) at 25 °C. The pH of the soil sample determined the pH of the enrichment media.

2.3 Isolation of bacterial strains by enrichment on crude oil

Figure 2.2 illustrates the bacteria enrichment and isolation steps adopted.

2.3.1 Media composition

Enrichment was carried out at pH 8.0 because the soil sample had an alkaline pH (8.3). Cultivations were carried out using four media that were sterilized by autoclaving at 121 °C and 15 psi for 20 min:

- (i) Rich Complete Medium (RCM) (g/L): casein (2.0), glycerol (2.5), asparagine (0.10), sodium propionate (4.0), K_2HPO_4 (0.50), $MgSO_4 \cdot 7H_2O$ (0.10), $FeSO_4 \cdot 7H_2O$ (0.001).
- (ii) Rich Incomplete Medium (RIM) as RCM but without casein and glycerol.
- (iii) Complete Mineral Medium (CMM) (g/L): starch (10.00), casein (0.30), $NaNO_3$ (0.85), KH_2PO_4 (0.56), Na_2HPO_4 (0.86); K_2SO_4 (0.17), $MgSO_4 \cdot 7H_2O$ (0.37), $CaCl_2 \cdot 6H_2O$ (0.007) and 2 mL of trace element solution: $ZnCl_2$ (0.042); $MnCl_2 \cdot 4H_2O$ (0.05); H_3BO_3 (0.30); $CuCl_2 \cdot 2H_2O$ (0.002); $Na_2MoO_3 \cdot 2H_2O$ (0.018); $CoCl_2 \cdot 6H_2O$ (0.19); $FeSO_4 \cdot 7H_2O$ (1.1); $NiCl_2 \cdot 6H_2O$ (0.024)) at pH 8.0 (25 °C).
- (iv) Incomplete Mineral Medium (IMM) as CMM without starch and casein.

2.3.2 Enrichment conditions

One gram of soil sample was suspended into 10 mL of culture media supplemented or not with 1 % (v/v) filter-sterilized Congo Bilondo crude oil and incubated at 20 °C, 27 °C and 35 °C at 75 rpm for 20 days. Thereafter, 1 ml aliquot of the enrichment cultures was transferred into fresh corresponding media and incubated for 14 days.

2.3.3 Isolation of bacteria

Aliquots (10 μ L and 100 μ L) of the enrichment cultures were spread on the corresponding 1.5 % agar media and incubated for 3 days at the same temperature as that used for the enrichment. For enrichments grown with the incomplete media, RIM and IMM agar media were supplemented with glucose (5 g/L) and yeast extract (5 g/L) or peptone (5 g/L) and yeast extract (5 g/L) or lactate (20 mM), acetate (20 mM) and yeast extract (5 g/L) as carbon source. Lysogeny broth (LB) agar, RCM agar and CMM agar were used for enrichments grown with RCM and CMM. Isolates were purified by two successive streaking on agar plates. The purity of isolates was confirmed by the morphological homogeneity of the colonies on agar plates, the presence of only one morphotype under the microscope and detection of a single 16S rRNA gene PCR product in the 16S rRNA genes sequencing chromatograms.

2.3.4 Screening of isolates on hydrocarbons

To identify isolates capable of utilizing a hydrocarbon, 5 mL IMM supplemented with 0.2 % (v/v) crude oil and 0.2 % (v/v) of a 50/50 mixture of *n*-decane and *n*-hexadecane was inoculated with 1 μ L loopful cell suspension of each isolate and incubated at 30 °C and 75 rpm. The isolates were also incubated in 5 mL IMM supplemented with propionate (4 g/L) and asparagine (0.1 g/L) to serve as a positive control. Growth was monitored every 72 h by optical density (OD) at 600 nm using a spectrophotometer (Spectronic Camspec, UK). LB media (5 mL) was each inoculated with 1 μ L loopful of isolates having the capability to utilize hydrocarbons and incubated at 30 °C and 75 rpm for 48 h. Then, aliquots (1.5 mL) of cultures were cryopreserved at -80 °C using 0.5 mL of 50 % glycerol while 250 μ L were used for DNA extraction to identify the isolates.

2.4 Molecular biology analysis

2.4.1 Genomic DNA extraction and Illumina sequencing

DNA was extracted from the soil sample (0.25 g) and enrichment cultures (250 μ L) using DNeasy® Power Soil® DNA Isolation Kit (Qiagen, Hilden, Germany) following the manufacturer's instructions. The extracted DNA samples were sequenced at MR DNA (www.mrdnalab.com, Shallowater, TX) on MiSeq following the manufacturer's guidelines. In summary, the V1-V3 variable region of 16S rRNA gene were amplified using the primers 8F-519R [200] with barcode on the forward primer in a 30 cycle PCR. PCR amplifications were performed using the HotStarTaq Plus Master Mix Kit (Qiagen, Germantown, MD) under the following conditions: 94 °C for 3 min, followed by 30 cycles of 94 °C for 30 s, 53 °C for 40 s and 72 °C for 1 min, followed by a final elongation step at 72 °C for 5 min. After amplification, PCR products were checked in 2 % agarose gel to determine the success of amplification and the relative intensity of bands. Multiple samples were pooled together in equal proportions using MR DNA's proprietary molarity model and purified using calibrated Ampure XP beads, before preparing the illumina DNA library. Sequence data were processed using version 2019_05 of MR DNA taxonomic analysis pipeline and database. Operational taxonomic units (OTUs) were defined by clustering at 3% divergence (97% similarity). Finally, OTUs were taxonomically classified using BLASTn against a curated database derived from RDPII and NCBI (<http://rdp.cme.msu.edu>, www.ncbi.nlm.nih.gov). The 16S rRNA gene sequences from the soil and enrichment samples were deposited to the NCBI Short Read Archive (SRA) under the BioProject accession number PRJNA883074.

2.4.2 Pacbio Sequel for bacterial identification

DNA extracted from isolates having the capability to utilize hydrocarbons were sequenced for identification. The 16S rRNA gene PCR primers, 8F-1492R, with barcode on the forward primer were used for amplification. After amplification, multiple samples were pooled together in equal proportions and purified using Ampure PB beads (Pacific Biosciences). SMRTbell libraries (Pacific Biosciences) were prepared and sequenced at MR DNA on the PacBio Sequel following the manufacturer's guidelines. After completion of initial DNA sequencing, each library undergoes a secondary analysis, Circular Consensus Sequencing (CCS), using PacBio's CCS2 algorithm. The CCS2 algorithm aligns the forward 'FWD' and reverse 'REV' subreads from each template to generate consensus sequences, thereby correcting the stochastic errors generated in the initial analysis. Thereafter, sequence data was processed using version 2019_08 of MR DNA taxonomic analysis pipeline and database. Nucleotide sequence of 16S rRNA gene were deposited at NCBI GenBank under the GenBank accession numbers ON383530 - ON383535. 16S rRNA sequences of type strains were obtained from EzBioCloud (www.ezbiocloud.net) for evolutionary analyses conducted in MEGA X.

2.5 Biodegradation studies

2.5.1 Biodegradation of *n*-hexadecane

Five millilitres of IMM inoculated with 1 μ L loopful of growing cell suspension of the selected bacteria and supplemented with *n*-hexadecane (0.1% v/v) as carbon source was used for biodegradation study. In parallel, 0.4 % (w/v) propionate as sole source of carbon was used as positive control while a medium supplemented with *n*-hexadecane with no inoculation served as negative control. Three replicates were incubated at 30 °C and 50 rpm. Experimental replicates of treatments and controls were sacrificed at day 0, 3, 6 and 10 to monitor protein concentration, residual *n*-hexadecane, and extracellular metabolites.

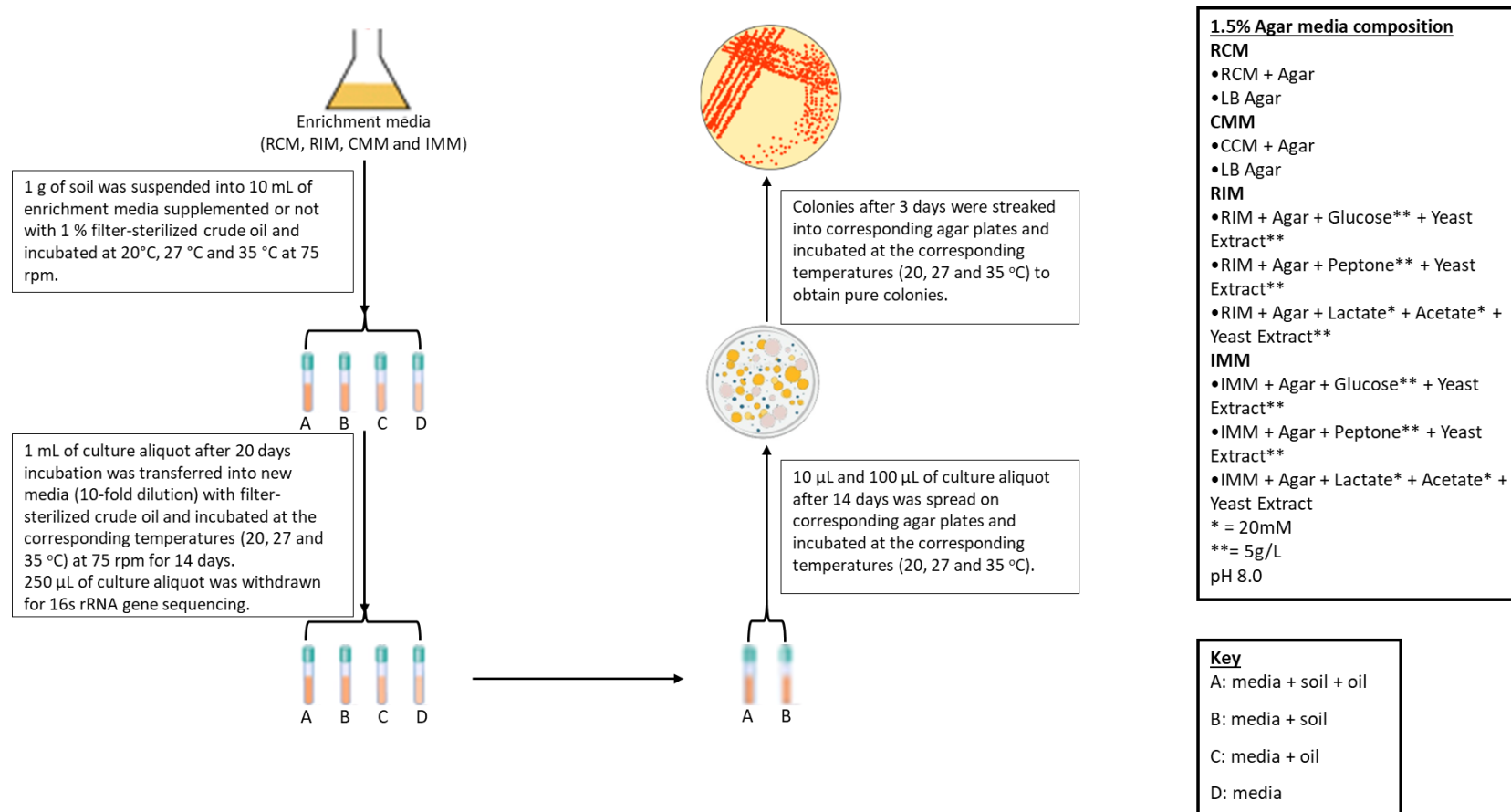


Figure 2.2: Bacteria enrichment and isolation workflow.

2.5.2 Biodegradation of saturate fraction of crude oil

2.5.2.1 SARA Fractionation of crude oil

Congo bilondo crude oil was fractionated using the method described elsewhere with modification [201]. The oil (85.2 g) was separated into maltene and asphaltene fractions using *n*-heptane (1:40, *w/v*). Thereafter, 10 g of the maltene fraction was fractionated by silica gel column chromatography and eluted with *n*-hexane, toluene, and DCM/methanol (9:1, *v/v*) to obtain saturates, aromatics and resin fractions, respectively.

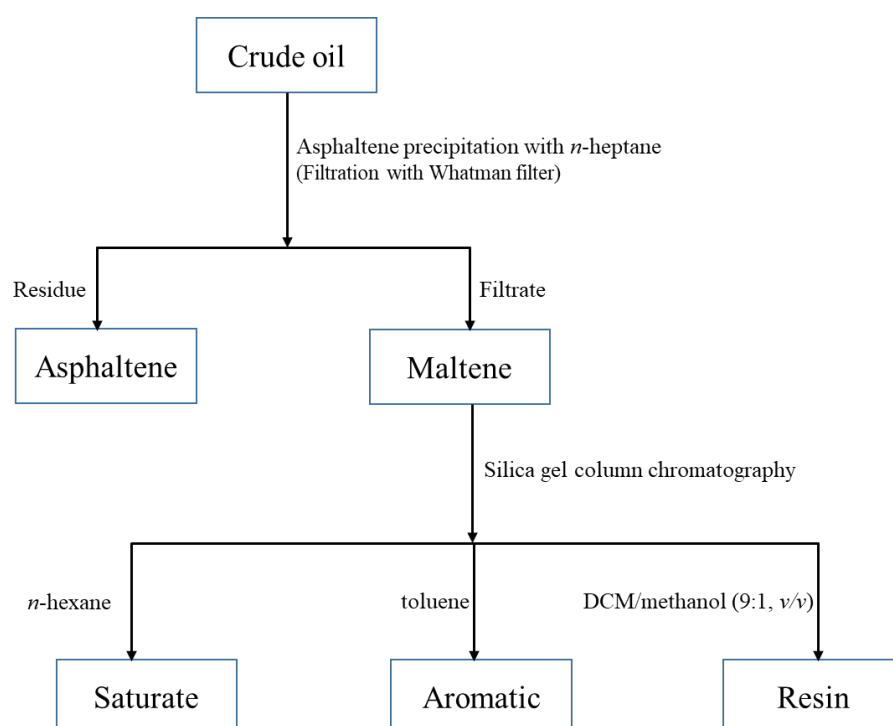


Figure 2.3: SARA fractionation scheme

2.5.2.2 Biodegradation of saturate fraction

Saturate fraction (0.1 %) was added to culture medium without bacteria (Control sample) and with bacteria. Culture media were incubated at 30 °C and 50 rpm. Experiments were stopped at day 0, 3, and 5 to monitor residual hydrocarbons, extra- and intracellular metabolites and protein concentration as described before.

2.5.3 Determination of protein concentration in culture

Ten microliters of 10 % SDS was added to 1 mL of culture and incubated at 90 °C for 2 min to solubilize proteins. Insoluble cell debris were removed by centrifugation at 13,000 rpm at room temperature. Protein concentration in the supernatant was determined using the Enhanced Protocol of Pierce™ BCA Protein Assay Kit (ThermoFisher Scientific, Rockford, IL), with bovine serum albumin (BSA) as standard.

2.5.4 GC-FID for residual hexadecane analysis

Five millilitres of *n*-hexane containing 0.1 % *n*-dodecane as internal standard were added to treatments (5 mL) to extract the residual *n*-hexadecane. The mixture was agitated at 400 min⁻¹ for 20 min. The organic phase was separated from the aqueous phase by freezing at -20 °C and analysed with GC-FID. In splitless mode, 1 µL sample was introduced into the GC-FID (6850 network GC system, Agilent Technologies, Santa Clara, CA) fitted with a HP-1 column (30 m × 0.320 mm × 0.25 µm i.d.) and nitrogen as carrier gas. The temperature program was: initial temperature: 50 °C, gradient at 20 °C /min to 130 °C, 1.50 °C /min to 150 °C, 4 °C /min to 172 °C held for 5 min.

2.5.5 GC-MS for residual saturate hydrocarbon analysis

An equal volume of *n*-hexane containing 0.1% deuterated dodecane as internal standard was added to media for extraction of residual saturated hydrocarbons. The mixture was agitated at 400 min⁻¹ for 20 min. The organic phase was separated from the aqueous phase by freezing at -20 °C and analysed in splitless mode using GC-MS (Thermo Scientific™ TRACE™ 1300 Series GC System, ThermoFisher Scientific, Illkirch-Graffenstaden, France) in EI ionization mode. The GC was fitted with a Zebron ZB-624_{PLUS} column (Phenomenex, Le Pecq, France) (30 m × 0.250 mm × 1.40 µm i.d.) and helium as carrier gas. The temperature program was: initial temperature: 50 °C held for 1 min, gradient at 20 °C /min to 150 °C, 10 °C /min to 250 °C, 15 °C /min to 300 °C held for 5.6 min. Chromeleon™ Chromatography Data System (CDS) software was used for data treatment. The obtained values were normalized against those of abiotic controls.

2.5.6 Sampling extracellular and intracellular metabolites

The culture was centrifuged at 15,300 *g* for 10 min. The obtained supernatant was filtered through 0.22 µm sterile Millex® syringe-driven filters (Merck Millipore, Darmstadt, Germany), and collected for extracellular metabolite screening. Likewise, the pelleted cells obtained after centrifugation were washed with miliQ water and sonicated for 2 min. The mixture after sonication

were extracted with 50 % cold acetone to precipitate proteins, and centrifuged at 14,000 rpm for 10 min at 4 °C. The clear supernatants were collected for intracellular metabolite screening.

2.5.7 LC-MS/MS for untargeted screening of metabolites

The chromatographic system used was an ultimate 3000 RSLC system (ThermoFisher Scientific, Germering, Germany), and the detection was ensured by a Q Exactive Plus high-resolution mass spectrometer (ThermoFisher Scientific, Bremen, Germany) operated in negative mode. A 10 µL aliquot was analyzed using Accucore™ C-18 column (150×2.1mm, 2.6µm, ThermoFisher Scientific). The flow rate was 0.45 mL/min, column temperature was 45 °C and the autosampler temperature was 5 °C. The mobile phase was (A) 10 mM ammonium acetate and (B) methanol (99.9 %). The LC separation was carried out with the following gradient: 0-1 min, 10 % B; 1-15 min, 10 to 95 % B; 15-18 min, 95 % B; 18-20 min, 10 % B. The resolution for MS¹ and MS² scans were set to 70,000 and 35,000, respectively, with mass range of 100 - 1000 *m/z*. Data processing was carried out using Compound Discoverer 2.1™ software (ThermoFisher Scientific, Waltham, MA). The software was fed with raw data from LC-MS/MS system, which was analyzed with a workflow and study factors illustrated in Figure S1 (supplementary data). Finally, Chempider and mzCloud databases were consulted to assign annotation accordingly.

2.5.8 LC-MS³ for structural elucidation of metabolites

Targeted analysis for extracellular metabolites were carried out using the Ultimate 3000 RSLC system coupled to Orbitrap Fusion Lumos Tribrid mass spectrometer (ThermoFisher Scientific, Waltham, MA). The same column, chromatographic conditions and ionization mode used in the untargeted screening were applied. Two fragmentation modes, collision-induced dissociation (CID) and higher-energy C-trap dissociation (HCD) were applied at collision energies ranging from 40 - 100.

2.5.9 Quantification of hydroxyhexadecanoic acid isomers

Calibration curve was prepared with 16-hydroxyhexadecanoic acid to quantify hydroxyhexadecanoic acid isomers detected as extracellular metabolites. The same column, chromatographic conditions and ionization mode used in the untargeted screening were applied.

2.6 Biofilm assays

2.6.1 Biofilm formation on liquid hydrophobic substrates

Quantification of biofilms grown at the interface between the liquid substrates (*n*-hexadecane and *n*-octadecane) and the aqueous phase was carried out in 100 mL bottles in 10 mL IMM containing

0.2 % substrate. After incubation, cultures were filtered through a nylon membrane of 33 μm porosity (Nitex[®]) using a vacuum pump. The biofilm retained on the filter was stained with 400 μL of 0.1 % crystal violet for 3 min, then washed with 10 ml of water. The dye was extracted with 10 mL of 10 % acetic acid, 50 % ethanol and 40 % water and absorbance of the resultant supernatant was read at 595 nm after 10-fold dilution. To compare planktonic and biofilm biomass measurement, the relationship between crystal violet absorbance at 595 nm and $\text{OD}_{600\text{nm}}$ was established for each strain. One microlitre of bacterial culture with known $\text{OD}_{600\text{nm}}$ (0, 0.25, 0.50, 0.75 and 1.00) were centrifuged at 13,000 rpm. The pelleted cells obtained were stained with 400 μL of 0.1 % crystal violet and incubated at room temperature for 3 minutes. Then, the cells were washed twice with 1 mL Milli-Q water. Cells retain the crystal violet and were decolorized with 1 mL solution of 10 % acetic acid and 50 % ethanol. The absorbance of the resultant supernatant was read at 595 nm after 10-fold dilution.

2.6.2 Biofilm formation as a mechanism to utilize *n*-hexadecane

A 6-well microplate with a Thincert[™] culture inserts having a transparent membrane filter of 0.4 μm porosity (Greiner Bio-One, Germany) was used. 3 ml of culture in exponential phase that was re-suspended in IMM at an $\text{OD}_{600\text{nm}}$ of 0.05 was added to the filters and wells. The filter compartments were supplemented with 0.2 % *n*-hexadecane and covered with parafilm to avoid evaporation into the wells. $\text{OD}_{600\text{nm}}$ of culture in the filter compartments and wells was read after 72 h. Two control experiments (A and B) were set up in parallel. Control A was to ensure bacteria could not cross the filters' membrane into the wells. It had cultures in the filter compartments supplemented with 0.4 % propionate while the wells had IMM with 0.4 % propionate and no bacteria. Control B had IMM in the filter compartments supplemented with 0.2 % *n*-hexadecane but no bacteria while the wells had bacteria and no carbon source. This was to know if bacteria growing in the wells were using soluble metabolites secreted by the biofilm formed in filters compartment.

2.6.3 Biofilm formation on solid hydrophobic substrates

Biofilm formation on solid substrates (alkane: paraffin, a wax ester: hexadecyl hexadecanoate and a triglyceride: tristearin) was assayed in IMM in 24-well polystyrene microplates with the wells coated with the substrates as previously described [202]. The plates were inoculated with 1 mL of culture in exponential phase re-suspended in IMM at an $\text{OD}_{600\text{nm}}$ of 0.1. After incubation, the culture medium was aspirated from the wells and used to quantify the planktonic cells by reading the OD at 600nm. The wells were washed twice with 1 mL of IMM. Biofilms adhering to the wells were stained at room temperature for 3 min with 400 μL of 0.1 % crystal violet. Then, each well was

washed twice with 1 mL water the crystal violet was eluted with 1 mL solution (10 % acetic acid, 50 % ethanol and 40 % water) and absorbance of the resultant supernatant was read at 595 nm after 10-fold dilution.

2.6.4 Microbial adhesion to hydrocarbon (MATH) assay

MATH assays were performed as described elsewhere [203]. In brief, 1 mL of buffer-washed aqueous cell suspensions obtained after growth on either propionate or *n*-hexadecane was mixed with an equal volume of *n*-hexadecane. After 2 min of vortexing, the mixture was left until the phases separated. OD of the aqueous phase was measured at 600 nm, and percentage of cell adherence was calculated from difference in OD before and after vortex.

2.6.5 Optical sectioning microscopy (ApoTome) of biofilm

Biofilms were grown on microscopic slides coated with paraffin and hexadecyl hexadecanoate immersed in 20 mL of IMM at 30 °C for 40 h. The slides were washed with IMM stained with 10 µM SYTO 9 (Invitrogen) and incubated for 20 min in the dark. Biofilms on the slides were covered with a coverslip and observed under a Zeiss AxioObserver Z1 inverted microscope equipped with an Apotome to perform optical sectioning, an oil immersion Plan-Apochromat 63x, NA 1.4 objective and the following filter sets: EX BP 470/40, FT 495, EM BP 525/50. Images were analysed using Zen 2.6 (blue edition) software. Biofilms were characterized using COMSTAT 2.1 (www.comstat.dk) as a plugin to ImageJ [204,205].

2.6.6 Screening for biosurfactant production

Strains were incubated in IMM with 1% (*v/v*) *n*-hexadecane at 30 °C and 50 rpm for 96 h. Thereafter, the culture was centrifuged at 15,300 *g* for 10 min, and the obtained supernatant was filtered through 0.22 µm sterile Millex[®] syringe-driven filters. Biosurfactant production was screened by drop collapse test, oil displacement test, and emulsification index (E_{24}) according to the methods described by Datta *et al.* [206]. Water and cell-free medium served as negative control while 1% SDS was used as the positive control. Furthermore, biosurfactant production was evaluated by measuring the interfacial tension (IFT) between culture supernatant and *n*-hexadecane as a function of time using a Trakcer pendant drop tensiometer (Interfacial Technology Concept, Quimper, France) [207].

Chapter three

Degradation of long-chain alkanes through biofilm formation by bacteria isolated from oil-polluted soil

3. Degradation of long-chain alkanes through biofilm formation by bacteria isolated from oil-polluted soil

3.1 Introduction

The approaches to clean up petroleum hydrocarbon pollution have progressively moved towards the more eco-friendly and sustainable intrinsic and enhanced bioremediation techniques [3,208]. Bioremediation of hydrocarbon depends essentially on microbial metabolism that leads to the degradation of hydrocarbons into carbon dioxide and water. Consequently, the metabolic potential of microorganisms [95], and the isolation of hydrocarbonoclastic microbes [106] are essential for bioremediation applications. This have driven the continual search for microorganisms with the appropriate metabolic capabilities for bioremediation application [16–18].

Microorganisms are considered as nature's ultimate scavenger due to their ability to acquire carbon and energy from numerous compounds [25]. Bacteria are capable of degrading hydrocarbons because of their energy and carbon needs for growth and reproduction, as well as surviving the stress and toxicity caused by hydrocarbons [209]. Petroleum polluted environment provide the ideal repository for isolating bacteria with capabilities to degrade hydrocarbons [26–28]. This is because the presence of hydrocarbons in an environment influences the diversity of the bacterial community [29–31]. Bacterial species belonging to the phyla *Proteobacteria*, *Actinobacteria*, *Acidobacteria*, *Bacteroidetes*, *Deinococcus-Thermus* and *Firmicutes* etc. have been reported of degrading petroleum hydrocarbons using diverse metabolic pathways that are mediated by specific enzyme system [9,209,210]. Most bacteria can efficiently degrade certain fractions of petroleum and classes of hydrocarbon. For instance, *Nocardia soli* Y48 and *Rhodococcus erythropolis* YF28-1 were reported to grow on *n*-alkanes (C₈-C₃₆) portion of crude oil [211], while *Bacillus cereus* utilized mono- and polyaromatic hydrocarbons as carbon source [212]. This could be attributed to bacteria strains having different catabolic enzymes, the toxic effects of the hydrocarbons, and in particular, the bioavailability and bioaccessibility to hydrocarbons.

Alkanes are major component of petroleum, and their solubility in water and biodegradability decreases with an increase in molecular weight. In aerobic degradation, alkanes are generally activated by enzymatic incorporation of molecular oxygen or in rare cases, peroxides [127] through terminal or sub-terminal oxidation to yield the corresponding primary or secondary alcohols. The primary alcohols are oxidized into aldehydes, which are further converted into fatty acids or ω -hydroxy fatty acids and dicarboxylic acids by ω -hydroxylation [41,129]. Ketones are generated from oxidation of the secondary alcohols and are further converted to esters and hydrolysed into fatty

acids. The fatty acids are converted into acetyl-CoA through the β -oxidation pathway and further metabolized in the tricarboxylic acid cycle to generate CO₂ and reducing equivalents that are channelled into the respiratory chain to produce energy and H₂O [127]. Chemical characterization of the metabolites of hydrocarbon biodegradation is very essential [213]. It gives an insight into the biochemical processes within and outside the cell during the biodegradation process. Such insights are important for the elucidation of hydrocarbon degradation mechanisms and pathways and design of more efficient bioremediation strategies. Moreover, characterizing extracellular metabolites provides crucial information about the bacterial response to the surrounding environment [214]. Metabolite profiling has been intensified in recent years due to the continuous development of robust analytical methods and instrumentation, especially mass spectrometry and chromatography, for characterizing compounds in complex matrices [149].

The low water solubility of hydrocarbons limits their accessibility and availability to bacteria as substrate. Hence, this necessitates specific assimilation mechanisms. Bacteria produce surface-active compounds known as biosurfactants to enhance the solubility and availability of hydrocarbons through emulsification, thereby facilitating hydrocarbons uptake and degradation [70]. Biosurfactants are amphipathic molecules that constitute heterogeneous group of biomolecules such as glycolipids, lipoproteins complexes and lipopolysaccharide-protein complexes. Recent studies have shown how biosurfactants promote hydrocarbon emulsification and solubility during biodegradation [76–80]. Another significant mechanism adopted by bacteria to overcome the poor solubility of hydrocarbons is biofilm formation. A Biofilm is referred to as microbial aggregates that are often embedded in a self-produced matrix of extracellular polymeric substances (EPS) and adhere to each other and/or to a surface [93]. The EPS serves as building material for the three-dimensional architecture of the biofilm and anchoring material for attachment to surfaces [120]. Biofilm formation during hydrocarbon degradation is an adaptation strategy and it is typically characterized by attachment of cells to hydrocarbons at the hydrocarbon-water interface [94–96]. Attachment to hydrocarbons relies on bacterial cell surface properties such as hydrophobicity, charge, roughness and extracellular appendages [96]. The adhesion of bacteria to the oil-water interface effectively enhances the rate of hydrocarbon assimilation by reducing the distance for mass transfer [108]. Additionally, the cells and secreted solubilisation factors such as exoenzymes, biosurfactants or proteins, that play important roles in hydrocarbon assimilation are retained and accumulated within the EPS matrix [96,122]. This retentive property of the matrix localizes and stabilizes solubilisation and enzymatic activities within the matrix and thus increase mass transfer of hydrocarbons toward the cell for degradation. Dasgupta *et al.* [94] reported that biofilm-forming

Pseudomonas strains degraded crude oil more readily and extensively than planktonic strains. Similarly, biofilm of *Stenotrophomonas acidaminihila* NCW-702 was able to degrade PAHs more efficiently than planktonic cells [98]. Recently, the effectiveness of bioaugmentation with biofilm-forming bacteria was reported [99]. Moreover, biofilm-forming bacteria revolves between planktonic growth and biofilm formation. When biofilm formation at the hydrocarbon-water interface becomes fully matured, cells begin to strategically detach from the biofilm in order to colonize new hydrocarbon surfaces [108]. Biofilm formation and planktonic-biofilm transition are complex and highly regulated processes [100,101].

The aim of this study was to study the mechanism of hydrocarbon degradation in soil by investigating the ability of bacterial strains isolated from a crude oil polluted soil by enrichment to utilize long chain alkanes through biofilm formation.

3.2 Materials and methods

All chemicals used in this study were of analytical grade and purchased from Merck (www.sigmaaldrich.com). Water produced from a MilliQ Purification System (ELGA[®], UK) was used throughout.

3.2.1 Sampling crude oil-polluted soil

The soil sample was collected using a soil auger at 15 cm depth in a Bodo West crude oil contaminated site (4° 37' 18.1" N, 7° 15' 53.4" E) in Ogoniland, Rivers State, Nigeria and stored in a clean plastic container. Soil pH was measured by suspending the soil in water (1:5 w/v). The slurry was vortexed for 1 min and let to settle down. pH was read with a pH meter (Cyberscan 510, EUTECH Instruments, Singapore) at 25 °C. The pH of the soil sample determined the pH of the enrichment media.

3.2.2 Isolation of bacterial strains by enrichment on crude oil

3.2.2.1 Media composition

Enrichment was carried out at pH 8.0 because the soil sample had an alkaline pH (8.3). Cultivations were carried out using four media that were sterilized by autoclaving at 121 °C and 15 psi for 20 min:

- (i) Rich Complete Medium (RCM) (g/L): casein (2.0), glycerol (2.5), asparagine (0.10), sodium propionate (4.0), K₂HPO₄ (0.50), MgSO₄.7H₂O (0.10), FeSO₄.7H₂O (0.001).
- (ii) Rich Incomplete Medium (RIM) as RCM but without casein and glycerol.

- (iii) Complete Mineral Medium (CMM) (g/L): starch (10.00), casein (0.30), NaNO₃ (0.85), KH₂PO₄ (0.56), Na₂HPO₄ (0.86), K₂SO₄ (0.17), MgSO₄·7H₂O (0.37), CaCl₂·6H₂O (0.007) and 2 mL of trace element solution: ZnCl₂ (0.042), MnCl₂·4H₂O (0.05), H₃BO₃ (0.30), CuCl₂·2H₂O (0.002), Na₂MoO₃·2H₂O (0.018), CoCl₂·6H₂O (0.19), FeSO₄·7H₂O (1.1), NiCl₂·6H₂O (0.024).
- (iv) Incomplete Mineral Medium (IMM) as CMM without starch and casein.

3.2.2.2 Enrichment conditions

One gram of soil sample was suspended into 10 mL of culture media supplemented or not with 1 % (v/v) filter-sterilized Congo Bilondo crude oil and incubated at 20 °C, 27 °C and 35 °C at 75 rpm for 20 days. Thereafter, 1 ml aliquot of the enrichment cultures was transferred into fresh corresponding media and incubated for 14 days.

3.2.2.3 Isolation of bacteria

Aliquots (10 µL and 100 µL) of the enrichment cultures were spread on the corresponding 1.5 % agar media and incubated for 3 days at the same temperature as that used for the enrichment. For enrichments grown with the incomplete media, RIM and IMM agar media were supplemented with glucose (5 g/L) and yeast extract (5 g/L) or peptone (5 g/L) and yeast extract (5 g/L) or lactate (20 mM), acetate (20 mM) and yeast extract (5 g/L) as carbon source. Lysogeny broth (LB) agar, RCM agar and CMM agar were used for enrichments grown with RCM and CMM. Isolates were purified by two successive streaking on agar plates. The purity of isolates was confirmed by the morphological homogeneity of the colonies on agar plates, the presence of only one morphotype under the microscope and detection of a single 16S rRNA gene PCR product in the 16S rRNA genes sequencing chromatograms.

3.2.2.4 Screening of isolates on hydrocarbons

To identify isolates capable of utilizing a hydrocarbon, 5 mL IMM supplemented with 0.2 % (v/v) crude oil and 0.2 % (v/v) of a 50/50 mixture of *n*-decane and *n*-hexadecane was inoculated with 1 µL loopful cell suspension of each isolate and incubated at 30 °C and 75 rpm. The isolates were also incubated in 5 mL IMM supplemented with propionate (4 g/L) and asparagine (0.1 g/L) to serve as a positive control. Growth was monitored every 72 h by optical density (OD) at 600 nm using a spectrophotometer (Spectronic Camspec, UK). LB media (5 mL) was each inoculated with 1 µL loopful of isolates having the capability to utilize hydrocarbons and incubated at 30 °C and 75 rpm for 48 h. Then, aliquots (1.5 mL) of cultures were cryopreserved at -80 °C using 0.5 mL of 50 % glycerol while 250 µL were used for DNA extraction to identify the isolates.

3.2.3 Molecular biology analysis

3.2.3.1 Genomic DNA extraction and Illumina sequencing

DNA was extracted from the soil sample (0.25 g) and enrichment cultures (250 μ L) using DNeasy® Power Soil® DNA Isolation Kit (Qiagen, Hilden, Germany) following the manufacturer's instructions. The extracted DNA samples were sequenced at MR DNA (www.mrdnalab.com, Shallowater, TX) on MiSeq following the manufacturer's guidelines. In summary, the V1-V3 variable region of 16S rRNA gene were amplified using the primers 8F-519R [200] with barcode on the forward primer in a 30 cycle PCR. PCR amplifications were performed using the HotStarTaq Plus Master Mix Kit (Qiagen, Germantown, MD) under the following conditions: 94 °C for 3 min, followed by 30 cycles of 94 °C for 30 s, 53 °C for 40 s and 72 °C for 1 min, followed by a final elongation step at 72 °C for 5 min. After amplification, PCR products were checked in 2 % agarose gel to determine the success of amplification and the relative intensity of bands. Multiple samples were pooled together in equal proportions using MR DNA's proprietary molarity model and purified using calibrated Ampure XP beads, before preparing the illumina DNA library. Sequence data were processed using version 2019_05 of MR DNA taxonomic analysis pipeline and database. Operational taxonomic units (OTUs) were defined by clustering at 3% divergence (97% similarity). Finally, OTUs were taxonomically classified using BLASTn against a curated database derived from RDPII and NCBI (<http://rdp.cme.msu.edu>, www.ncbi.nlm.nih.gov). The 16S rRNA gene sequences from the soil and enrichment samples were deposited to the NCBI Short Read Archive (SRA) under the BioProject accession number PRJNA883074.

3.2.3.2 Pacbio Sequel for bacterial identification

DNA extracted from isolates having the capability to utilize hydrocarbons were sequenced for identification. The 16S rRNA gene PCR primers, 8F-1492R, with barcode on the forward primer were used for amplification. After amplification, multiple samples were pooled together in equal proportions and purified using Ampure PB beads (Pacific Biosciences). SMRTbell libraries (Pacific Biosciences) were prepared and sequenced at MR DNA on the PacBio Sequel following the manufacturer's guidelines. After completion of initial DNA sequencing, each library undergoes a secondary analysis, Circular Consensus Sequencing (CCS), using PacBio's CCS2 algorithm. The CCS2 algorithm aligns the forward 'FWD' and reverse 'REV' subreads from each template to generate consensus sequences, thereby correcting the stochastic errors generated in the initial analysis. Thereafter, sequence data was processed using version 2019_08 of MR DNA taxonomic analysis pipeline and database. Nucleotide sequence of 16S rRNA gene were deposited at NCBI

GenBank under the GenBank accession numbers ON383530 - ON383535. 16S rRNA sequences of type strains were obtained from EzBioCloud (www.ezbiocloud.net) for evolutionary analyses conducted in MEGA X.

3.2.4 Biodegradation of *n*-hexadecane

Five millilitres of IMM inoculated with 1 μ L loopful of growing cell suspension of the selected bacteria and supplemented with *n*-hexadecane (0.1% v/v) as carbon source was used for biodegradation study. In parallel, 0.4 % (w/v) propionate as sole source of carbon was used as positive control while a medium supplemented with *n*-hexadecane with no inoculation served as negative control. Three replicates were incubated at 30 °C and 50 rpm. Experimental replicates of treatments and controls were sacrificed at day 0, 3, 6 and 10 to monitor protein concentration, residual *n*-hexadecane, and extracellular metabolites.

3.2.4.1 Determination of protein concentration in culture

Ten microliters of 10 % SDS was added to 1 mL of culture and incubated at 90 °C for 2 min to solubilize proteins. Insoluble cell debris were removed by centrifugation at 13,000 rpm at room temperature. Protein concentration in the supernatant was determined using the Enhanced protocol of Pierce™ BCA Protein Assay Kit (ThermoFisher Scientific, Rockford, IL), with bovine serum albumin (BSA) as standard.

3.2.4.2 GC-FID for residual hexadecane analysis

Five millilitres of *n*-hexane containing 0.1 % *n*-dodecane as internal standard were added to treatments (5 mL) to extract the residual *n*-hexadecane. The mixture was agitated at 400 min⁻¹ for 20 min. The organic phase was separated from the aqueous phase by freezing at -20 °C and analysed with GC-FID. In splitless mode, 1 μ L sample was introduced into the GC-FID (6850 network GC system, Agilent Technologies, Santa Clara, CA) fitted with a HP-1 column (30 m \times 0.320 mm \times 0.25 μ m i.d.) and nitrogen as carrier gas. The temperature program was: initial temperature: 50 °C, gradient at 20 °C /min to 130 °C, 1.50 °C /min to 150 °C, 4 °C /min to 172 °C held for 5 min.

3.2.4.3 Sampling extracellular metabolites

The culture was centrifuged at 15,300 *g* for 10 min. The obtained supernatant was filtered through 0.22 μ m sterile Millex® syringe-driven filters (Merck Millipore, Darmstadt, Germany), and collected for extracellular metabolite screening by LC-MS/MS.

3.2.4.4 LC-MS/MS for untargeted screening of extracellular metabolites

The chromatographic system used was an ultimate 3000 RSLC system (ThermoFisher Scientific, Germering, Germany), and the detection was ensured by a Q Exactive Plus high-resolution mass spectrometer (ThermoFisher Scientific, Bremen, Germany) operated in negative mode. A 10 μ L aliquot was analyzed using Accucore™ C-18 column (150 \times 2.1mm, 2.6 μ m, ThermoFisher Scientific). The flow rate was 0.45 mL/min, column temperature was 45 °C and the autosampler temperature was 5 °C. The mobile phase was (A) 10 mM ammonium acetate and (B) methanol (99.9 %). The LC separation was carried out with the following gradient: 0-1 min, 10 % B; 1-15 min, 10 to 95 % B; 15-18 min, 95 % B; 18-20 min, 10% B. The resolution for MS¹ and MS² scans were set to 70,000 and 35,000, respectively, with mass range of 100 - 1000 m/z . Data processing was carried out using Compound Discoverer 2.1™ software (ThermoFisher Scientific, Waltham, MA). The software was fed with raw data from LC-MS/MS system, which was analyzed with a workflow and study factors illustrated in Figure 3.1 (supplementary data). Finally, Chempider and mzCloud databases were consulted to assign annotation accordingly.

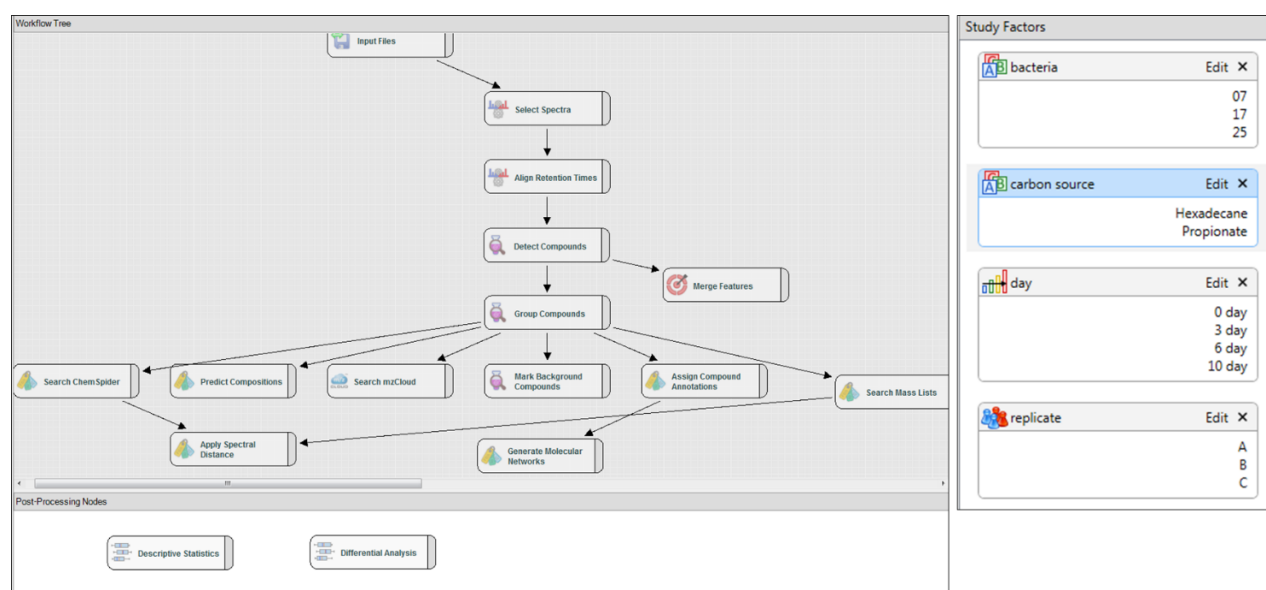


Figure 3.1: Workflow tree of untargeted screening of *n*-hexadecane metabolites using Compound Discoverer 2.1™. The software detects each chromatographic peak from the data batch of HPLC-MS/MS. A peak equals signal at a given m/z ratio and a retention time, all within a Gaussian shape.

3.2.4.5 LC-MS³ for structural elucidation of extracellular metabolites

Targeted analysis for extracellular metabolites were carried out using the Ultimate 3000 RSLC system coupled to Orbitrap Fusion Lumos Tribrid mass spectrometer (ThermoFisher Scientific, Waltham, MA). The same column, chromatographic conditions and ionization mode used in the

untargeted screening were applied. Two fragmentation modes, collision-induced dissociation (CID) and higher-energy C-trap dissociation (HCD) were applied at collision energies ranging from 40 - 100.

3.2.4.6 Quantification of extracellular metabolites

Calibration curve was prepared with 16-hydroxyhexadecanoic acid to quantify hydroxyhexadecanoic acid isomers detected as extracellular metabolites. The same column, chromatographic conditions and ionization mode used in the untargeted screening were applied.

3.2.5 Biofilm assays

3.2.5.1 Biofilm formation on liquid alkanes

Quantification of biofilms grown at the interface between the liquid substrates (*n*-hexadecane and *n*-octadecane) and the aqueous phase was carried out in 100 mL bottles in 10 mL IMM containing 0.2 % substrate. After incubation, cultures were filtered through a nylon membrane of 33 μm porosity (Nitex[®]) using a vacuum pump. The biofilm retained on the filter was stained with 400 μL of 0.1 % crystal violet for 3 min, then washed with 10 ml of water. The dye was extracted with 10 ml of 10 % acetic acid, 50 % ethanol and 40 % water and absorbance of the resultant supernatant was read at 595 nm after 10-fold dilution.

3.2.5.2 Biofilm formation on solid alkanes and lipids

Biofilm formation on solid substrates (alkane: paraffin, a wax ester: hexadecyl hexadecanoate and a triglyceride: tristearin) was assayed in IMM in 24-well polystyrene microplates with the wells coated with the substrates as previously described [202]. The plates were inoculated with 1 mL of culture in exponential phase re-suspended in IMM at an $\text{OD}_{600\text{nm}}$ of 0.1. After incubation, the culture medium was aspirated from the wells and used to quantify the planktonic cells by reading the OD at 600nm. The wells were washed twice with 1 mL of IMM. Biofilms adhering to the wells were stained at room temperature for 3 min with 400 μL of 0.1 % crystal violet. Then, each well was washed twice with 1 mL water the crystal violet was eluted with 1 mL solution (10 % acetic acid, 50 % ethanol and 40 % water) and absorbance of the resultant supernatant was read at 595 nm after 10-fold dilution. To compare planktonic and biofilm biomass measurement, the relationship between crystal violet colouration at 595 nm and $\text{OD}_{600\text{nm}}$ was established for each strain. One microlitre of bacterial culture with known $\text{OD}_{600\text{nm}}$ (0, 0.25, 0.50, 0.75 and 1.00) were centrifuged at 13,000 rpm. The pelleted cells obtained were stained with 400 μL of 0.1 % crystal violet and incubated at room temperature for 3 minutes. Then, the cells were washed twice with 1 mL Milli-Q

water. Cells retain the crystal violet and were decolorized with 1 mL solution of 10 % acetic acid and 50 % ethanol. The absorbance of the resultant supernatant was read at 595 nm after 10-fold dilution.

3.2.5.3 Microbial adhesion to hydrocarbon (MATH) assay

MATH assays were performed as described elsewhere [203]. In brief, 1 mL of buffer-washed aqueous cell suspensions obtained after growth on either propionate or *n*-hexadecane was mixed with an equal volume of *n*-hexadecane. After 2 min of vortexing, the mixture was left until the phases separated. OD of the aqueous phase was measured at 600 nm, and percentage of cell adherence was calculated from difference in OD before and after vortex.

3.2.5.5 Optical sectioning microscopy (ApoTome) of biofilm

Biofilms were grown on microscopic slides coated with paraffin and hexadecyl hexadecanoate immersed in 20 mL of IMM at 30 °C for 40 h. The slides were washed with IMM stained with 10 µM SYTO 9 (Invitrogen) and incubated for 20 min in the dark. Biofilms on the slides were covered with a coverslip and observed under a Zeiss AxioObserver Z1 inverted microscope equipped with an Apotome to perform optical sectioning, an oil immersion Plan-Apochromat 63x, NA 1.4 objective and the following filter sets: EX BP 470/40, FT 495, EM BP 525/50. Images were acquired using Zen 2.6 (blue edition) software and analyzed using COMSTAT 2.1 (www.comstat.dk) as a plugin to ImageJ [204,205].

3.2.5.6 Screening for biosurfactant production

Strains were incubated in IMM with 1% (*v/v*) *n*-hexadecane at 30 °C and 50 rpm for 96 h. Thereafter, the culture was centrifuged at 15,300 *g* for 10 min, and the obtained supernatant was filtered through 0.22 µm sterile Millex[®] syringe-driven filters. Biosurfactant production was screened by drop collapse test, oil displacement test, and emulsification index (E_{24}) according to the methods described by Datta *et al.* [206]. Water and cell-free medium served as negative control while 1% SDS was used as the positive control. Furthermore, biosurfactant production was evaluated by measuring the interfacial tension (IFT) between culture supernatant and *n*-hexadecane as a function of time using a Trakcer pendant drop tensiometer (Interfacial Technology Concept, Quimper, France) [207].

3.3 Results

3.3.1 Isolation and taxonomic identity of selected strains

The soil sample used for strains isolation, contained a high diversity of bacteria as revealed by 16S rRNA gene sequencing (Figure 3.2). A total of 12 phyla, 33 classes, 62 orders, 127 families, and 250 bacterial genera were detected in the soil sample. *Proteobacteria* (46.01 %) and *Actinobacteria* (31.34 %) constituted major proportion of the phyla while *Chloroflexi* (0.15 %) and *Deinococcus* (0.13 %) were the least abundant. During enrichment, 16S rRNA gene sequencing showed that cultures exhibited high proportion of *Proteobacteria* followed by *Bacteroidetes* and *Firmicutes* (Figure 3.3).

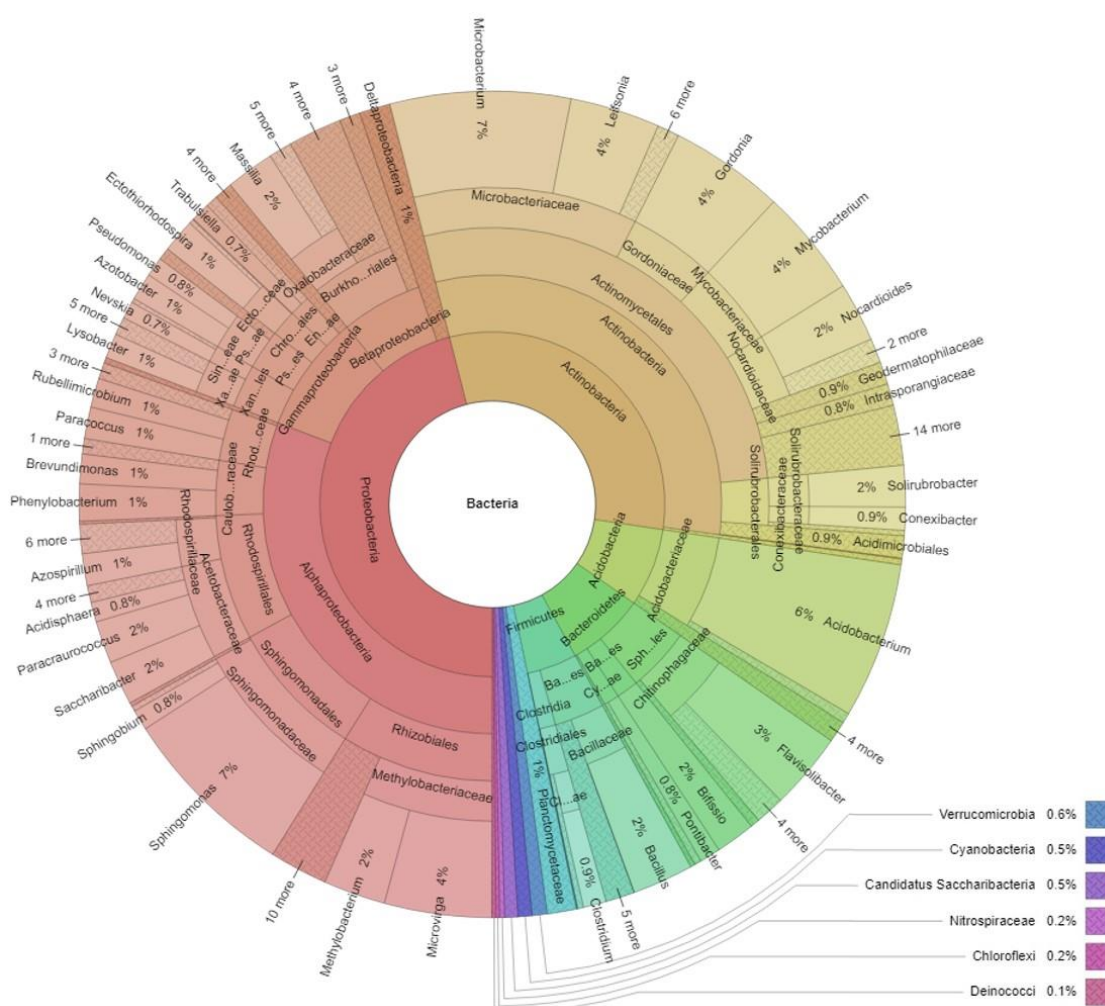


Figure 3.2: Krona chart showing the bacterial diversity in the crude oil contaminated soil sample. The chart illustrates (from the inner core to the exterior) the bacterial diversity across the phyla, class, order, family, and genus. The 16S rRNA gene sequences from the soil was deposited to the NCBI Short Read Archive (SRA) under the BioProject number PRJNA883074 and accession number SRR21708976.

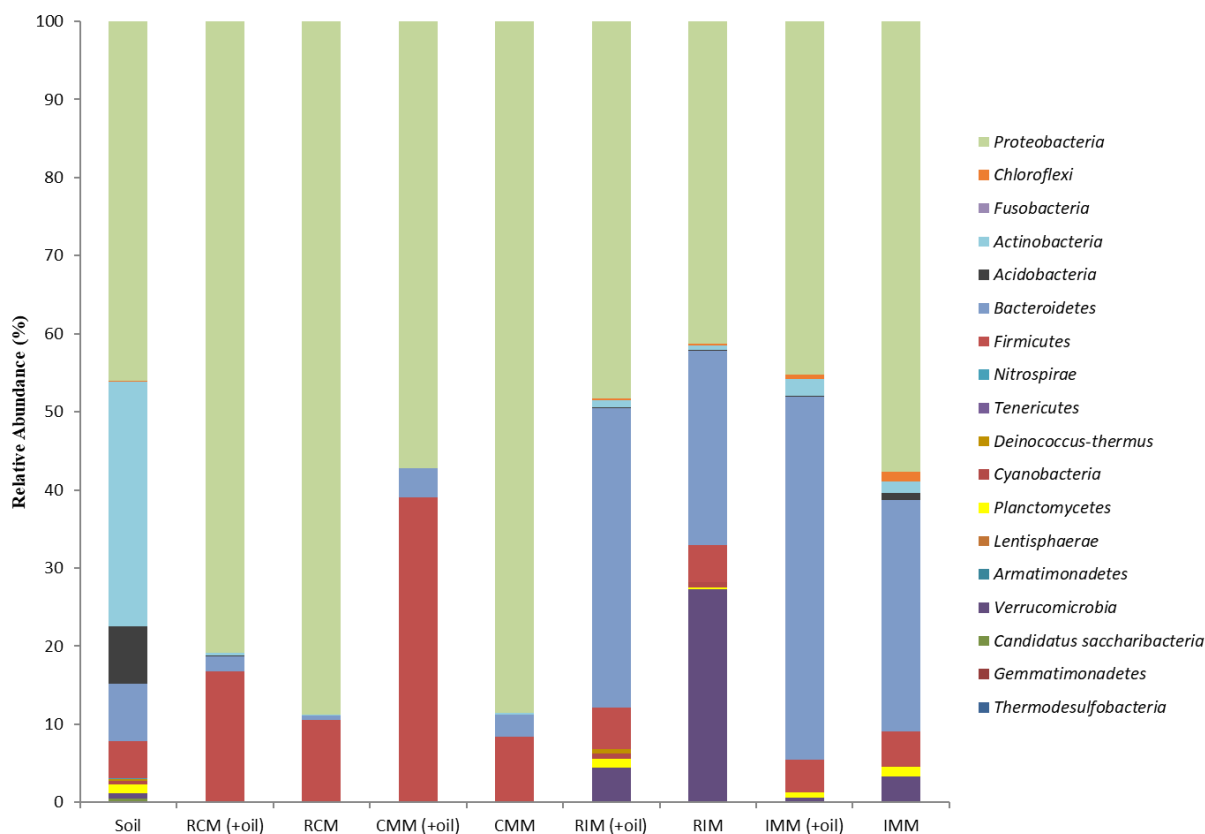


Figure 3.3: Relative abundance of bacterial phyla during soil enrichment carried out using four media with or without 1 % (v/v) filter-sterilized Congo Bilondo crude oil. The 16S rRNA gene sequences from the enrichment samples were deposited to the NCBI Short Read Archive (SRA) under the BioProject number PRJNA883074 and accession numbers SRR21677267 - SRR21677274.

After isolation of bacteria, 95 recovered isolates were screened for growth on 0.2 % (v/v) crude oil and 0.2 % (v/v) of a 50/50 mixture of *n*-decane and *n*-hexadecane. Six strains had the ability to grow on crude oil or the *n*-alkane mixture as sole carbon and energy source. These strains belong to the phyla; *Proteobacteria*, *Actinobacteria* and *Firmicutes* (Figure 3.4). Strains that exhibited the fastest growth, *Novosphingobium* sp. S1, *Gordonia amicalis* S2 and *Gordonia terrae* S5 were selected for further study. The *Novosphingobium* and *Gordonia* genera represented 0.20 % and 4.49 %, respectively, of the total bacteria community found in the soil sample. The *Gordonia* strains characteristically form orange-red circular colonies while *Novosphingobium* sp. S1 forms yellowish circular colonies. The three strains are short rod shaped and non-motile (Figure 3.5).

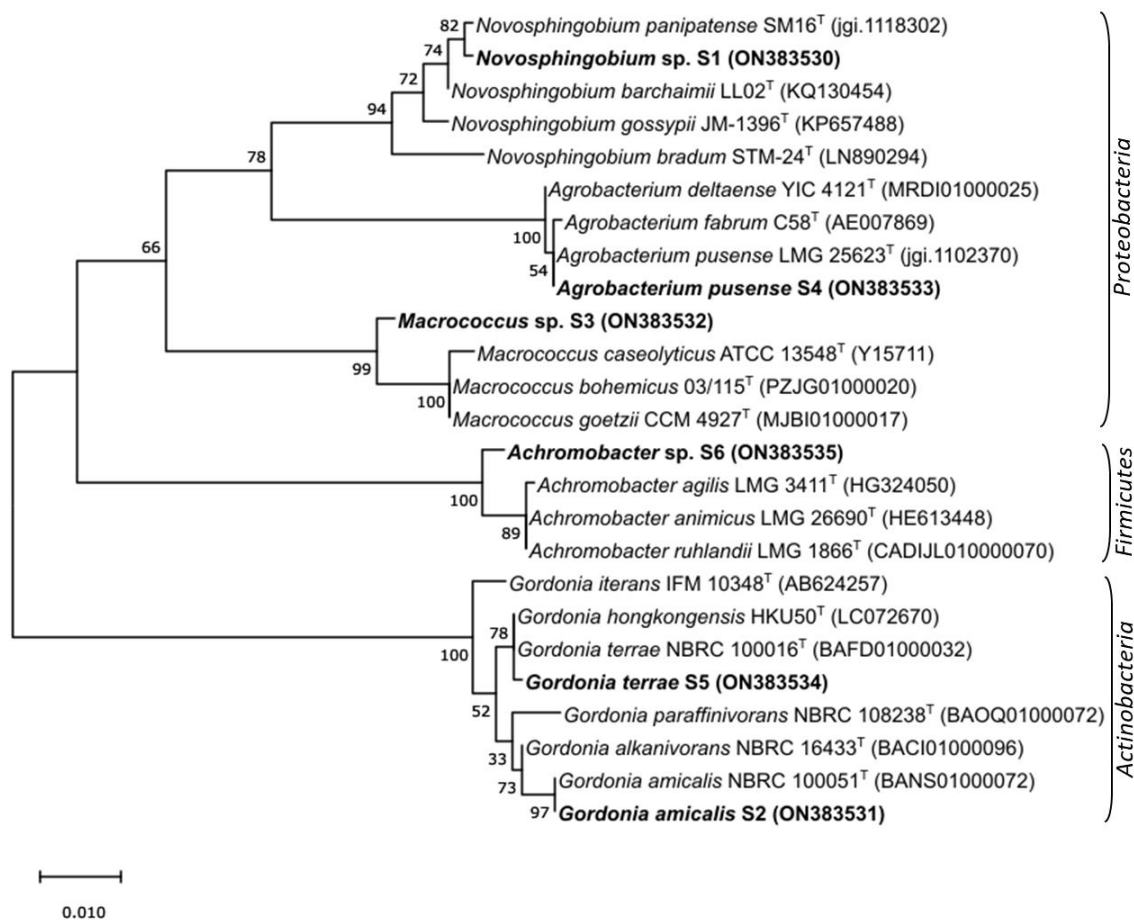


Figure 3.4: Phylogenetic tree, based on 16S rRNA gene sequences, showing the relationships between the isolated strain and closely related representative strains. The tree was constructed by using the Maximum Likelihood method and Jukes-Cantor model. The percentage of replicate trees in which the associated taxa clustered together in the bootstrap test (1000 replicates) are shown next to the branches. The tree is drawn to scale, with branch lengths in the same units as those of the evolutionary distances used to infer the phylogenetic tree.

3.3.2 Biodegradation of *n*-hexadecane

Figure 3.6 shows the removal of more than 70 % of *n*-hexadecane among the three bacteria on day 10. Equally, the increase in bacteria growth, as expressed by protein concentration, correlates with the disappearance of *n*-hexadecane in cultures. This illustrates that *n*-hexadecane served as source of carbon and energy for the bacteria strains. Biofilm formation at the hexadecane-water interface of the culture was observed (Figure 3.7). Turbidity in the aqueous phase was observed only in *Novosphingobium* sp. S1, indicating the presence of planktonic cells. Consequently, studies on the dynamics of biofilm formation by the three strains using various hydrophobic carbon sources were carried out.

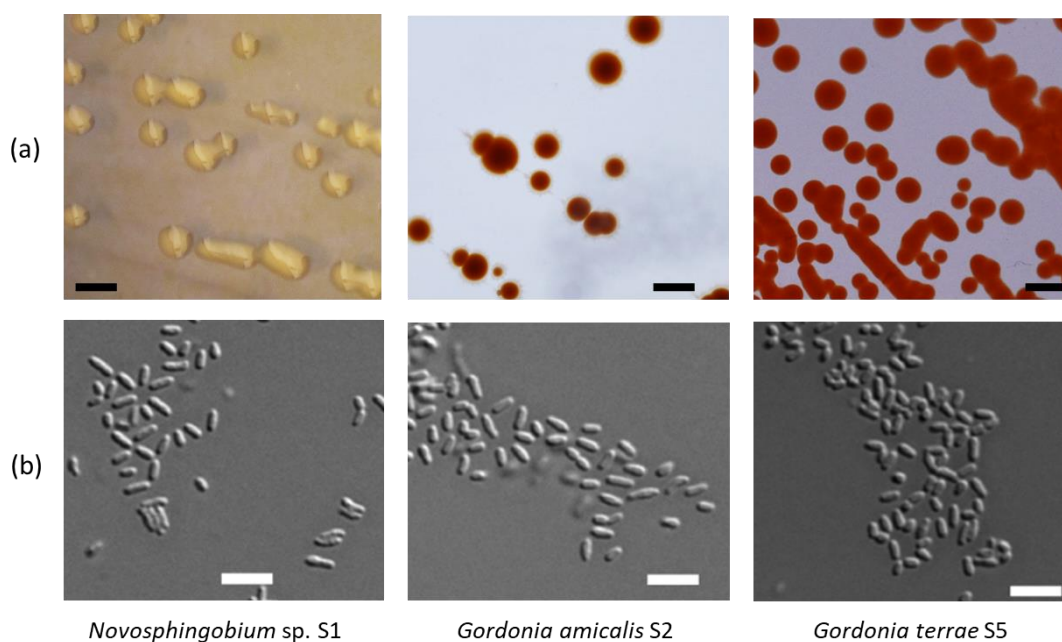


Figure 3.5: (a) Pictures of colonies of the isolated strains; Scale bar = 2 mm. (b) Microscopic images of cells of the isolated strains; Scale bar = 5 μm . Microscopic images were obtained with the Zeiss AxioObserver.Z1/7 microscope with an oil immersion Plan-Apochromat 63x/1.40 DIC M27 objective.

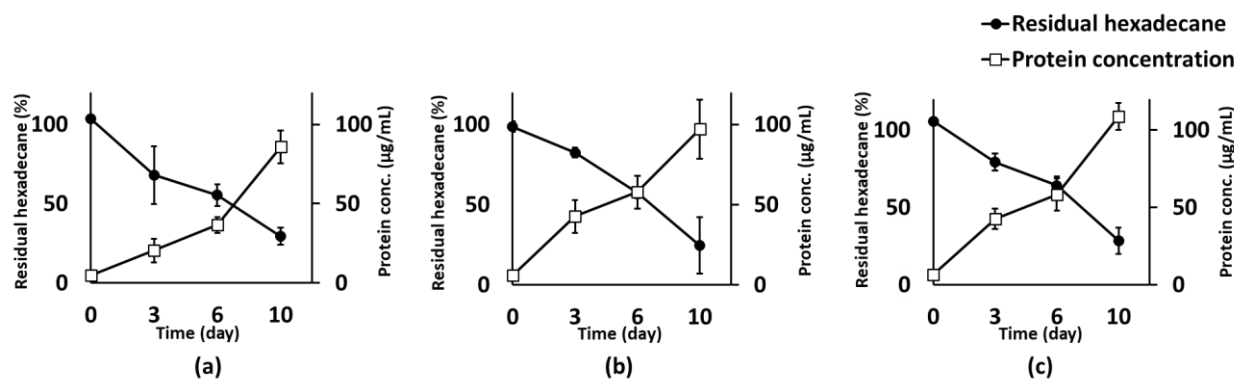


Figure 3.6: Residual *n*-hexadecane and protein concentration in culture media of (a) *Novosphingobium* sp. S1, (b) *Gordonia amicalis* S2 and (c) *Gordonia terrae* S5. A 100 % residual *n*-hexadecane corresponds to 0.1 % (v/v) *n*-hexadecane in culture medium.

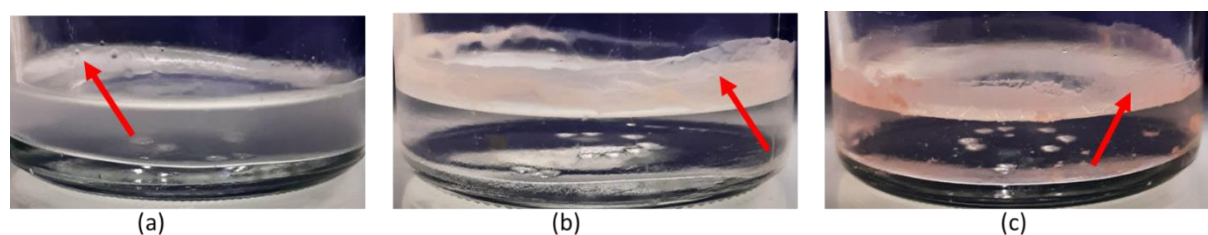


Figure 3.7: Images of oleolytic biofilm formed by (a) *Novosphingobium* sp S1, (b) *Gordonia amicalis* S2 and (c) *Gordonia terrae* S3 on *n*-hexadecane by day 3.

3.3.3 Biofilm formation on hydrocarbons and lipids

To better characterise the mode of growth of the three strains in the presence of alkanes, the biomass in biofilm and in the aqueous phase were quantified during growth. Biofilm biomass was quantified using crystal violet staining (see material and methods) while the planktonic biomass was measured by the OD at 600 nm. To compare planktonic and biofilm biomass measurement, the relationship between crystal violet colouration at 595 nm and OD_{600nm} was established for each strain (Figure 3.8). Biofilm development was studied on *n*-alkanes of different chain lengths: *n*-hexadecane (C₁₆), *n*-octadecane (C₁₈) and paraffin, a mixture of long chain alkanes (>C₁₉ with 94 % > C₂₂). *n*-hexadecane and *n*-octadecane were liquid at the incubation temperature while paraffin was solid. As it was reported that *Marinobacter hydrocarbonoclasticus* SP17 can degrade alkanes as well as lipids through the formation of oleolytic biofilms [202], lipids; hexadecyl hexadecanoate, a wax ester and tristearin, a triglyceride were included in this study. *Novosphingobium* sp. S1 grew on *n*-hexadecane and *n*-octadecane by forming biofilm at the hydrocarbon-water interface (Figure 3.7), while exhibiting an increase in OD_{600nm} in the aqueous phase (Figure 3.9). A faster detachment of cells from the biofilm could be a possible reason. On wax ester, the cells were equally distributed between the biofilm and the planktonic states. *G. amicalis* S2 formed biofilm on *n*-hexadecane, *n*-octadecane, wax ester and paraffin. However, biofilm formed by *G. amicalis* S2 on *n*-hexadecane was very delicate, and was poorly retained by the nylon membrane (33 µm porosity) during biofilm quantification. It is therefore very likely that biofilm quantification on *n*-hexadecane is underestimated. Notably, *G. terrae* S5 formed biofilm on *n*-hexadecane, *n*-octadecane and paraffin, as well as on the wax ester with very low planktonic cells increase. None of the bacteria grew on tristearin.

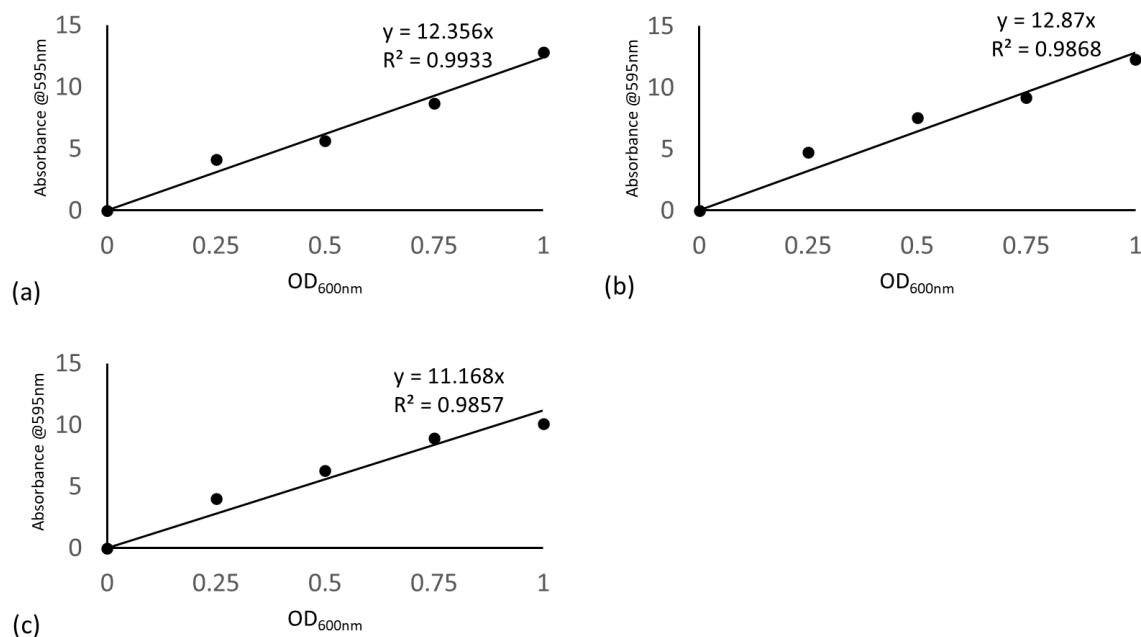


Figure 3.8: Calibration curve establishing the relationship between crystal violet colouration at 595 nm and OD_{600nm} for (a) *Novosphingobium* sp S1, (b) *Gordonia amicalis* S2 and (c) *Gordonia terrae* S3. In summary, 1 mL of bacterial culture with known OD_{600nm} (0, 0.25, 0.50, 0.75 and 1) were centrifuged at 13,000 rpm. The pelleted cells obtained were stained with 400 μ L of 0.1 % crystal violet and incubated at room temperature for 3 minutes. Then, the cells were washed twice with 1 mL Milli-Q water. Cells retained the crystal violet and were decolorized with 1 mL solution of 10 % acetic acid and 50 % ethanol. The absorbance of the resultant supernatant was read at 595 nm after 10-fold dilution. Note that the values presented are absorbance after correction for dilution.

Growth of the three strains on alkanes or lipids which are nearly insolubles in water, resulted in the development of biofilm and planktonic populations although at different extent depending on the strains and substrate. This raised the question of the relationship between the two populations. To gain insight on this point, cultures were performed in 6-well plates containing within each well an insert with 0.4 μ m pore size membrane. This constituted a culture system with two compartments: the insert and the well, the two being separated by a membrane.

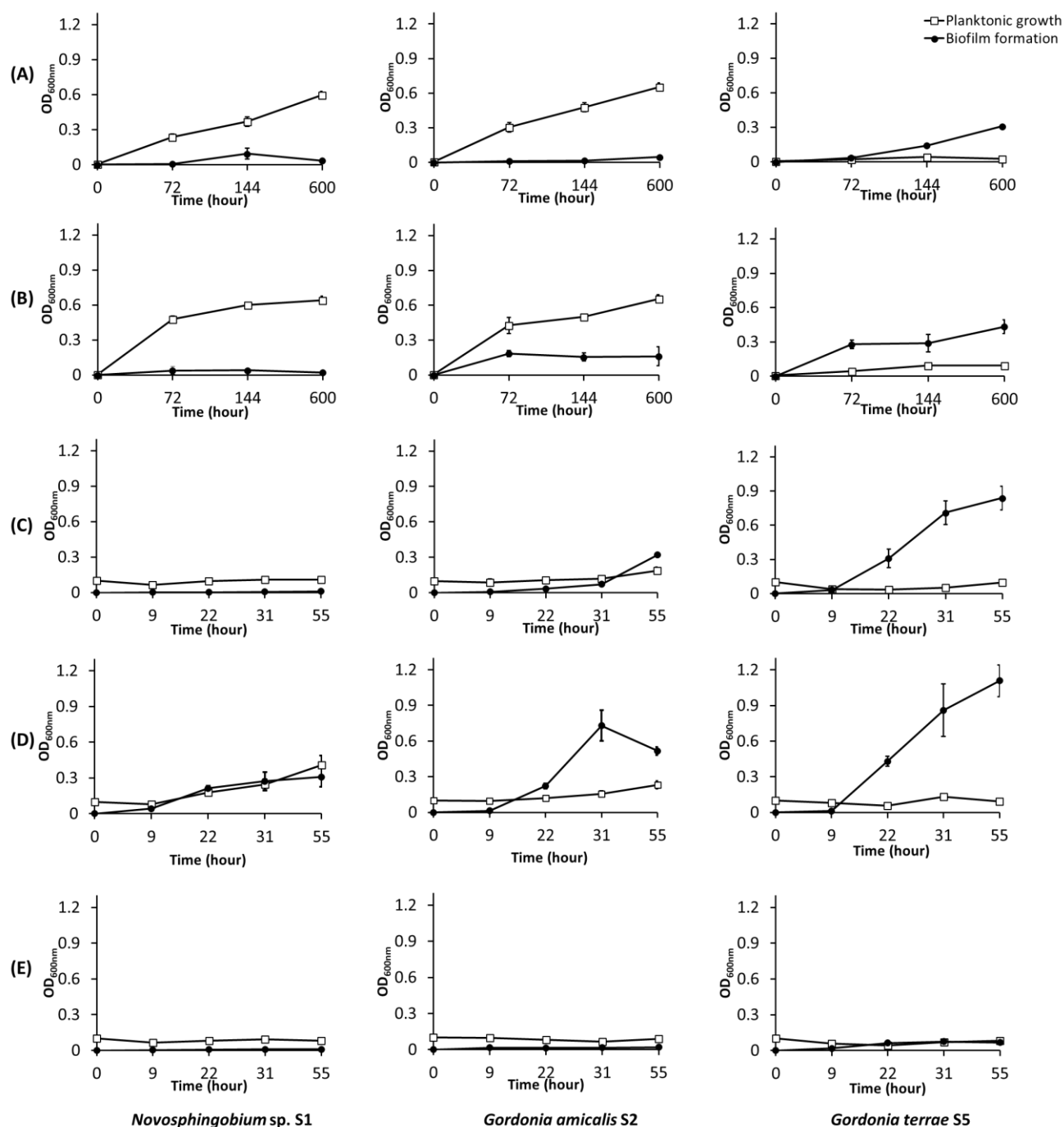


Figure 3.9: Planktonic growth and biofilm formation on (A) *n*-hexadecane, (B) *n*-octadecane (C) paraffin, (D) hexadecyl hexadecanoate and (E) tristearin by *Novosphingobium* sp. S1, *Gordonia amicalis* S2 and *Gordonia terrae* S5.

In a first experiment, the two compartments contained IMM medium with 0.4% propionate. After inoculation of the inserts only at an OD of 0.05 and incubation, no cells were observed in the wells, indicating that they were not able to cross the membrane (Figure 3.10a). In the second experiment, the inserts contained 0.2% *n*-hexadecane and the wells containing no carbon source were inoculated

at an OD_{600nm} of 0.1. In this configuration, cells were separated from the *n*-hexadecane by the porous membrane. After incubation, the cell populations in the wells did not increase (Figure 3.10b). This experiment indicated that the cells of the three strains could assimilate *n*-hexadecane only if they were able to reach the hexadecane-water interface. In another experiment, the wells and the inserts were fill with the medium without carbon source and both inoculated at an OD_{600nm} of 0.1. The substrate, *n*-hexadecane, was then added only in the inserts. After incubation, a biofilm developed in the inserts at the hexadecane-water interface and the cell density increased in the inserts while the population in the wells did not change (Figure 3.10c). This indicated that the planktonic cells observed in culture of the three strains on *n*-hexadecane originated from the biofilm and hence were not actually growing. Moreover, the biofilm did not release water soluble metabolites that could feed the planktonic population.

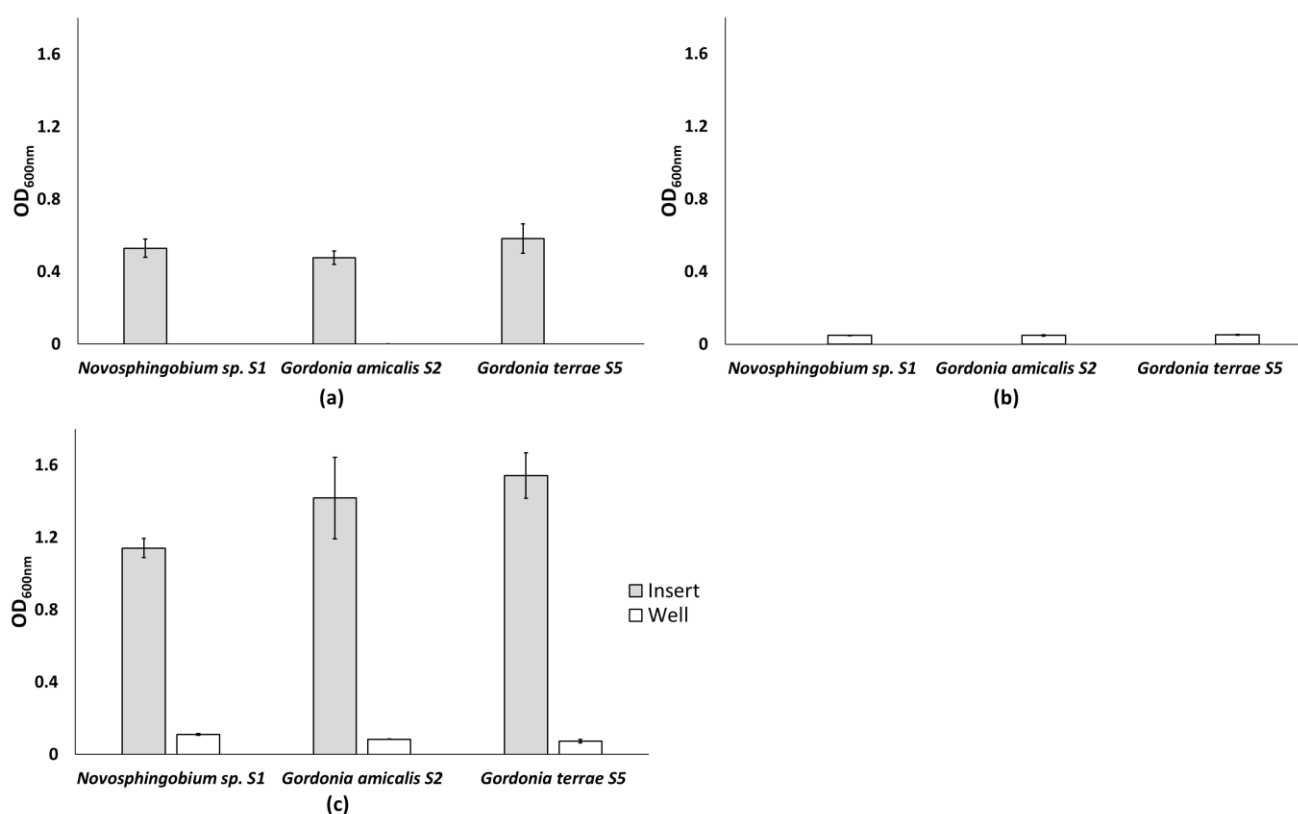


Figure 3.10: Comparative growth profile of *Novosphingobium* sp. S1, *Gordonia amicalis* S2 and *Gordonia terrae* S5 in culture insert and well compartment separated by a membrane filter. OD_{600nm} of culture in the filter compartments and wells was read after 72 h incubation at 30 °C.

The structural characteristics of the biofilm formed on paraffin and hexadecyl hexadecanoate by *G. terrae* S5 were investigated by microscopy. The biofilms formed by the two other strains were too

weak to be imaged. Microscopic characterization of the biofilm formed on paraffin showed a flat homogeneous biofilm with a low cell density (indicated by total surface coverage) with little increase of thickness and volume between 24 and 40 hour (Figure 3.11a and 3.11b). However, biofilm formed on wax ester was patchy with average biofilm thickness of 6.76 ± 1.66 and $6.85 \pm 2.54 \mu\text{m}$ at 24 and 40 h, respectively (Table 3.1). In comparison, results indicated that *G. terrae* S5 colonized paraffin more than the wax ester. Nevertheless, the hollowed surface feature of the wax ester could be a suggested reason (Figure 3.12).

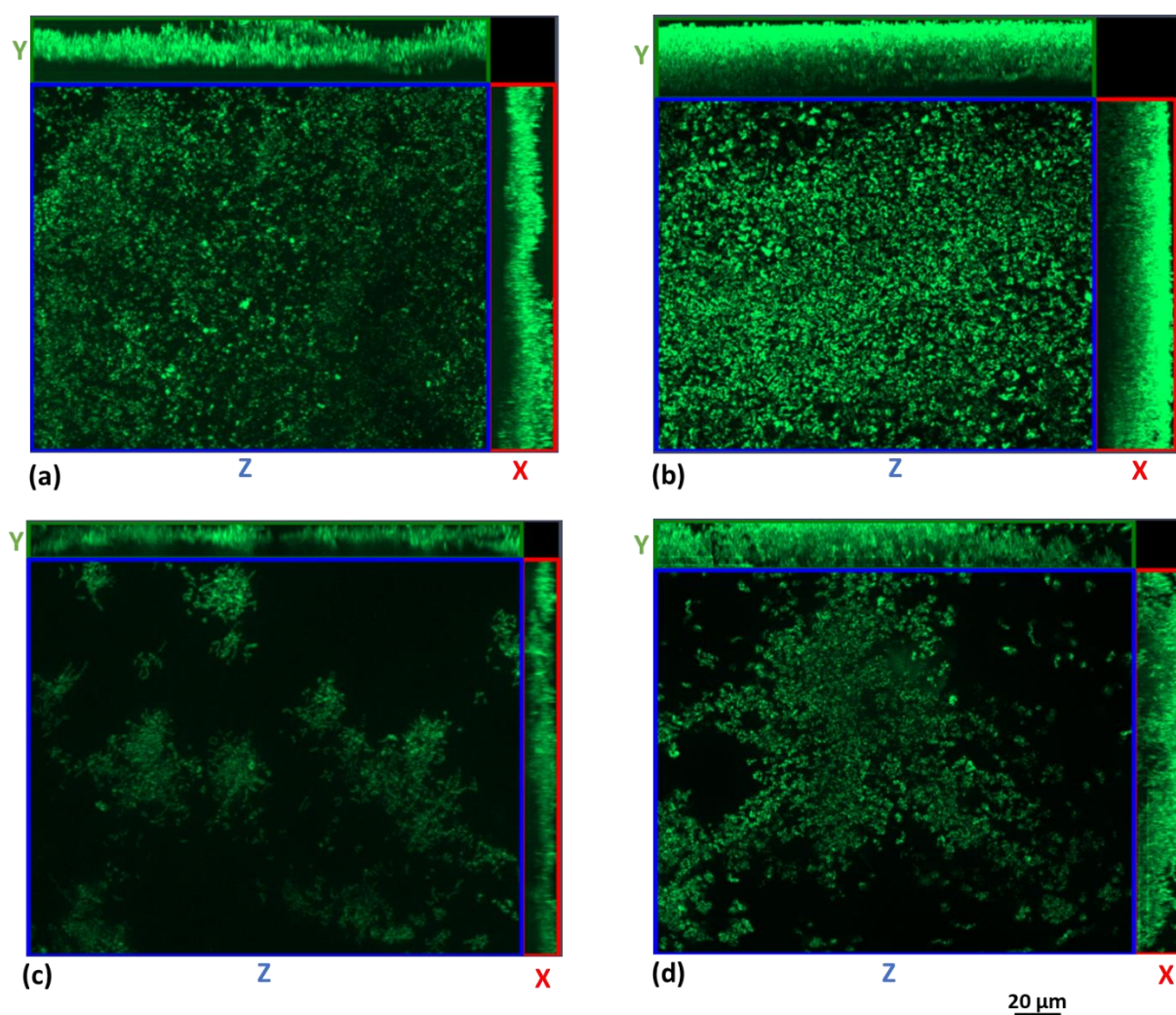
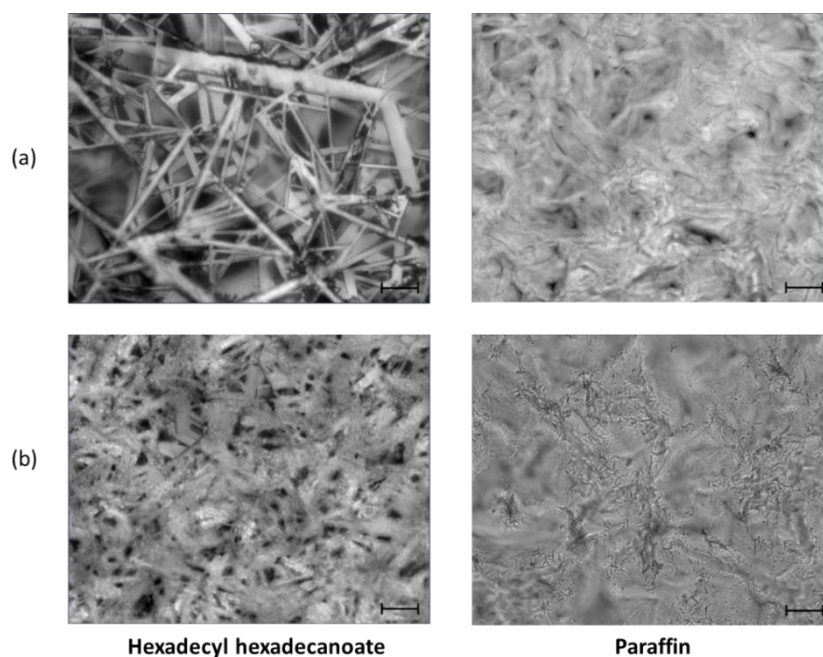


Figure 3.11: Maximum Intensity Projection (X:Y:Z plane) of biofilm formed by *Gordonia terrae* S5 on paraffin wax after (a) 24 h and (b) 40 h and hexadecyl hexadecanoate after (c) 24 h and (d) 40 h. Scale bar = 20 μm . Biofilms were stained with 0.1 % SYTO 9 (green).

Table 3.1: Volumetric and topological characterization of biofilms by *Gordonia terrae* S5 on paraffin and hexadecyl hexadecanoate. Values are means and standard deviation of data from 5 image stacks.

	Time (hour)	Substrate	
		Paraffin wax	Hexadecyl hexadecanoate
Bio-volume ($\mu\text{m}^3/\mu\text{m}^2$)	24	4.7 ± 1.9	1.7 ± 0.6
	40	6.2 ± 1.1	1.3 ± 0.7
Maximum biofilm thickness (μm)	24	26.3 ± 3.8	16.7 ± 4.2
	40	30.4 ± 4.8	21.7 ± 5.1
Average biofilm thickness (μm)	24	17.9 ± 6.9	6.8 ± 1.7
	40	23.1 ± 4.6	6.9 ± 2.5
Substratum coverage (μm^2)	24	5397.8 ± 1715.6	3071.9 ± 1097.9
	40	6376.1 ± 1025.5	2038.3 ± 1287.3
Total substratum coverage (%)	24	16.9 ± 5.4	9.6 ± 3.4
	40	20.0 ± 3.2	6.4 ± 4.0
Roughness Coefficient (Ra^*)	24	1.1 ± 0.1	1.4 ± 0.2
	40	1.2 ± 0.1	1.6 ± 0.2

Figure 3.12: Microscopic images of the surface of Hexadecyl hexadecanoate and paraffin (a) before and (b) after biofilm formation by *Gordonia terrae* S5. Microscopic images were obtained with the Zeiss AxioObserver.Z1/7 microscope with an oil immersion Plan-Apochromat 63x/1.40 DIC M27 objective. Scale is 20 μm .

MATH test was used to assess the ability of the strains to adhere to hydrocarbons (Figure 3.13). Cells of *G. terrae* S5 and *G. amicalis* S2 partitioned almost completely into the *n*-hexadecane indicating a high affinity for the hydrocarbon. In contrast, *Novosphingobium* sp. S1 cell mostly remained in the aqueous phase indicating a low affinity to hydrocarbons. The properties of the cells of the three strains did not change in respect of the growth substrate: propionate or *n*-hexadecane. This suggests that the ability to adhere to hydrocarbons is constitutive.

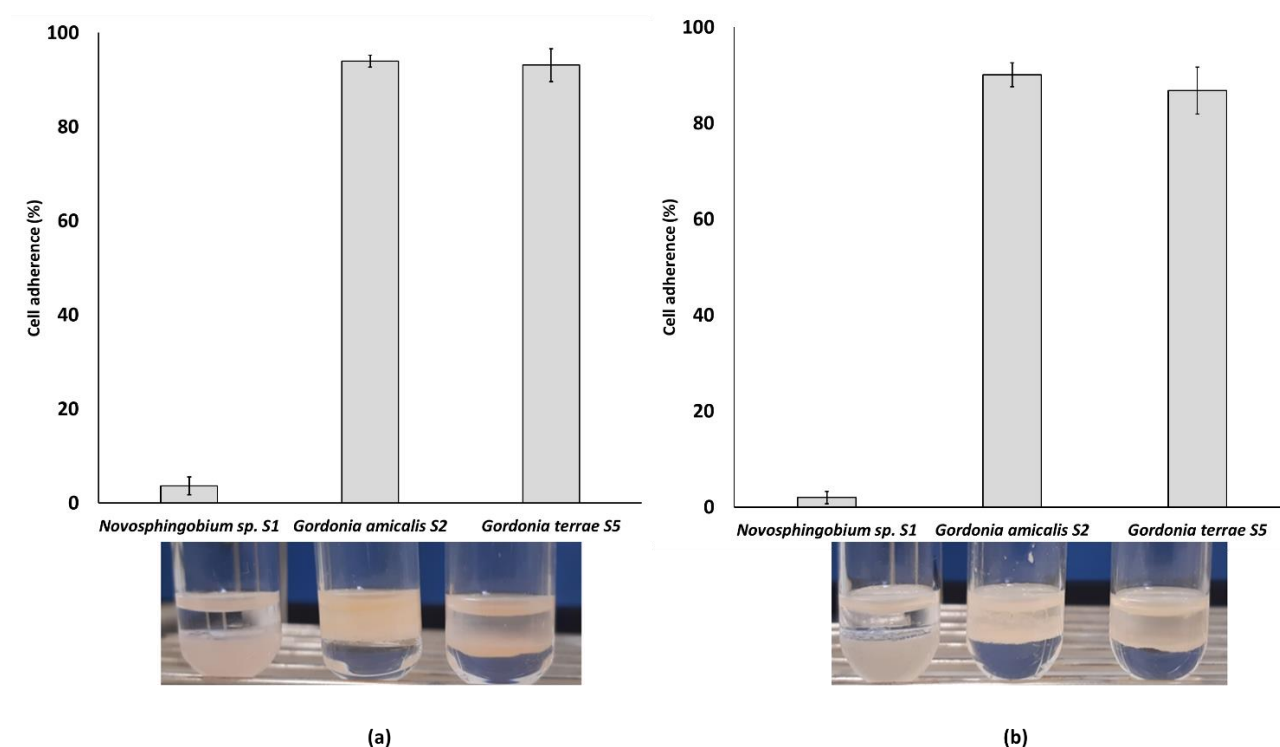


Figure 3.13: Adhesion of *Novosphingobium* sp. S1, *Gordonia amicalis* S2 and *Gordonia terrae* S5 to hexadecane grown on (a) propionate and (b) *n*-hexadecane. Insert: images of *Novosphingobium* sp. (left), *Gordonia amicalis* (middle) and *Gordonia terrae* (right) adhering to *n*-hexadecane. Adherent cells rose with the hydrocarbon, forming a "creamy" upper layer and a clear aqueous phase after allowing to stand.

Bacteria can produce biosurfactant to facilitate interaction at the interface between the aqueous and hydrocarbon systems for enhanced solubility. However, as shown in Table 3.2, a negative result from the drop collapse and E₂₄ tests demonstrated that the three strains did not produce biosurfactant. Similarly, results from oil displacement test were very low when compared to 1 % SDS. The lowering of interfacial tension after 180 sec observed in cultures of *Novosphingobium* sp. S1, *G. amicalis* S2 and *G. terrae* S5 were 49.7, 60.4 and 50.8 mN m⁻¹, respectively, while that of the

uninoculated medium (control) was 62.5 mN m^{-1} (Table 3.2). This confirmed that none of the strains produced biosurfactant during growth on *n*-hexadecane.

Table 3.2: Screening for biosurfactant production by bacteria. Key: + = positive, - = negative and ND = not determined.

	Drop collapse	Oil displacement (cm)	Emulsification index (%)	Interfacial tension (mN m^{-1})
MilliQ water	-	-	-	ND
Cell-free medium	-	-	-	62.5
<i>Novosphingobium</i> sp. S1	-	0.5 ± 0.2	-	49.7
<i>Gordonia amicalis</i> S2	-	0.3 ± 0.1	-	60.4
<i>Gordonia terrae</i> S5	-	0.4 ± 0.1	-	50.8
SDS (1 %)	+	2.4 ± 0.1	75.3 ± 0.6	ND

3.3.4. Screening for extracellular metabolites by untargeted HPLC-MS/MS

The release of extracellular metabolites is reported to influence the exometabolome of bacteria cell and its microenvironment [215]. Thus, to further gain insight into the mechanism of *n*-hexadecane metabolism by the selected strains, extracellular metabolite characterization during biodegradation was carried out. In the process of selection of compounds specific to *n*-hexadecane biodegradation, compounds found in the instrumental blank, abiotic control, culture medium with propionate, and at the start of the experiment (day 0) were ignored. Compounds that were not present in the triplicate samples were disregarded. In addition, the area ratio between samples at different time point, which signifies the appearance and disappearance of a compound, was used to highlight compounds. Structures were assigned to selected compounds based on number of carbon atoms (C) and the ratio of the number of hydrogen to carbon atoms (H/C) and database match. Furthermore, FISh scoring (Fragment Ion Search) was carried out to match theoretical and experimental MS^2 fragments. Particularly, we ignored hexadecanoic acid because it was found to be a carry-over contaminant during LC method development.

Untargeted screening of the extracellular metabolites revealed 8-hydroxyhexadecanedioic acid (m/z 301.2021) and 16-hydroxyhexadecanoic acid (m/z 271.2280) as tentative metabolites (Figure 3.14). However, 16-hydroxyhexadecanoic acid, which was annotated with a full match on mzCloud and ChempSpider database, was detected at two retention times, suggesting the presence of isomers. Furthermore, the retention time of the standard, 16-hydroxyhexadecanoic acid (RT 13.16 min) showed that the compounds at 12.45 min and 12.22 min were not 16-hydroxyhexadecanoic acid. The 8-hydroxyhexadecanedioic acid was produced by *Novosphingobium* sp. S1 and *G. amicalis* S2 while the hydroxyhexadecanoic acid isomers were detected from *G. terrae* S5. These compounds were specific to *n*-hexadecane biodegradation because they were not detected in the control samples. To confirm the identity of these metabolites, their structures were elucidated using targeted MS^2/MS^3 analysis.

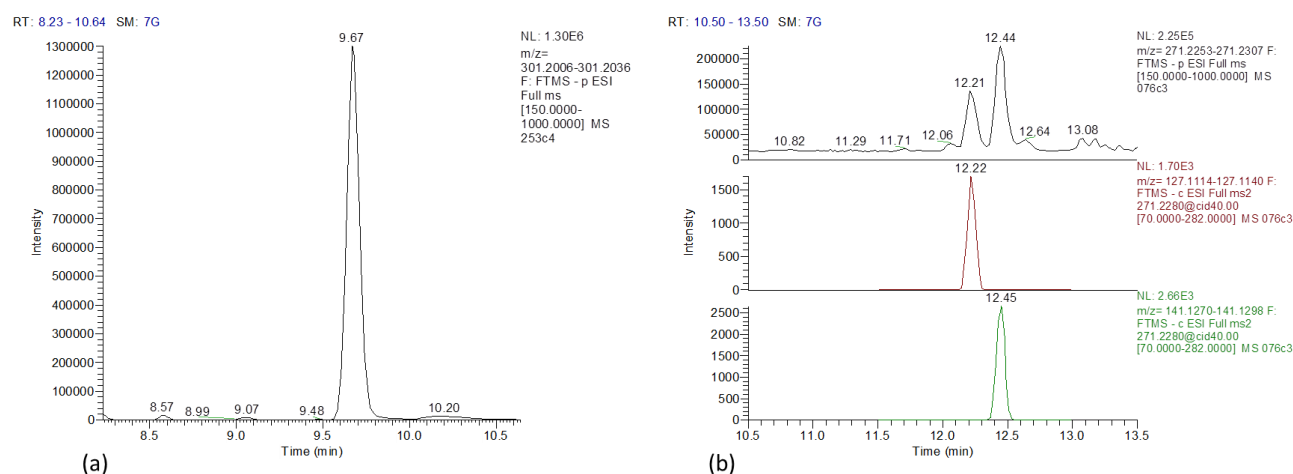


Figure 3.14: Extracted chromatogram of (a) 8-hydroxyhexadecanedioic acid (m/z 301.2021) at RT 9.67 min and (b) hydroxyhexadecanoic acid (m/z 271.2280) at RT 12.22 and 12.45 min. Specific signals for the two isomers were extracted with specific fragments m/z 127.112.

3.3.5 Structural elucidation of metabolites by targeted HPLC- MS^2 and MS^3

Better fragmentation was achieved using CID. Therefore, CID was used as the preferred fragmentation mode.

3.3.5.1 Structural elucidation of 8-hydroxyhexadecanedioic acid

The metabolite, 8-hydroxyhexadecanedioic acid (m/z 301.2021), had two significant product fragments in MS^2 (Figure 3.15) that were obtained in CID40 scans. The two fragments, m/z 283.1916 and m/z 241.1802 were further monitored by MS^3 at CID45 to elucidate the structure of the metabolite. Fragments of m/z 265.1810, m/z 239.2018 and m/z 221.1912 were product fragments

obtained from m/z 283.1916. The structure of these fragments was elucidated by also observing those of similar compounds on mzCloud (www.mzcloud.org). The fragment, m/z 265.1810, indicated the loss of two molecules of water from the precursor compound (m/z 301.2021) at both ends. This observation strongly supports the position of the -OH group between carbon atoms 4 and 13. Furthermore, this was corroborated by product fragments obtained from m/z 241.1802. However, there was no more fragment(s) or mass spectral data to identify the exact position of the hydroxyl group. Therefore, the initial assigned name, 8-hydroxyhexadecanedioic acid, was retained for this metabolite.

3.3.5.2 Structural elucidation of hydroxyhexadecanoic acid isomers

The identity and structure of the isomers (m/z 271.2280) were elucidated based on specific product fragments in MS² obtained at CID50 (Figure 3.16). MS² fragmentation showed that the isomers had a common fragment of m/z 253.2176 (loss of H₂O) and m/z 225.225 (loss of CO). The same fragmentation pattern was observed for the standard, 16-hydroxyhexadecanoic acid, indicating they are structural isomers. Nonetheless, the peak at 12.22 min had a specific final fragment of m/z 127.1127 and the structure of this fragment denotes that this metabolite is 8-hydroxyhexadecanoic acid. On the other hand, the second isomer showed these specific fragments, m/z 141.1284 and m/z 113.0968. Likewise, the structure of the m/z 113.0968 fragment signified that this isomer is 7-hydroxyhexadecanoic acid. Due to the lower abundance of this metabolite, there were no fragments obtained for MS³ scans.

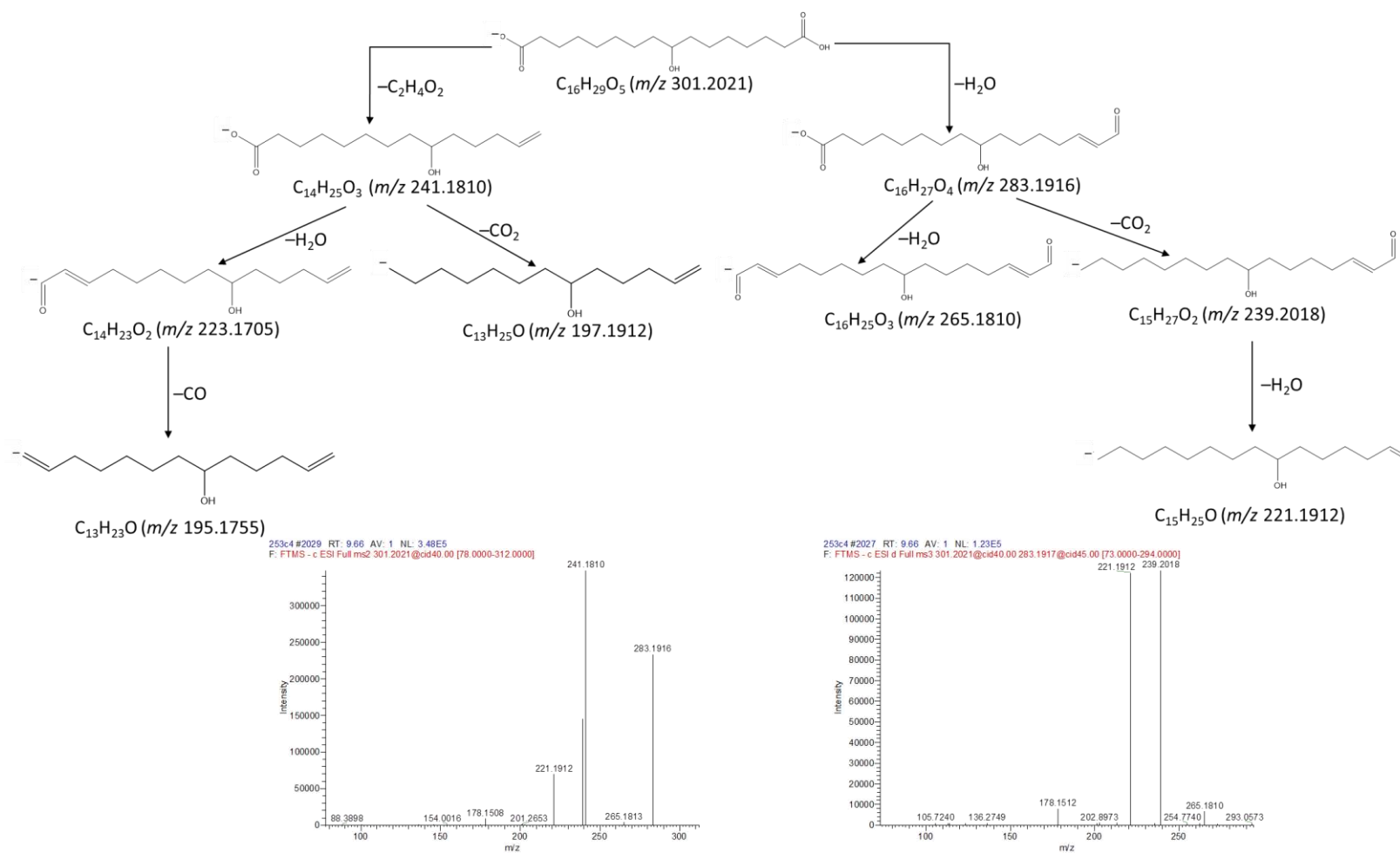


Figure 3.15: Structural elucidation of 8-hydroxyhexadecanedioic acid by MS³ fragmentation. Insert: MS³ mass spectrum showing the product fragments from *m/z* 241.1802 and *m/z* 283.1916. Peaks of *m/z* 178 and *m/z* 148 are regarded as artefacts.

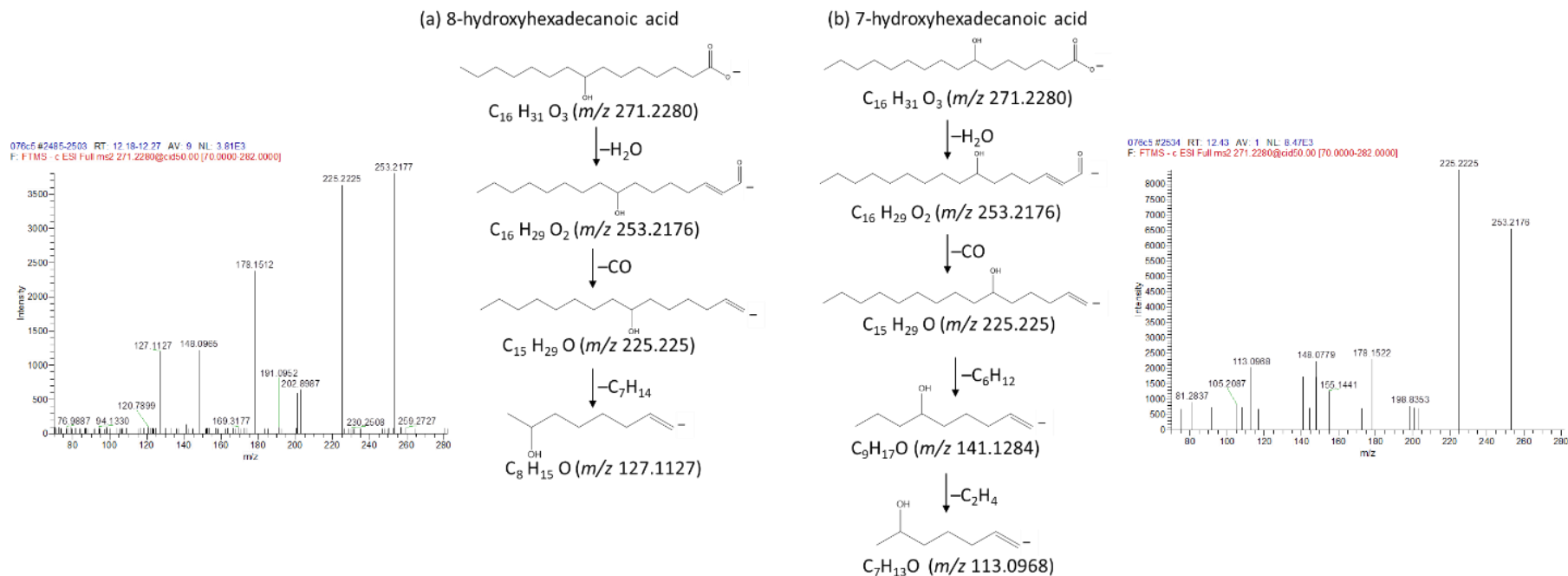


Figure 3.16: Structural elucidation of 8-hydroxyhexadecanoic acid and 7-hydroxyhexadecanoic acid by MS^2 fragmentation. Insert: MS^2 mass spectrum showing the product fragments from each isomer. Peaks of m/z 178 and m/z 148 are regarded as artefacts.

Therefore, 8-hydroxyhexadecanedioic, 8-hydroxyhexadecanoic acid and 7-hydroxyhexadecanoic acid were described as the metabolites specific of the growth on *n*-hexadecane (Table 3.3).

Table 3.3: Metabolites detected and elucidated by HPLC-MS² and MS³ (ESI-) during biodegradation of *n*-hexadecane.

Bacteria strain	Metabolite	Molecular formula	Molecular weight	Retention time
<i>Novosphingobium</i> sp. S1 <i>Gordonia amicalis</i> S2	8-hydroxyhexadecanedioic acid	C ₁₆ H ₃₀ O ₅	302.209	9.67
<i>Gordonia terrae</i> S5	8-hydroxyhexadecanoic acid 7-hydroxyhexadecanoic acid	C ₁₆ H ₃₂ O ₃	272.235	12.22 12.45

8-hydroxyhexadecanedioic acid was detected on day 3 of the biodegradation study with a significant decrease in intensity on day 6 for both *Novosphingobium* sp. S1 and *G. amicalis* S2 (Figure 3.11). Comparably, there was a 2.6 times intensity of 8-hydroxyhexadecanedioic acid produced by *G. amicalis* S2 on day 3. We could not detect this metabolite on day 10 for either strain. 8-hydroxyhexadecanoic acid and 7-hydroxyhexadecanoic acid were detected on day 3 through day 10, the intensity increased from day 3 to a maximum on day 6.

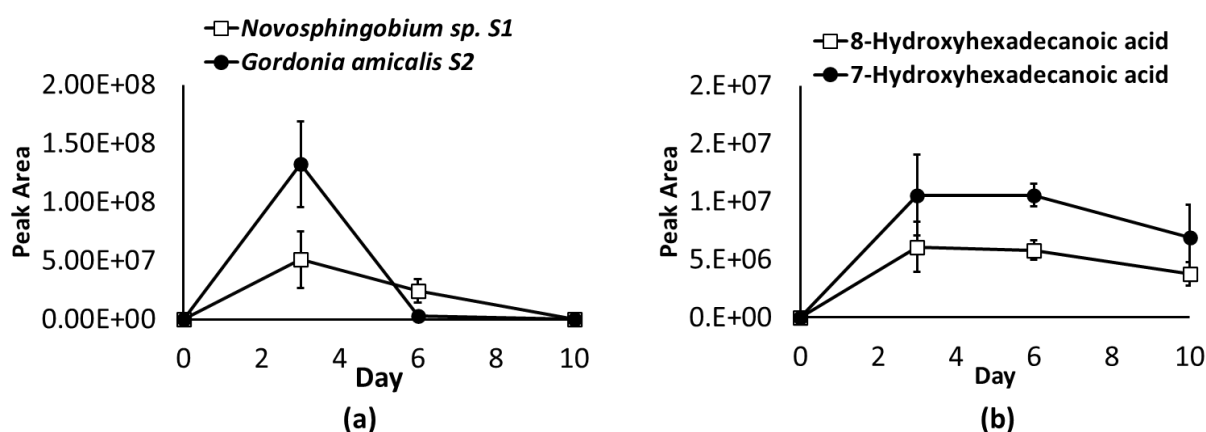


Figure 3.17: Evolution of (a) 8-hydroxyhexadecanedioic acid abundance in culture during *n*-hexadecane degradation by *Novosphingobium* sp. S1 and *Gordonia amicalis* S2 and (b) 8-hydroxyhexadecanoic acid and 7-hydroxyhexadecanoic by *Gordonia terrae* S5. Note the difference in the y-axis scales which were chosen for the best presentation.

Table 3.4 illustrates the estimation of 7-hydroxyhexadecanoic acid and 8-hydroxyhexadecanoic acid in culture from *Gordonia terrae* S5 using 16-hydroxyhexadecanoic acid as a standard (Figure 3.18). The compounds were quantified using the common fragment of m/z 225.225 (loss of CO). Quantification revealed that 7-hydroxyhexadecanoic acid concentration decreased from 3.4 ± 1.7 to 2.5 ± 1 ng/mL on day 3 to day 10, although the change in concentration was not significant at $p < 0.05$. Similarly, 8-hydroxyhexadecanoic acid decreased from 1.1 ± 0.6 to 0.7 ± 0.3 ng/mL. In the absence of a suitable standard, 8-hydroxyhexadecanedioic acid was not quantified.

Table 3.4: Concentrations of 7-hydroxyhexadecanoic acid and 8-hydroxyhexadecanoic acid in culture of *Gordonia terrae* S5. Data are presented as means \pm standard deviations of triplicates with a limit of detection of 0.1 ng/mL. Means of each compound across sampling time were compared using one-way ANOVA, Tukey honestly significant difference (HSD) on IBM® SPSS® Statistics. Different superscript within the same row shows significant difference ($p < 0.05$).

Compound	Amount (ng/mL)			
	Day 0	Day 3	Day 6	Day 10
7-hydroxyhexadecanoic acid	0 ^a	3.4 ± 1.7^b	2.7 ± 0.1^b	2.5 ± 1.0^{ab}
8-hydroxyhexadecanoic acid	0 ^a	1.1 ± 0.6^b	0.8 ^{ab}	0.7 ± 0.3^{ab}

3.4 Discussion

The dominance of *Proteobacteria* and *Actinobacteria* among microbial communities inhabiting oil-contaminated soils was reported elsewhere [28,39,216]. Interestingly, similar bacterial diversity was reported for an oil-contaminated soil sample obtained from Bodo West community [30]. These phyla are known to play important roles in carbon, nitrogen and other nutrition cycling in soil [217]. Additionally, this group of bacteria significantly influence the transformation and fate of petroleum hydrocarbons in the environment [209]. Whereas, several hydrocarbonoclastic taxa may be present in a polluted soil, bacteria with higher growth rates are likely dominant during enrichment [31]. *Actinobacteria* are considered suitable for biodegradation applications because of their high metabolic capability [17,52]. *Gordonia* species, having the ability to degrade petroleum hydrocarbons were isolated from soil and sediments before. *G. rubripertincta* SBUG 1971 and *G. rubripertincta* SBUG 1972, as well as, *G. iterans* Co17 were reported to degrade a wide range of aliphatic, alicyclic, and aromatic hydrocarbons [134,218]. Similarly, *G. paraffinivorans*, *G. alkanivorans* and *Gordonia* sp. Q8 could degrade PAHs [219–221]. Furthermore, *G. amicalis* HS-

11 utilized squalene and *n*-hexadecane as sole carbon and energy source. On the other hand, *Novosphingobium* species are well known for their ability to degrade a variety of polycyclic aromatic hydrocarbons, and these were characterized recently [25,222]. However, alkane degradation by *Novosphingobium* strains are very rare [223].

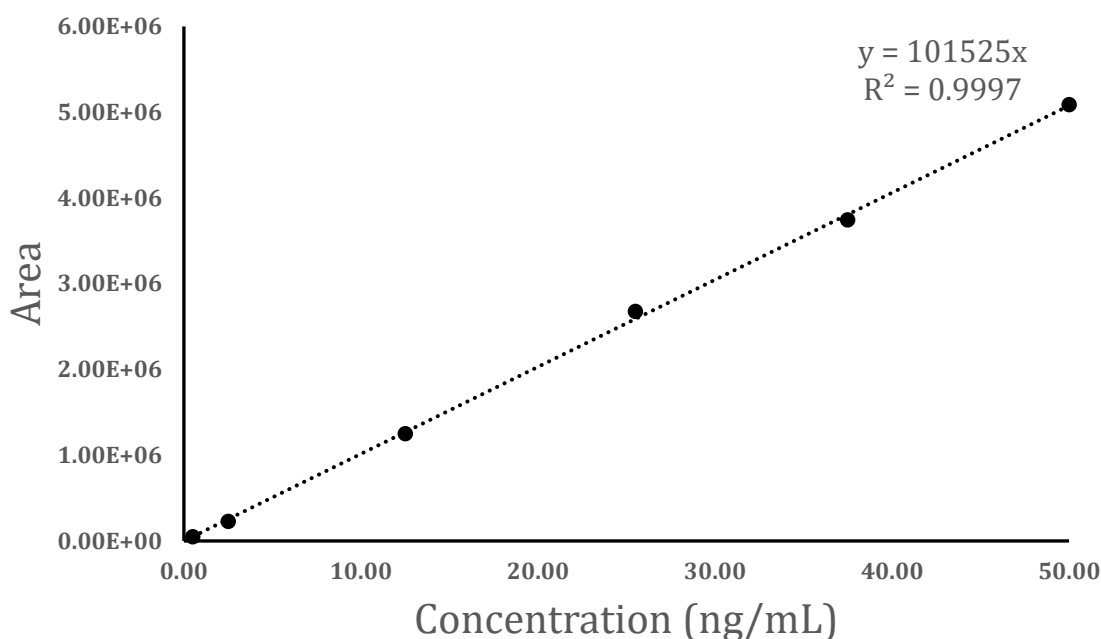


Figure 3.18: Standard curve of 16-hydroxyhexadecanoic used for the quantification of 7-hydroxyhexadecanoic acid and 8-hydroxyhexadecanoic acid.

The degradative capability of the *Gordonia* strains in this study is comparable with that of *G. amicalis* HS-11 [44] and *G. paraffinivorans* and *G. sihwensis* [224] isolated from a hydrocarbon contaminated tropical soil and compost, respectively. Biodegradation of hydrocarbons requires that microorganisms utilize hydrocarbons as growth substrates. But this depends on the ability of the bacteria to access the hydrocarbons, which is inherently unavailable in aqueous media [67]. The three stains isolated during this study formed biofilms at the alkane-water interface. Biofilm allow cells to stay in the vicinity of the alkane surface favoring mass transfer of the substrate to the cells [31, 58]. The interfacial access to alkanes is supported by the absence of biosurfactant in the supernatant of the cultures. Biosurfactant make hydrocarbons available in the aqueous phase by pseudo-solubilization. Biofilm formation would allow for accessing to alkane without the need of biosurfactant production. Similarly, in a culture of *Marinobacter hydrocarbonoclasticus* SP17, growth on *n*-hexadecane occurred uniquely at the oil-water interface [225].

The paraffin used in this study is a mixture of long-chain alkanes ($>C_{19}$ with 94 % $> C_{22}$) that is solid at the incubation. Although these features greatly decrease bioavailability and bioaccessibility, *G. terrae* S5 and *G. amicalis* S2 were able to utilize it for growth through biofilm formation. Notably, these two strains exhibited a very high adhesion to *n*-hexadecane and *G. terrae* S5 which had the highest growth rate and yield on paraffin formed the biggest biofilm. In contrast, *Novosphingobium* sp. S1 which did not grow on paraffin, formed relatively little biofilm on other alkanes, most of the cells being in the planktonic state and exhibited a very low adhesion to *n*-hexadecane. These observations point to the importance of the interaction of cells with the alkane-water interface to overcome the low bioavailability of alkanes. The emerging trends is that assimilation of less soluble alkanes requires stronger interactions with the alkane-water interface that intervene during adhesion and biofilm development. Another interpretation could be that the mechanism of biofilm formation at liquid-liquid interfaces differs from biofilm formation on solid-liquid interfaces [112].

Adsorption of bacteria at the liquid interface is an initial and essential step in biofilm formation, and could be influenced by the surface properties of the bacteria [112,226]. *G. amicalis* S2 and *G. terrae* S5 exhibited adhesion to *n*-hexadecane capability after been grown on propionate and *n*-hexadecane. In contrast, *Novosphingobium* sp. S1 displayed a very low adhesion to *n*-hexadecane and had reduced biofilm formation. Nevertheless, the degradation of *n*-hexadecane by this strain was remarkable with no significant difference when compared to the degradation efficiency of the *Gordonia* strains that adhere strongly to *n*-hexadecane. This observation suggests that even a weak adhesion is enough to allow for efficient biodegradation, implying that the initial adhesion is not the limiting step in *n*-hexadecane degradation. Even if adhesion is not limiting, it is however an obligate step for uptake of medium and long-chain *n*-alkanes for bacteria that do not produce biosurfactant as demonstrated by [109,110]. Biodegradation of petroleum hydrocarbons by *Bacillus subtilis* BL-27, a strain with weak hydrophobicity, aided by addition of surfactants was reported [47].

Adhesion to hydrocarbons was demonstrated for many actinobacteria such as *G. amicalis* that was reported to grow on *n*-hexadecane by attachment to large droplets [227]. Adhesion of bacteria to hydrocarbons can be mediated by extracellular appendages (fimbriae, fibrils and pili) and molecules such as outer membrane lipids, and proteins present on the cell surface [112,209,210]. Once attached, the cell proliferates in the presence of the hydrocarbons and develop into cell aggregates, and further into mature biofilms [113]. Cell-bound surface active compounds and glycosylated peptidolipid (Gordonin) were shown to be responsible for enhanced cell hydrophobicity in *Gordonia* sp. BS29 and *Gordonia hydrophobica*, respectively, [115,116].

The experiments performed with the culture system separated by a porous membrane, demonstrated that growth occurred only in the compartment containing the interface and hence, the formation of biofilm and lack of growth amongst the planktonic population. The amount of biofilm in the culture resulted therefore from the ratio of the growth rate at the interface to the rate of detachment from the biofilm. This could explain why *Novosphingobium* sp. S1 that made a weak biofilm, degraded *n*-hexadecane as fast as the strong biofilm formers. The exclusive growth at the interface reported here was also described in the case of *M. hydrocarbonoclastiicus* SP17 [225] and is consistent with a requirement of cell adhesion to the alkane-water interface for biodegradation as demonstrated by [109]. This observation points to the importance of the interaction, at least at the macroscopic scale, of cells at the alkane-water interface to overcome the low bioavailability of alkanes. This reinforced the view that biofilm formation would be a strategy to overcome the poor bioavailability of hydrocarbons in soils.

It was previously reported that the marine *Gammaproteobacteria*, *M. hydrocarbonoclasticus* SP17 that utilizes long chain alkanes was also capable to assimilate a variety of lipids [39]. In this study, it was shown that the three strains were able to grow on the wax ester hexadecyl hexadecanoate through biofilm formation. The biofilms formed by *G. terrae* S5 on paraffin and wax ester had significant structural differences. The reason of this could be differences in the structure of surface of the solid substrates, paraffin having a smoother surface than hexadecyl hexadecanoate that is more crystalline. Alternatively, it could be due to the nature of carbon source, alkane and lipid, which could affected the structure of biofilms as described for *Pseudomonas aeruginosa* PAO1 [228]. Assimilation of this lipid by the three strains support the view of biofilm formation as be a general mechanism for assimilation of non-dissolved organic carbon and not restricted to hydrocarbons [31].

The search for hexadecane-specific extracellular metabolites revealed the hydroxylated carboxylic acids, 8-hydroxyhexadecanedioic acid, as an extracellular metabolite for *Novosphingobium* sp. S1 and *G. amicalis* S2 while 8-hydroxyhexadecanoic acid and 7-hydroxyhexadecanoic acid were identified for *G. terrae* S5 during *n*-hexadecane degradation. To the best of our knowledge, this is the first report associating these metabolites with *n*-hexadecane biodegradation. The presence of these acids in the extracellular medium could be through oxidation of *n*-hexadecane outside of the cell (or within the EPS) prior to its uptake across the cell membrane [105]. These metabolites could originate from the lysis of cells [215]. Rodrigues *et al.* reported the production of hydroxylated fatty acid by *Rhodococcus rhodochrous* TRN7 and *Nocardia farcinica* TRH1 when growing on hexadecane [229]. They proposed that the hydroxylation of fatty acids is a possible strategy to

increase the affinity of the cell surface towards hexadecane and to remain at the oil-water interface. Note that hydroxycarboxylic acids generated during both aerobic and anaerobic biodegradation of crude oil were considered to be biosurfactants [230]. Also, dicarboxylic acids were speculated elsewhere to be associated to or secreted by the cells to act as biosurfactants [166,231]. However, biosurfactant production by the strains in this study could not be detected as interfacial tension, emulsification index, oil displacement and drop collapse tests were negative. The evolution of 8-hydroxyhexadecanedioic acid showed that this metabolite was transient, with no accumulation in the culture media after day 6. Also, 8-hydroxyhexadecanoic acid and 7-hydroxyhexadecanoic acid peaked on day 3, then gradually decreased. The concentration of the hydroxyhexadecanoic acid isomers observed in ng/mL also indicates that there was no accumulation of these metabolites in culture. Hence, this indicates that as the metabolites were produced, they were either assimilated by the cell, converted into the subsequent metabolites or their production stopped when their physiological role were no longer required.

3.5 Conclusion

The bioavailability and bioaccessability of hydrocarbon to the degrading bacteria is important for efficient bioremediation. Our findings showed that biofilm formation was beneficial for the assimilation of long chain alkanes. Furthermore, the ability of *G. amicalis* S2 and *G. terrae* S5 to adhere to alkanes is certainly an important property of these strains to form a biofilm and utilize *n*-hexadecane as a carbon and energy source. Interestingly, results showed *Novosphingobium* sp. S1 effectively utilized *n*-hexadecane and *n*-octadecane as a carbon source despite a poor adhesion to *n*-hexadecane. The production of hydroxylated carboxylic acids substantiates the degradation of *n*-hexadecane by the strains although the physiological role of these compounds remain to be elucidated. This highlights their potential for the development of bioremediation technologies of hydrocarbon-contaminated sites. Biofilm-mediated bioremediation is a promising approach for efficient hydrocarbon cleanup.

Chapter four
**Biodegradation of saturated fraction of crude oil and
signature carboxylic acids production**

4. Biodegradation of saturated fraction of crude oil and signature carboxylic acids production

4.1 Introduction

Crude oil is projected to remain a major energy source and feedstock for industries in the future [1]. However, crude oil is considered a major source of hydrocarbon pollution that has remained inevitable during exploration, production, refining, transportation, and storage. Crude oil pollution causes environmental and health problems especially in oil producing environment. Bioremediation is a sustainable technique for the cleanup of hydrocarbon pollution because it's less expensive, non-invasive, and more eco-friendly. Bioremediation largely depends on microorganisms such as bacteria to degrade pollutants such as hydrocarbons into CO₂ and H₂O. Consequently, the metabolic potential and genetic machinery of microorganisms are assets in bioremediation. Additionally, there is now much focus on improving the efficiency of the biodegradation. Saturated hydrocarbons represent the highest composition in most oil types with an estimated abundance of 20 - 50 % compared to aromatic hydrocarbons and nitrogen-sulphur-oxygen (NSO) containing compounds [8,110]. Saturated hydrocarbons are characterized by low chemical reactivity and poor water solubility for microorganisms due to the strong and localized carbon to carbon bond, and lack of reactive functional groups [232]. The carbon chains could be aliphatic (*n*-alkanes), branched (iso-alkanes and acyclic isoprenoids) or cyclic (cyclo-alkanes and cyclic isoprenoids) containing one or more saturated rings. Additionally, saturates also exist in three states at ambient temperature: gaseous (C₁ – C₄), liquid (C₅ – C₁₆) and solid (>C₁₇). The *n*-alkanes are classified based on their chain length as short chain (<C₉), medium chain (C₁₀ – C₁₅) and long chain (>C₁₅).

Few bacterial strains belonging to the genera, *Pseudomonas*, *Bacillus*, *Rhodococcus*, *Staphylococcus*, *Gordonia*, *Dietzia* and *Acinetobacter* are reported to biodegrade a wide range of saturated hydrocarbons [46,233,234]. This makes the isolation and characterization of strains with the capacity to degrade a wide range of saturated hydrocarbon of crucial importance for bioremediation of oil contamination. The low molecular weight alkanes are sparingly soluble in water for effective mass transfer to bacteria. Also, they are toxic to bacteria and are rapidly lost due to their high volatility. The high molecular weight alkanes are much more insoluble in the aqueous medium. So, alkanes are degraded by a biosurfactant-mediated process or by biofilm formation that facilitate adhesion of cells to the hydrocarbon for pseudo-solubilization and assimilation [70,94,96]. Branched chain and long-chain alkanes as well as isoprenoids, hopanes and steranes are more resistant to microbial biodegradation [235]. Aerobic degradation of saturated hydrocarbons involves

terminal and/or subterminal oxidation that generates corresponding alcohols, which are subsequently oxidized to carboxylic acids. Both terminal and sub-terminal oxidation can co-exist in some bacteria, resulting in the production of isomers [232]. However, both ends of the alkane molecule can be oxidized through ω -hydroxylation of fatty acids producing ω -hydroxy fatty acids that are further converted into dicarboxylic acids [129]. The production of carboxylic acids during biodegradation was reported as a viable indicator for biodegradation [155]. Particularly, [126] established carboxylic acids as a valuable tool for tracing microbial activity in oilfields. This is plausible given that these metabolites are found at the intersection of the various biodegradation pathways. While carboxylic acids are indicative of active biodegradation, they are also descriptive of the mechanism or pathways adopted by the degrading bacteria.

Collectively, the residual hydrocarbons and metabolites formed during biodegradation are useful to evaluating and understanding the degradation process. This is achieved by using analytical techniques to monitor chemical endpoints derived from the biotransformation [168]. Gas chromatography (GC) or liquid chromatography (LC), connected to mass spectrometry (MS) remains analytical tool of choice to characterize hydrocarbon biodegradation with ultra-high resolution and mass accuracy. Although GC-MS is the traditional technique for analysing hydrocarbon biodegradation, it is not amenable to the analysis of the produced carboxylic acids, which are polar or non-volatile metabolites, without cumbersome derivatization. Characterization using LC-MS provides an easy, rapid, robust, and quantitative detection of the produced carboxylic acids without prior derivatization [157]. Nevertheless, residual hydrocarbon analysis is generally preferred through GC because of their non-polar and thermally stable properties.

Therefore, this study investigates the capability as well as understanding the mechanism to degrading a wide range of hydrocarbons in the saturated fraction of Congo Bilondo crude oil by three bacteria strains, *Novosphingobium* sp. S1, *Gordonia amicalis* S2 and *Gordonia terrae* S5, that were isolated from a crude oil polluted soil. The study adopts a differential analytical approach that combined the efficiency of GC-MS and LC-MS for characterizing the hydrocarbons and comprehensive screening of carboxylic acid metabolites, respectively.

4.2 Materials and methods

4.2.1 Bacteria strains

The three bacteria strains, *Novosphingobium* sp. S1, *Gordonia amicalis* S2 and *Gordonia terrae* S5, used in this study were isolated from a crude oil polluted soil by enrichment with crude oil (to be published elsewhere).

4.2.2 Biodegradation of saturate fraction of Congo Bilondo crude oil

4.2.2.1 SARA fractionation of Congo Bilondo crude oil

Congo Bilondo crude oil (85.2 g) was separated into maltene and asphaltene fractions using *n*-heptane (1:40, w/v) [201]. Thereafter, 10 g of the maltene fraction was fractionated by silica gel column chromatography and eluted with *n*-hexane, toluene, and DCM/methanol (9:1, v/v) to obtain saturates, aromatics and resin fractions, respectively.

4.2.2.2 Biodegradation of the saturated fraction

Saturate fraction (0.1 % v/v) was added to culture medium without bacteria (abiotic control) and with bacteria (*Novosphingobium* sp. S1, *G. amicalis* S2 and *G. terrae* S5) in triplicate. Culture media were incubated at 30 °C and 50 rpm. Experiments were stopped at day 0, 3, and 5 to monitor residual hydrocarbons, and extracellular metabolites.

4.2.2.3 Sampling extracellular metabolites

The culture was centrifuged at 15,300 g for 10 min. The obtained supernatant was filtered through 0.22 µm sterile Millex[®] syringe-driven filters (Merck Millipore, Darmstadt, Germany), and collected for extracellular metabolite screening.

4.2.3 Analytical analysis and identification of extracellular metabolites

4.2.3.1 GC-MS for residual saturate hydrocarbon analysis

An equal volume of *n*-hexane containing 0.1% deuterated dodecane as internal standard was added to media for extraction of residual *n*-hexadecane. The mixture was agitated at 400 min⁻¹ for 20 min. The organic phase was separated from the aqueous phase by freezing at -20 °C and analysed with GC-MS. In splitless mode, 1 µL sample was introduced into the GC-MS (Thermo Scientific[™] TRACE[™] 1300 Series GC System, ThermoFisher Scientific, Illkirch-Graffenstaden, France) fitted with a 30 m × 0.250 mm × 1.40 µm Zebron ZB-624_{PLUS} column (Phenomenex, Le Pecq, France) and helium as carrier gas. The temperature program was: initial temperature: 50 °C held for 1 min,

gradient at 20 °C /min to 150 °C, 10 °C /min to 250 °C, 15 °C /min to 300 °C held for 5.6 min. Chromeleon™ Chromatography Data System (CDS) software was used for data treatment.

4.2.3.2 Evaluating biodegradation efficiency

The quantitative analyses of *n*-alkanes (C₁₀ - C₂₄) present in the saturate fraction were obtained using a calibration curve of standard alkane mix (C₁₀ - C₂₄). Furthermore, the obtained concentration was used to calculate the biodegradation efficiency against those of abiotic controls using the equation below.

$$\text{Biodegradation efficiency (\%)} = \frac{C_A - C_B}{C_A} \times 100 \quad (1)$$

where CA and CB are the concentration of the *n*-alkanes (C₁₀–C₂₄) in abiotic control and bacteria treated samples, respectively.

Biodegradation efficiency of the other hydrocarbons was estimated using their Response ratio (*R*). The Response ratio is defined by equation 2:

$$\text{Response ratio (R)} = \frac{PS}{PI} \quad (2)$$

PS is the peak area of each compound in the saturate fraction; and PI is the peak area of the internal standard (0.1% deuterated dodecane).

Subsequently, the estimated *R* was used to calculate the biodegradation efficiency using the equation below.

$$\text{Biodegradation efficiency (\%)} = \frac{R_A - R_B}{R_A} \times 100 \quad (3)$$

RA and RB are the Response ratio (*R*) in abiotic control and bacteria treated samples, respectively.

4.2.3.3 LC-MS/MS for untargeted screening of metabolites

The chromatographic system used was an ultimate 3000 RSLC system (ThermoFisher Scientific, Germering, Germany), and the detection was ensured by a Q Exactive Plus high-resolution mass spectrometer (ThermoFisher Scientific, Bremen, Germany) operated in negative mode. A 10 μL aliquot was analyzed using Accucore™ C-18 column (150×2.1mm, 2.6μm, ThermoFisher Scientific). The flow rate was 0.45 mL/min, column temperature was 45 °C and the autosampler temperature was 5 °C. The mobile phase was (A) 10 mM ammonium acetate and (B) methanol (99.9 %). The LC separation was carried out with the following gradient: 0-1 min, 10 % B; 1-15 min, 10 to 95 % B; 15-18 min, 95 % B; 18-20 min, 10% B. The resolution for full MS¹ Orbitrap (OT) and ddMS² OT scans were set to 70,000 and 35,000, respectively, with mass range of 100 - 1000 *m/z*.

Data processing was carried out using Compound Discoverer 2.1™ software (ThermoFisher Scientific, Waltham, MA). The software was fed with raw data from LC-MS/MS system, and Chemspider and mzCloud databases were consulted to assign annotation accordingly.

4.2.3.4 LC-MS³ for structural elucidation of metabolites

Targeted analysis for extracellular metabolites were conducted using the Ultimate 3000 RSLC system coupled to Orbitrap Fusion Lumos Tribrid mass spectrometer (ThermoFisher Scientific, Waltham, MA). The same column, chromatographic conditions and ionization mode used in the untargeted screening were applied. The fragmentation mode, collision-induced dissociation (CID) was applied at collision energies ranging from CID15 to CID45 with full MS Ion trap scan mode.

4.3 Results and discussion

4.3.1 SARA fractionation of Congo Bilondo crude oil

To obtain the saturate fraction of Congo Bilondo crude oil, SARA fractionation was employed to separate the oil into fractions before biodegradation study. SARA fractionation is commonly used to separate crude oil into fractions (saturates, aromatics, resins, and asphaltenes) based on solubility and polarity. This permits the study of each fraction without interference by the other fractions. The results from the fractionation are presented in Table 4.1. Firstly, asphaltenes were precipitated using *n*-heptane due to the irreversible adsorption affinity of asphaltenes to the stationary phase (silica gel). Asphaltene precipitation yielded 0.3 % asphaltene and 99 % maltene by weight. The low amount of asphaltene indicates that the crude oil is a paraffinic crude oil. Subsequent fractionation of the maltene (10 g) produced saturates (50.4 ± 1.7 %), aromatics (32.8 ± 1.3 %) and resin (14.4 ± 0.8 %) by weight with 97.59 ± 1.42 % recovery.

Table 4.1: Calculated weight distribution of the different fractions of Congo Bilondo crude oil

Composition of fraction (%/weight)			Recovery (%)
Asphaltene	Maltene		
0.3	99.6		99.9
	Saturates	Aromatics	Resin
	50.4±1.7	32.8±1.3	14.4±0.8
			97.6±1.4

The saturated fraction was observed as a yellowish green liquid with the lowest viscosity. The aromatics fraction is brownish and more viscous while the resin fraction is a very sticky dark brown matter (Figure 4.1). Meanwhile, the asphaltene fraction was a black dry flake.

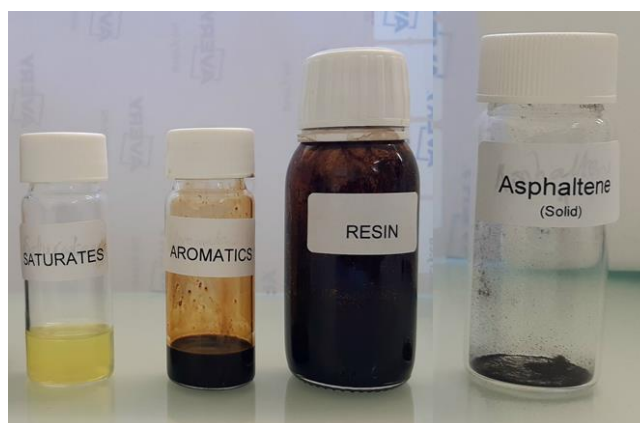


Figure 4.1: Picture of the fractions obtained from the SARA procedure of Congo Bilondo crude oil.

4.3.2 Characterization of the saturate fraction by GC-MS

The obtained saturate fraction was characterized by GC-MS, and the obtained chromatogram is shown in Figure 4.2.

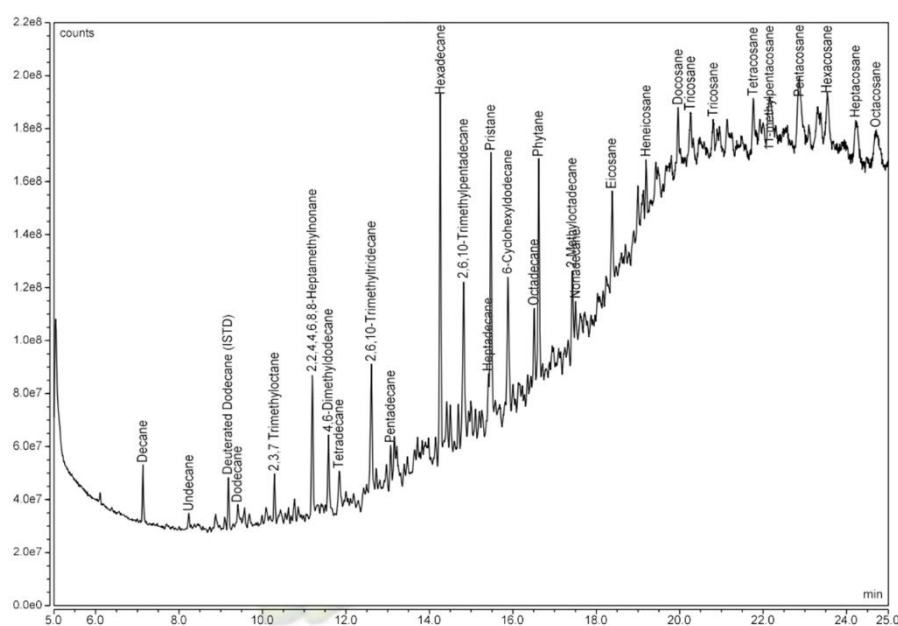
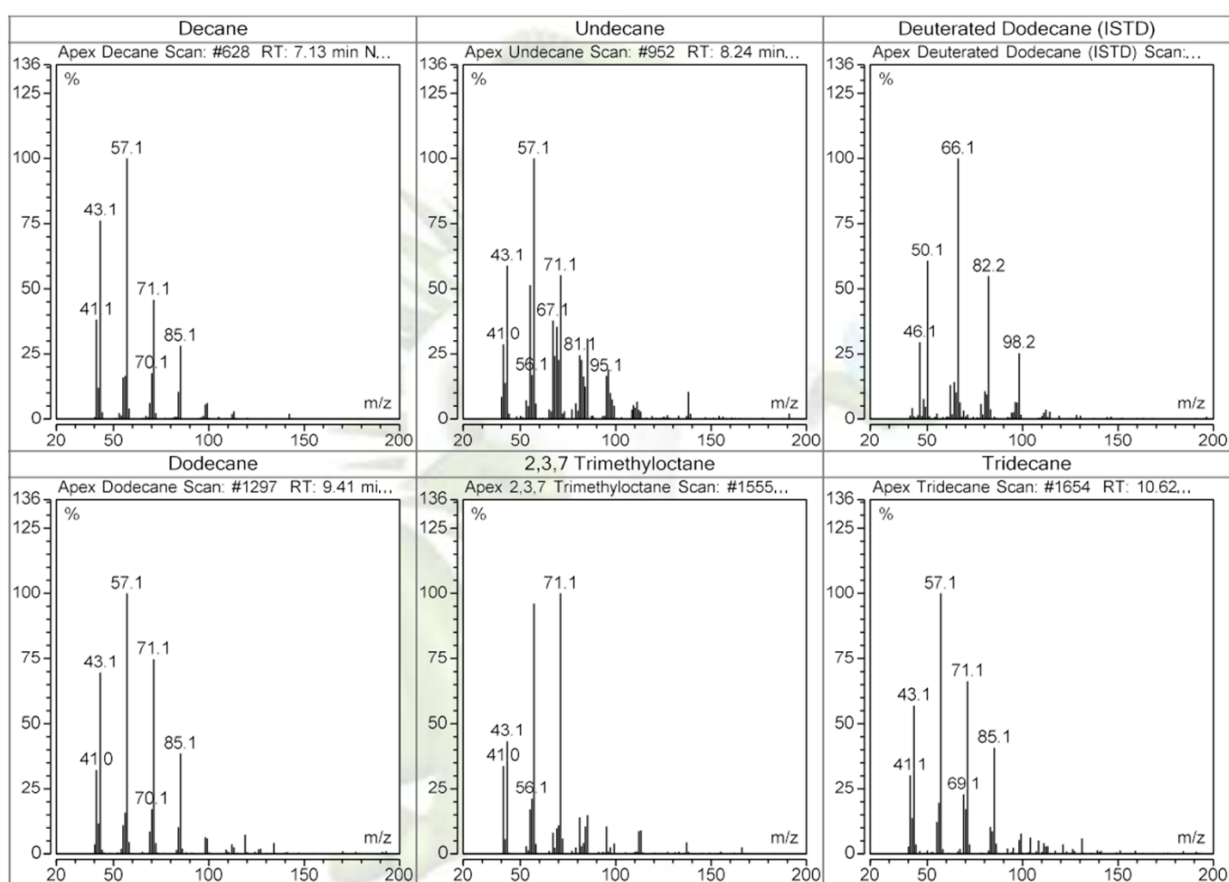
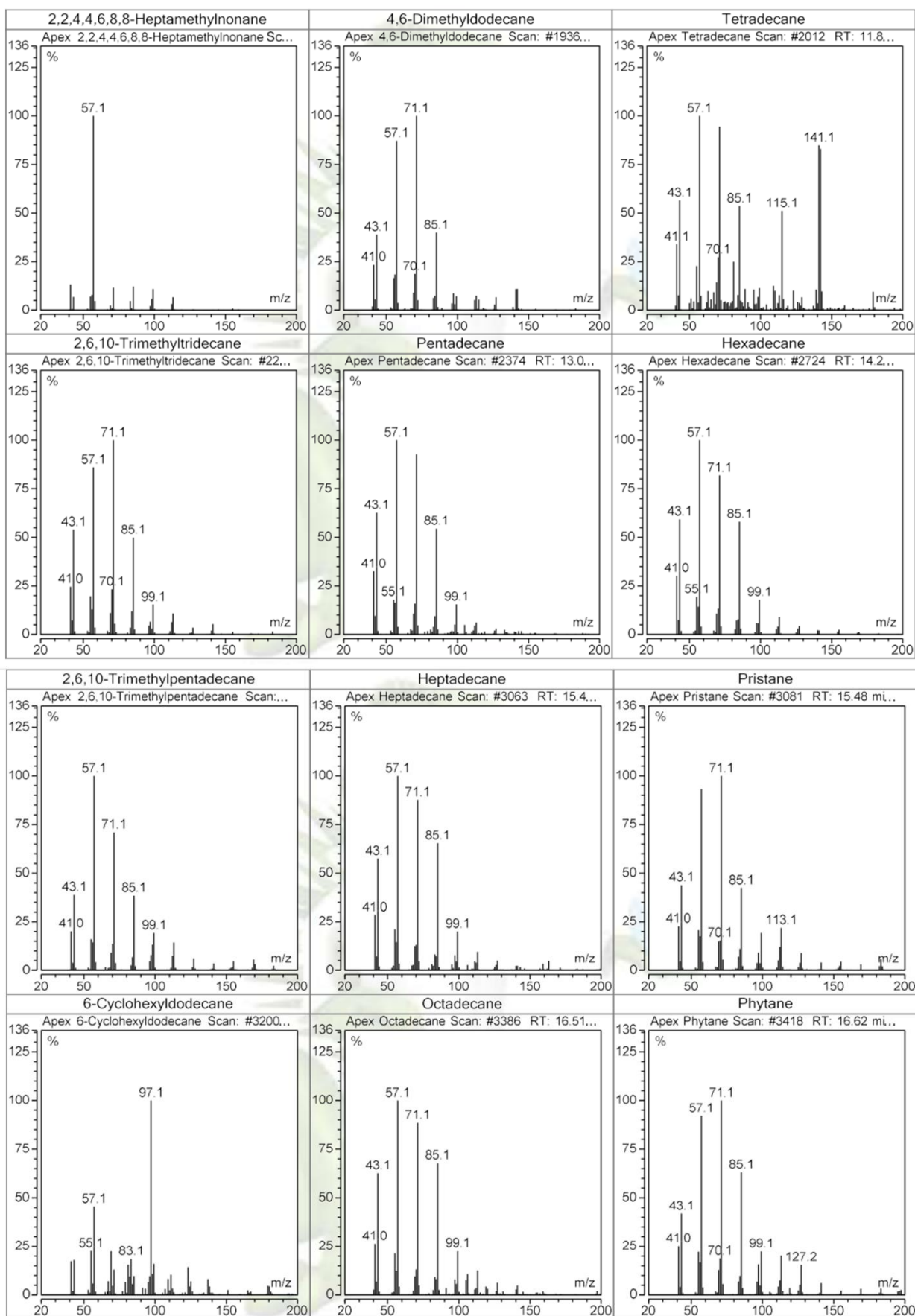


Figure 4.2: Chromatographic profiles of hydrocarbons in the saturated fraction of Congo Bilondo crude oil with deuterated dodecane as internal standard.

Saturated hydrocarbons detected in the fraction included *n*-alkanes (C₁₀ - C₂₈) and various monomethyl-, dimethyl-, trimethyl-, and tetramethyl-substituted alkanes (isoprenoids). These hydrocarbons were annotated based on their characteristic fragments at *m/z* 43, *m/z* 57, *m/z* 71 and *m/z* 85 (Figure 4.3) and match with standards and the NIST database. The short chain alkanes were not detected in the fraction probably due to loss during SARA fractionation. The risk of the loss of more volatile compounds during sample processing and solvent removal is one limitation of SARA fractionation. *n*-Hexadecane was observed as the most abundant among the described hydrocarbons with a concentration of $337.7 \pm 67.9 \mu\text{g/L}$ (Table 4.2). This was significantly followed by *n*-dodecane ($262.3 \pm 45.6 \mu\text{g/L}$) and *n*-tetradecane ($202 \pm 18.1 \mu\text{g/L}$). *n*-Hexadecane was reported elsewhere as a major component of oil among the alkanes [74,105] and is widely used as a model hydrocarbon to study the biodegradation of the long-chain alkanes. The most abundant isoprenoids were pristane (2,6,10,14-tetramethyl pentadecane) and phytane (2,6,10,14-tetramethyl hexadecane) [236]. Some hydrocarbons could not be readily resolved and identified by GC-MS.





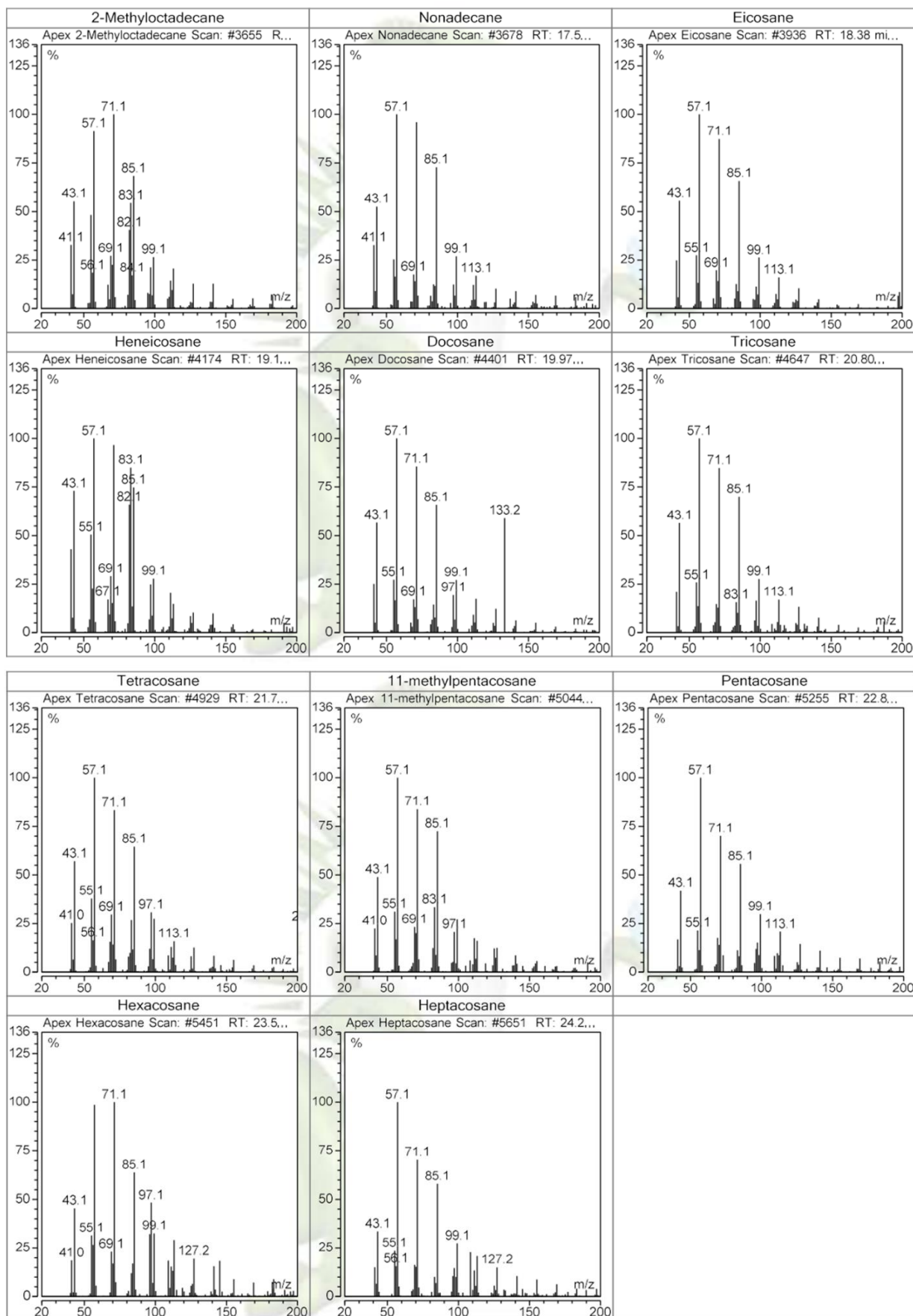
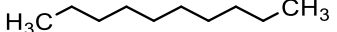

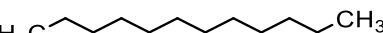
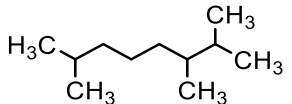

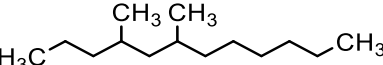
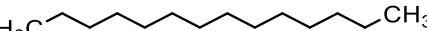
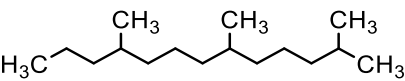

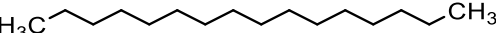
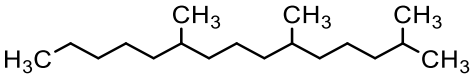

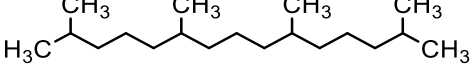
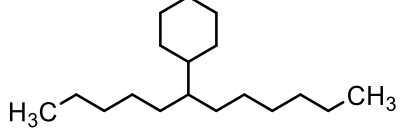
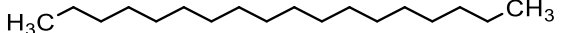
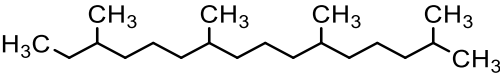
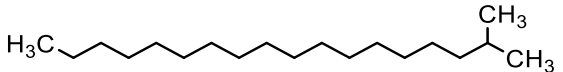
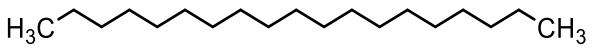
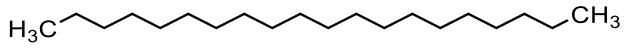

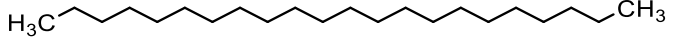

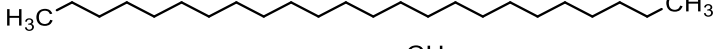
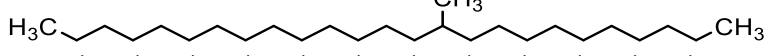

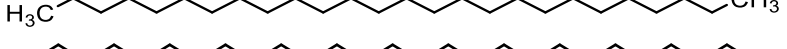




Figure 4.3: Ion chromatogram typical for *n*-alkanes and isoprenoid alkanes (m/z 43, m/z 57, m/z 71 and m/z 85).

Table 4.2: Hydrocarbons detected by GC-MS in the saturated fractions of Congo Bilondo crude oil. Key: ND = not determined.

Hydrocarbon	RT (min)	Chemical formular	Chemical structure	Amount ($\mu\text{g/L}$)	Quant. Ion (m/z)
Decane	7.14	$\text{C}_{10}\text{H}_{22}$		12.7 ± 0.6	57.0
Undecane	8.24	$\text{C}_{11}\text{H}_{24}$		31.7 ± 7.8	57.0
Dodecane	9.41	$\text{C}_{12}\text{H}_{26}$		262.3 ± 45.6	57.0
2,3,7 Trimethyloctane	10.29	$\text{C}_{11}\text{H}_{24}$		ND	
Tridecane	10.62	$\text{C}_{13}\text{H}_{28}$		105.3 ± 9.0	57.0
4,6-Dimethyldodecane	11.58	$\text{C}_{14}\text{H}_{30}$		ND	
Tetradecane	11.84	$\text{C}_{14}\text{H}_{30}$		202 ± 18.1	57.0
2,6,10-Trimethyltridecane	12.61	$\text{C}_{16}\text{H}_{34}$		ND	
Pentadecane	13.07	$\text{C}_{15}\text{H}_{32}$		48.3 ± 2.1	57.0
Hexadecane	14.26	$\text{C}_{16}\text{H}_{34}$		337.7 ± 67.9	57.0
2,6,10-Trimethylpentadecane	14.82	$\text{C}_{18}\text{H}_{38}$		ND	
Heptadecane	15.41	$\text{C}_{17}\text{H}_{36}$		42.0 ± 2.6	57.0
Pristane	15.48	$\text{C}_{19}\text{H}_{40}$		ND	
6-Cyclohexyldodecane	15.89	$\text{C}_{18}\text{H}_{36}$		ND	
Octadecane	16.51	$\text{C}_{18}\text{H}_{38}$		16.3 ± 4.0	57.0

Hydrocarbon	RT (min)	Chemical formular	Chemical structure	Amount (µg/L)	Quant. Ion (m/z)
Phytane	16.62	C ₂₀ H ₄₂		ND	
2-Methyloctadecane	17.42	C ₁₉ H ₄₀		ND	
Nonadecane	17.50	C ₁₉ H ₄₀		157.7 ± 41.1	57.0
Eicosane	18.38	C ₂₀ H ₄₂		14 ± 3.5	57.0
Heneicosane	19.20	C ₂₁ H ₄₄		96.7 ± 19.6	57.0
Docosane	19.96	C ₂₂ H ₄₆		152.3 ± 28.6	57.0
Tricosane	20.26	C ₂₃ H ₄₈		68±3	57.0
Tetracosane	21.77	C ₂₄ H ₅₀		4±1	43.0
11-Methylpentacosane	22.14	C ₂₆ H ₅₄		ND	
Pentacosane	22.86	C ₂₅ H ₅₂		ND	
Hexacosane	23.54	C ₂₆ H ₅₄		ND	
Heptacosane	24.21	C ₂₇ H ₅₆		ND	
Octacosane	24.75	C ₂₈ H ₅₈		ND	

4.3.3 Biodegradation of the saturated fraction

Figure 4.4 presents the GC-MS chromatograms of the saturated hydrocarbons on day 3 and day 5 of biodegradation. The chromatograms showed that the profile of the saturate fraction changed significantly among the bacteria in comparison to the abiotic control, although at different extents. An important observation is that the three strains can efficiently use as carbon and energy source the *n*-alkanes (C₁₀ - C₂₈) as well as the methyl-substituted alkanes (C₁₁ - C₂₆). This proved that the strains have the metabolic capabilities to biodegrade a wide spectrum of saturated hydrocarbons. Additionally, the three strains were observed growing at the oil-water interface by forming biofilm. This is believed to have enhanced the rate of hydrocarbon assimilation by reducing the distance for mass transfer [108]. Cells and secreted solubilisation factors such as exoenzymes were reported to be localized within the biofilm matrix [96,122].

The biodegradation efficiency of each hydrocarbon of the saturated fraction among the bacterial strains is shown in Table 4.3. The medium-chain *n*-alkanes (C₁₀ - C₁₅) were efficiently degraded by strains, with degradation rates above 70 % on day 5. Most odd-number carbon *n*-alkanes (C₁₅ - C₁₉) were completely degraded. This could be attributed to the loose configuration of their carbon atoms compared to even-number carbon *n*-alkanes. The latter are more symmetrical, making them more difficult for bacteria to utilize [46]. However, the degradation rates of long-chain alkanes (C₂₀ - C₂₈) were relatively higher between *Novosphingobium* sp. S1 and *G. amicalis* S2 than with *G. terrae* S5. Likewise, *Gordoniae* strains were reported to degrade alkanes in the range of C₈ - C₃₆ [134,218]. *n*-Alkanes (C₈ - C₄₀) were also significantly degraded by salt-tolerant bacteria isolated from an oil field [234,237]. Interestingly, *Novosphingobium* sp. S1 showed a high capability to degrade a wide spectrum of the saturated hydrocarbons even though this genus are well known to majorly degrade a broad range of mono- and polyaromatic aromatic hydrocarbons [222].

Furthermore, the methyl-substituted alkanes were efficiently degraded by the three strains. For instance, 2,3,7 trimethyloctane, 2,6,10-trimethyltridecane and 2,6,10-trimethylpentadecane were completely degraded on day 5. Although pristane and phytane are considered relatively resistant to biodegradation due to being highly branched, they were degraded with degradation efficiency reaching 87.4 ± 7.1 and 100 %, respectively, on day 5 for *Novosphingobium* sp. S1. Equally, biodegradation efficiency of pristane and phytane were 91.2 ± 3.8 and 97.9 ± 1.9 %, respectively, on day 5 for *G.amicalis* S2 but were 77.4 ± 5.4 and 69 ± 3.5 % for *G. terrae* S5. In contrast, pristane and phytane remained detected within 90 days of biodegradation using *Pseudomonas aeruginosa* XJ16, *Bacillus cereus* XJ20, and *Acinetobacter lwoffii* XJ19 [46]. Result from this study showed that the biodegradation of *n*-alkanes and isoprenoids occurred relatively at the same rate. Similarly,

a near complete degradation of phytane and pristane after 20 days was reported using a consortium of *Serratia marcescens* PL and *Raoultella ornithinolytica* PS enriched from oil contaminated soil [216]. Pristane and phytane are reported to be degraded mainly via mono-, di-terminal and sub-terminal oxidation with initial activation by hydroxylation [127].

4.3.4 Identification of carboxylic acids metabolites and elucidation of degradation pathway

The separation efficiency of the carboxylic acids in the culture medium and their ionization conditions were optimized using 10 mM ammonium acetate solution (pH 6.8) and methanol (99.9 %). The method was validated by analyzing three standard carboxylic acids (Figure 4.5). It showed a good separation efficiency and sensitivity. However, hexadecanoic acid was observed to be a carry-over contaminant during LC method development. Therefore, this compound was ignored during subsequent screening and selection of metabolites.

Furthermore, the rapid development in MS techniques has made acquired data set (m/z , retention times, intensities etc.) larger and complex. One way of overcoming this challenge is developing workflows for a focused analytical effort. As such, in selecting compounds specific to the biodegradation process, the area ratio between samples at different time point, that indicates the appearance and disappearance of a compound, was used to highlight compounds of interest. In addition, compounds found in the instrumental blank, abiotic control, and at the beginning of the experiment (day 0) were ignored. Compounds that were not present in the triplicate samples were disregarded. Finally, structures were assigned to selected compounds based on number of carbon atoms (C) and the ratio of the number of hydrogen to carbon atoms (H/C), database match and fragmentation pattern.

Fourteen carboxylic acids were identified as extracellular metabolites during the degradation of the saturate fraction by the three strains (Table 4.4). The carboxylic acids ranged from C₁₀ to C₂₀ and comprised of monocarboxylic acids, hydroxylated carboxylic acids, and dicarboxylic acids. While most of the carboxylic acids were found on database search, a fragmentation pattern characteristic of dehydration, decarboxylation and dealkylation was observed for all compounds (Table 4.5). However, short chain fragments were not obtained, even in MS³, as increase of the fragmentation energy beyond CID45 resulted in the loss of the precursor.

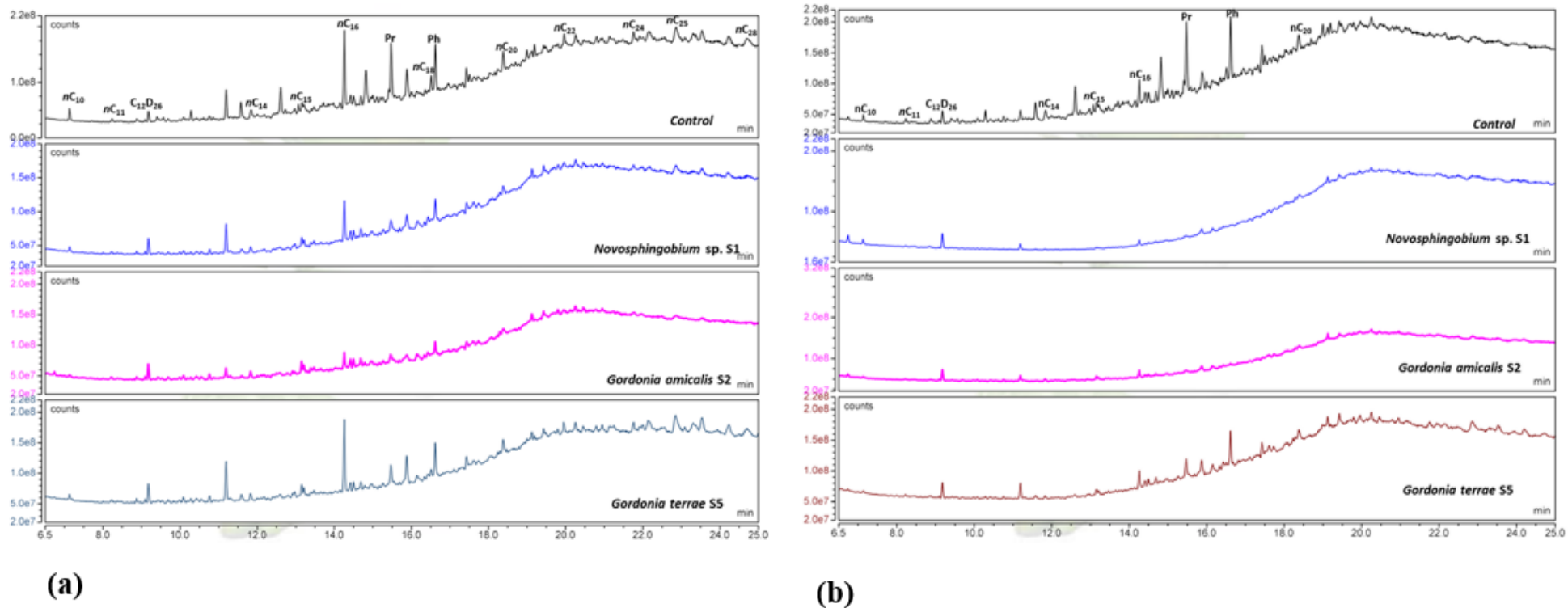


Figure 4.4: Chromatogram showing the relative changes in the distribution and abundance of alkanes on (a) day 3 and (b) day 5 of biodegradation study

Table 4.3: Relative biodegradation efficiency for each alkane on day 3 and day 5 of biodegradation study

Hydrocarbon	Biodegradation efficiency (%)					
	<i>Novosphingobium</i> sp. S1		<i>Gordonia amicalis</i> S2		<i>Gordonia terrae</i> S5	
	day 3	day 5	day 3	day 5	day 3	day 5
Decane	63.5 ± 9.9	71.9 ± 9.1	79.1 ± 8.8	80.7 ± 2.7	60.5 ± 8.1	78.8 ± 18.9
Undecane	68 ± 0.7	74.8 ± 11.6	64.2 ± 3.4	80.8 ± 14.8	59.4 ± 17.3	86.2 ± 13.4
Dodecane	76.1 ± 21.8	87.4 ± 12.6	70 ± 21.5	81.1 ± 14.9	78.6 ± 16.3	86.8 ± 13.1
Tridecane	44.8 ± 1 2.5	75.5 ± 21.7	62 ± 17.8	81.4 ± 6.2	61 ± 9.7	82.7 ± 15.8
Tetradecane	66.9 ± 5.2	77.8 ± 11.4	62.9 ± 15.2	82.7 ± 2.4	70.9 ± 7	80.2 ± 2.5
Pentadecane	100	100	87.6 ± 10.7	100	79.1 ± 18.4	100
Hexadecane	50.2 ± 16.9	75.1 ± 9.9	62.4 ± 24.8	69.3 ± 9.7	46.6 ± 17.3	59.2 ± 12
Heptadecane	100	100	100	100	100	100
Octadecane	80.9 ± 16.8	82.3 ± 16.3	70.3 ± 17.9	84.7 ± 4.6	68.3 ± 9.2	75.3 ± 21.6
Nonadecane	100	100	100	100	100	100
Eicosane	62.1 ± 12.3	67.2 ± 28.2	72.8 ± 1.7	80.2 ± 5.2	60.9 ± 1.1	65.5 ± 4.6
Heneicosane	77.4 ± 2.9	80.2 ± 2	64.7 ± 3.2	73.4 ± 6.5	58.3 ± 6	60.1 ± 7.8
Docosane	57.7 ± 18.3	71.9 ± 24.7	75.8 ± 12.8	81.3 ± 16.8	57.5 ± 24.9	58.9 ± 6.4
Tricosane	55.9 ± 0.9	72.2 ± 24.1	70.9 ± 6.4	78.7 ± 20	58 ± 5.9	61.6 ± 5.7
Tetracosane	64.5 ± 14.4	73.7 ± 22.8	71.6 ± 16.5	77.7 ± 20	55.7 ± 13.5	56.1 ± 9.9
Pentacosane	37.1 ± 4.4	60 ± 8.2	61.6 ± 1.6	79.2 ± 4.1	32.9 ± 6.4	33.6 ± 0.5
Hexacosane	35.9 ± 9	67.8 ± 28	65.1 ± 8.4	86.6 ± 6.1	27.7 ± 4.1	42.3 ± 8.2
Heptacosane	41.4 ± 8.3	79.9 ± 17.4	71.1 ± 24.5	73.1 ± 28.8	31.2 ± 6.3	46.4 ± 4.1
Octacosane	32.1 ± 10.4	70.2 ± 25.8	55.9 ± 13.2	72 ± 24.9	43.8 ± 5.3	54.8 ± 18.8

Hydrocarbon	Biodegradation efficiency (%)					
	<i>Novosphingobium</i> sp. S1		<i>Gordonia amicalis</i> S2		<i>Gordonia terrae</i> S5	
	day 3	day 5	day 3	day 5	day 3	day 5
2,3,7 Trimethyloctane	94 ± 10.4	100	94.7 ± 5.7	100	100	100
4,6-Dimethyldodecane	80 ± 1.7	83.6 ± 16.4	91.2 ± 1	91.7±7.8	79.3 ± 3.8	80.4 ± 2.5
2,6,10-Trimethyltridecane	100	100	95.6 ± 3.8	100	96.5 ± 3	100
2,6,10-Trimethylpentadecane	100	100	100	100	93.9 ± 10.5	100
Pristane	77 ± 14.5	87.4 ± 7.1	83.4 ± 10.5	91.2 ± 3.8	72.2 ± 16.3	77.4 ± 5.4
6-Cyclohexyldodecane	29.8 ± 4.3	63.5 ± 1.3	52.2 ± 11.9	66.1 ± 1.2	8.2 ± 2.1	26.2 ± 4.3
Phytane	73.4 ± 23.1	100	89.4 ± 6	97.9 ± 1.9	53.6 ± 2.9	62.4 ± 6.8
2-Methyloctadecane	86 ± 24.3	87 ± 11.4	84.1 ± 9.2	98.6 ± 2.5	67 ± 6.9	69 ± 3.5

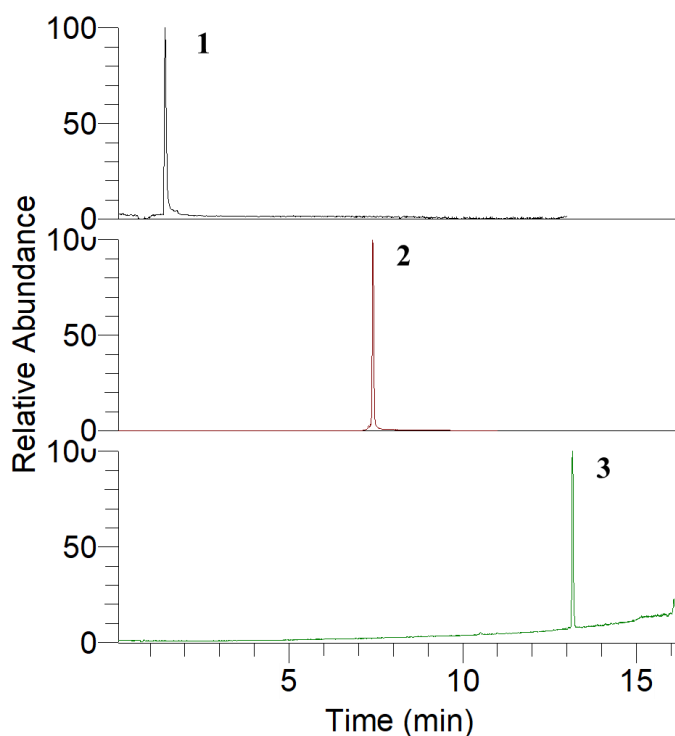


Figure 4.5: Optimization of the LC separation and detection of standard metabolites (1) 50 ppb benzoic acid, (2) 200 ppb hexadecanoic acid and (3) 0.5 ppb 16-hydroxyhexadecanoic acid. Benzoic acid, in particular, was spiked into the mobile phase, water and culture medium to evaluate matrix effect.

The appearance of C_{10} - C_{20} straight chain carboxylic acids reflects the active degradation of the corresponding n - C_{10} to C_{20} alkanes as illustrated in Table 4.4. For instance, undecanoic acid is produced from undecanoic acid while tetradecanoic, 14-tetradecanoic and tetradecanedioic acid are produced from the degradation of tetradecane. Bacteria are known to degrade alkanes through mono-terminal, bi-terminal or sub-terminal pathways, with the first found to be most prevalent. These pathways are catalyzed by oxygenases such as the membrane anchored AlkB family of alkane hydroxylases or the soluble cytochrome CYP153A enzymes [129]. However, the series of mono-, hydroxy- and dicarboxylic acids found in this study suggests their production was via the bi-terminal oxidation or dicarboxylic acid pathway. To the best of our knowledge, this is the first report associating these bacterial species with bi-terminal oxidation of alkanes. The alkane-activating monooxygenase are known to overcome the low reactivity of the alkanes by producing reactive oxygen species [232]. After the formation of the initial terminal oxidation products (Primary alcohol and aldehyde), without breaking of the carbon chain, the degradative pathway branches into bi-terminal oxidation (Figure 4.6). The ω -hydroxylation of fatty acids produces ω -hydroxy fatty acids that are further converted into dicarboxylic acids which are then passed into β -oxidation [129]. The production of hydroxylated fatty acid by *Rhodococcus rhodochrous* TRN7 and *Nocardia farcinica* TRH1

when growing on hexadecane was observed by Rodrigues *et al.* [229]. Likewise, several long-chain α,ω -dicarboxylic acids were observed during the degradation of *n*-octacosane.

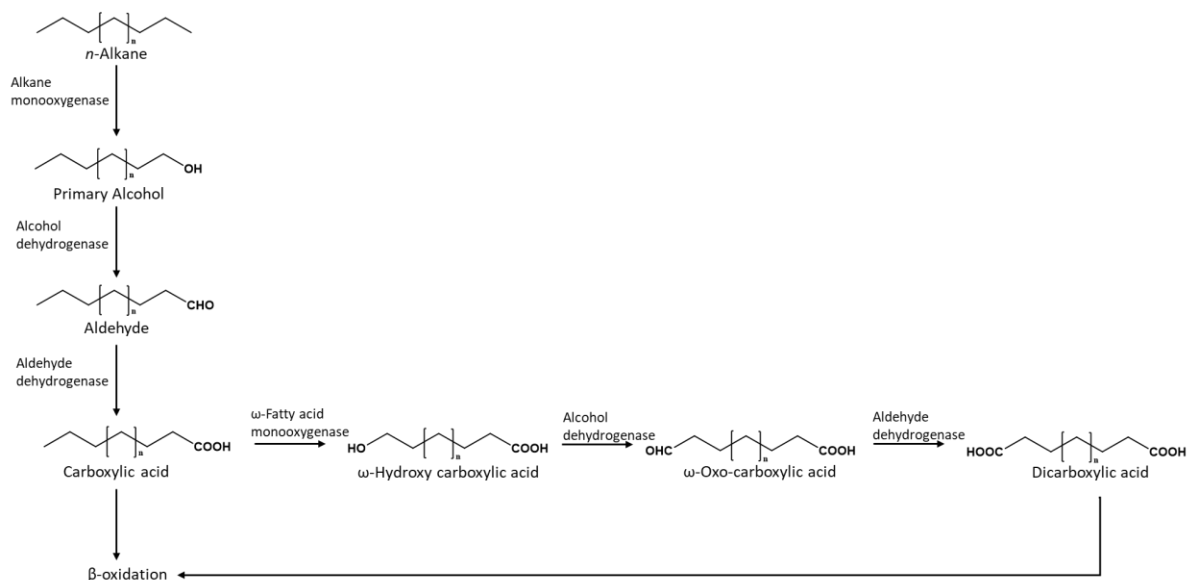


Figure 4.6: Proposed alkane degradation pathway for the bacteria strains. monocarboxylic acids either enter β -oxidation or be oxygenated further by the ω -fatty acid monooxygenases to form dicarboxylic acid

Though the presence of these metabolites indicates active degradation of hydrocarbon, the essence of their presence in the extracellular matrix remains unclear. Nonetheless, the oxidation of *n*-hexadecane outside of the cell prior to its uptake across the cell membrane was reported [105]. Furthermore, the strains used in this study form biofilm in the presence of hydrocarbon. Thus, one speculation about the presence of these acids in the extracellular medium could be through digestion within the extracellular polymeric substance (EPS). The extracellular matrices of biofilm was regarded as an external digestion system that enables a tight coupling between external digestion or solubilization of substrates and their uptake by cells [96]. These metabolites could also originate from the lysis of cells involving disruptive (lysis and cell death) and non-disruptive (active or passive excretion, leaky of cell envelope due to cell stress or cell growth/division) processes [215].

Table 4.4: Extracellular metabolites produced by *Novosphingobium* sp. S1, *Gordonia amicalis* S2 and *Gordonia terrae* S5

Compound	Molecular formula	Molecular mass	RT	Day detected in culture			Probable precursor
				<i>Novo.</i> sp. S1	<i>G. amicalis</i> S2	<i>G. terrae</i> S5	
10-Hydroxydecanoic acid	C ₁₀ H ₂₀ O ₃	188.14	6.45	3 and 5	3 and 5	3 and 5	Decane
Undecanoic acid	C ₁₁ H ₂₂ O ₂	186.16	12.44	3 and 5	3 and 5	3 and 5	Undecane
Dodecanedioic acid	C ₁₂ H ₂₂ O ₄	230.15	6.37	3 and 5	3 and 5	3 and 5	Dodecane
Tridecanoic acid	C ₁₃ H ₂₆ O ₂	214.19	13.83	3 and 5	3 and 5	3 and 5	Tridecane
10-Propoxydecanoic acid	C ₁₃ H ₂₆ O ₃	230.18	10.62	-	3	3 and 5	
Tetradecanoic acid	C ₁₄ H ₂₈ O ₂	228.20	15.01	3	3 and 5	3	Tetradecane
14-Hydroxytetradecanoic acid	C ₁₄ H ₂₈ O ₃	244.20	11.63	3	3	3 and 5	Tetradecane
Tetradecanedioic acid	C ₁₄ H ₂₆ O ₄	258.18	9.40	3 and 5	3 and 5	3	Tetradecane
15-Hydroxypentadecanoic acid	C ₁₅ H ₃₀ O ₃	258.21	12.36	3 and 5	3 and 5	3 and 5	Pentadecane
Hexadecandioic acid	C ₁₆ H ₃₀ O ₄	286.21	11.37	3 and 5	5	3 and 5	Hexadecane
8-Hydroxyhexadecanedioic acid	C ₁₆ H ₃₀ O ₅	302.20	7.50	3 and 5	3 and 5	3 and 5	Hexadecane
Heptadecanedioic acid	C ₁₇ H ₃₂ O ₄	300.23	11.99	3 and 5	3 and 5	3 and 5	Heptadecane
(15Z)-9,12,13-trihydroxy-15-octadecenoic acid	C ₁₈ H ₃₄ O ₅	330.24	9.52	-	3 and 5	3 and 5	
Icosanedioic acid	C ₂₀ H ₃₈ O ₄	342.27	13.76	3 and 5	3 and 5	3 and 5	Icosane

Table 4.5: Annotation and fragmentation pattern of detected extracellular metabolites. Most of the carboxylic acids were found on database search and a fragmentation pattern characteristic of dehydration, decarboxylation and dealkylation was commonly observed.

Compound	Formula	[M-H] ⁻ (m/z)	Mass spectral match		Fragment ions (m/z)	
			MzCloud	Chemspider	MS ² (loss moiety)	MS ³ (loss moiety)
10-Hydroxydecanoic acid	C ₁₀ H ₁₉ O ₃	187.1337	Full	Full	169.1230 (-H ₂ O) 141.1281 (-CH ₂ O ₂) 125.0967 (-CH ₂ O ₃)	113.1333 (-C ₃ H ₆ O ₂)
Undecanoic acid	C ₁₁ H ₂₁ O ₂	185.1543	Full	Full	167.0710 (-H ₂ O) 141.0917 (-CO ₂) 123.0811 (-C ₃ H ₁₀ O)	
Dodecanedioic acid	C ₁₂ H ₂₁ O ₄	229.1440	Full	Full	211.1335 (-H ₂ O) 167.1437 (-CH ₂ O ₃)	139.0811 (-C ₃ H ₁₀ O)
Tridecanoic acid	C ₁₃ H ₂₅ O ₂	213.1856	Full	Full	195.1023 (-H ₂ O) 169.1020 (-C ₃ H ₈) 151.1126 (-C ₃ H ₁₀ O)	
10-Propoxydecanoic acid	C ₁₃ H ₂₅ O ₃	229.1803	Full	Full	211.1699 (-H ₂ O) 183.1750 (-CO) 167.1438 (-C ₂ H ₆ O ₂)	
Tetradecanoic acid	C ₁₄ H ₂₇ O ₂	227.2012	Full	Full	209.1178 (-H ₂ O) 183.1175 (-CO ₂) 165.1218 (-C ₃ H ₁₀ O)	
14-Hydroxytetradecanoic acid	C ₁₄ H ₂₇ O ₃	243.1960	Full	Partial	225.1855 (-H ₂ O) 197.1906 (-CH ₂ O ₂) 183.1749 (-C ₂ H ₄ O ₂)	
Tetradecanedioic acid	C ₁₄ H ₂₅ O ₄	257.1753	Full	Full	239.1647 (-H ₂ O) 213.1855 (-CO ₂)	

15-Hydroxypentadecanoic acid	$C_{15}H_{29}O_3$	257.2117	No	Full	195.1750 (-CH ₂ O ₃) 239.2011 (-H ₂ O) 211.2062 (-CH ₂ O ₂) 197.1907 (-C ₂ H ₄ O ₂) 195.1950 (-C ₂ H ₆ O ₂)	
Hexadecandioic acid	$C_{16}H_{29}O_4$	285.2065	No	Full	267.1960 (-H ₂ O) 241.2168 (-CO ₂) 223.2062 (-CH ₂ O ₃) 195.1950 (-C ₃ H ₆ O ₃)	
8-Hydroxyhexadecanedioic acid	$C_{16}H_{29}O_5$	301.2020	No	Full	283.1908 (-H ₂ O) 265.1803 (-H ₄ O ₂) 239.2010 (-CH ₂ O ₃) 221.1905 (-CH ₄ O ₄)	
Heptadecanedioic acid	$C_{17}H_{31}O_4$	299.2222	No	Full	281.2116 (-H ₂ O) 255.2324 (-CO ₂) 237.2218 (-CH ₂ O ₃)	209.1333 (-C ₂ H ₂ O ₄)
(15Z)-9,12,13-trihydroxy-15-octadecenoic acid	$C_{18}H_{33}O_5$	329.2333	Full	Full	311.2221 (-H ₂ O) 293.2117 (-H ₄ O ₂) 267.2322 (-CH ₂ O ₃) 249.2219 (-CH ₄ O ₄)	
Icosanedioic acid	$C_{20}H_{37}O_4$	341.2693	No	Full	323.2587 (-H ₂ O) 297.2431 (-C ₂ H ₄ O) 279.2689 (-CH ₂ O ₃)	

Figure 4.7 shows the evolution of the carboxylic acids during the study for each bacterial strain. The results demonstrate that the carboxylic acids were transient. In some cases, such as, 14-hydroxytetradecanoic acid was detected only on day 3 for *Novosphingobium* sp. S1 and *G. amicalis* S2 but was at relatively the same level for *G. terrae* S5 during day 3 and 5. 10-propoxydecanoic acid, tetradecanoic acid and (15Z)-9,12,13-trihydroxy-15-octadecenoic acid were not detected for *Novosphingobium* sp. S1.

4.4 Conclusion

The biodegradation of a wide range of hydrocarbons is a desirable characteristic for enhancing the bioremediation oil pollution. This study demonstrated the high capacity of *Novosphingobium* sp. S1, *Gordonia amicalis* S2 and *Gordonia terrae* S5 to utilize a wide spectrum of the alkanes present in the Congo Bilondo crude oil. Furthermore, the comprehensive determination of produced carboxylic acids was diagnostic for specific alkanes degradation and it permitted the identification of the bi-terminal oxidation pathway as the most likely pathway used by the strains. Finally, the results highlight the potential application of the strains in bioremediation of crude oil contaminated sites.

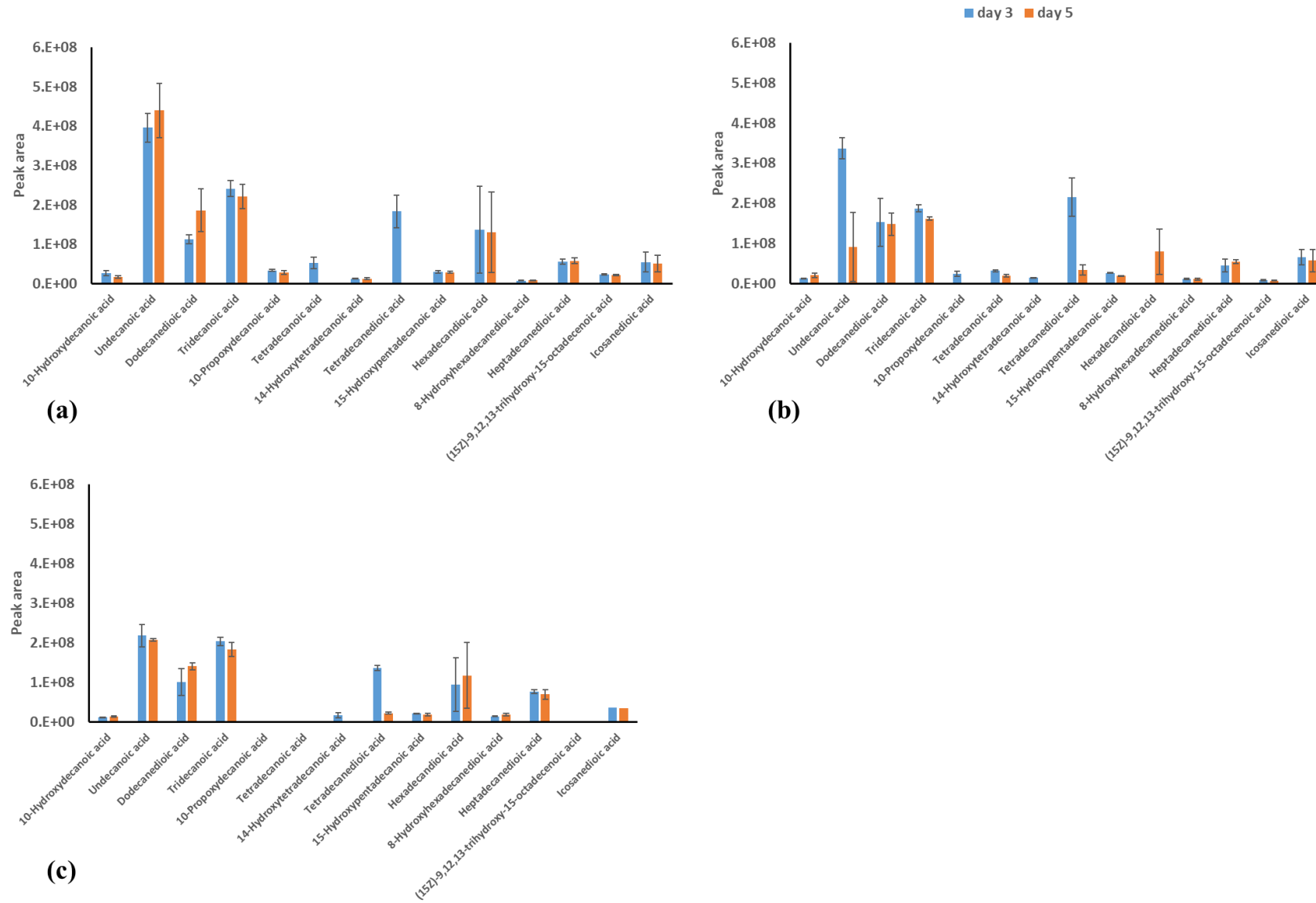


Figure 4.7: Levels of carboxylic acids in culture medium of (a) *Novosphingobium* sp. S1 (b) *Gordonia amicalis* S2 and (c) *Gordonia terrae* S5 on day 3 and 5.

Chapter five

Conclusions and perspectives

5. Conclusions and perspectives

The energy and economic benefits of crude oil as well as the health and environmental impact of crude oil spill cannot be overemphasized. Decades of research have clearly demonstrated that microbial degradation remains the viable, efficient, eco-friendly, and economical alternative to cleaning up crude oil spill. Consequently, in recent times, focus has shifted to improving the efficiency of the degradation process. This interest has further driven the search for strains with versatile metabolic capability to access, assimilate and degrade hydrocarbons. Furthermore, elucidation of hydrocarbon degradation mechanisms and pathways through the characterization of signatures metabolites, such as carboxylic acids, produced during the degradation process has become crucial to designing more efficient bioremediation strategies. This has been supported by the extensive and robust developments of analytical platforms, particularly in terms of chromatographic and mass spectrometric methods.

The three bacteria, *Novosphingobium* sp. S1, *Gordonia amicalis* S2 and *Gordonia terrae* S5, isolated from a crude oil polluted soil showed high potential to degrade a wide range of saturated hydrocarbons. The isolation and characterization of bacteria with the capacity to degrade a wide range of hydrocarbons is of crucial importance for bioremediation of crude oil contamination. Although none of the strains produced biosurfactant into the culture medium, growth occurred only when the cells had access to the alkane-water interface through biofilm formation. This interfacial access to alkanes was also supported by the ability of the strains to adhere to hydrocarbons, with the *Gordonia* species exhibiting a much stronger adhesion than *Novosphingobium* sp. S1. Furthermore, the ability of *G. amicalis* S2 and *G. terrae* S5 to adhere to alkanes was an important property of these strains to form a biofilm and utilize hydrocarbons as carbon and energy source.

The comprehensive determination of carboxylic acid metabolites in culture medium by LC-MS during degradation of alkanes provided sufficient information to elucidate the degradative pathway adopted. The series of mono-, hydroxy- and dicarboxylic acids found in this study confirmed the active biodegradation of the alkanes and suggested that their degradation was via the bi-terminal oxidation or dicarboxylic acid pathway. Likewise, the production of hydroxylated fatty acid was also suggested as a possible strategy that increased the affinity of *Novosphingobium* sp. S1 during *n*-hexadecane degradation.

Finally, the study highlights the potential of *Novosphingobium* sp. S1, *G. amicalis* S2 and *G. terrae* S5 for the development of bioremediation technologies of hydrocarbon-contaminated sites. Biofilm-mediated bioremediation is a promising approach for efficient hydrocarbon cleanup.

Indeed, biofilm formation and the planktonic-biofilm transition are complex and highly regulated processes. High-throughput genomics approaches are necessary to provide a large array of information on biofilm modulating genes and regulation mechanism. Understanding these mechanisms and the enzymes and/or gene involved would immensely contribute to the development of new strategies for bioremediation of hydrocarbons.

As the development of metabolomics and petroleomics continues, further progress in MS and chromatographic techniques is expected. The democratization of FT-ICR MS, as a standalone technique or as a detector for GC or HPLC, would result in the acquisition of comprehensive characterization data soon. Additionally, the ongoing developments in Orbitrap and TOF MS would offer attractive and effective alternatives for direct infusion ultra-high-resolution analysis. This, in combination with metagenomic data, is likely to facilitate the identification of metabolic pathways leading to the development of efficient and eco-friendly bioremediation technologies.

The aim of crude oil bioremediation is to degrade the toxic hydrocarbons into CO₂ and H₂O or convert them into non-toxic forms. However, biodegradation can sometimes result into incomplete mineralization and formation of metabolites with poorly recognized or unknown chemical and toxicological characteristics. Moreover, these metabolites can become increasingly polar and bioavailable posing more danger to health and the environment. Chemical analysis does not always consider the effects of these metabolites and practical information on the bioavailability of these metabolites is also not sufficiently covered. Thus, it would be imperative to complement chemical analysis by monitoring ecotoxicity of biodegraded oil.

Scientific publications and communications

Journal publications

- **Kevin Iyere Ehiosun**, Régis Grimaud, Ryszard Lobinski
Mass spectrometric analysis for carboxylic acids as viable markers of petroleum hydrocarbon biodegradation. *Trends in Environmental Analytical Chemistry* (under review).
- **Kevin Iyere Ehiosun**, Simon Godin, Laurent Urios, Ryszard Lobinski, Régis Grimaud
Degradation of long-chain alkanes through biofilm formation by bacteria isolated from oil-polluted soil. *International Biodeterioration and Biodegradation* (under review).
- Biodegradation of saturated fraction of crude oil and signature carboxylic acids production (to be submitted soon).

Oral communications

- **Kevin Iyere Ehiosun**, Régis Grimaud, Ryszard Lobinski
Hydrocarbonoclastic bacteria isolated from oil-polluted soil degrade long-chain alkanes through biofilm formation.
3rd International Environmental Chemistry (EnviroChem) Congress, Kemer–Antalya, Turkey, 01-04 November 2021.
- **Kevin.I. Ehiosun** and Ryszard Lobinski
Mass spectrometry insights into hydrocarbon biodegradation: from natural bioattenuation to bioremediation technologies.
CAPES/PrInt workshop, Universidade Federal de Santa Maria, Brazil. 28 October 2021.

References

- [1] J.G. Speight, Sources and Types of Organic Pollutants, in: J.G. Speight (Ed.), *Environ. Org. Chem. Eng.*, Elsevier, 2017: pp. 153–201. <https://doi.org/10.1016/B978-0-12-804492-6.00004-6>.
- [2] Y. Teng, W. Chen, Soil Microbiomes—a Promising Strategy for Contaminated Soil Remediation: A Review, *Pedosphere*. 29 (2019) 283–297. [https://doi.org/10.1016/S1002-0160\(18\)60061-X](https://doi.org/10.1016/S1002-0160(18)60061-X).
- [3] M. Baniasadi, S.M. Mousavi, A Comprehensive Review on the Bioremediation of Oil Spills, in: *Microb. Action Hydrocarb.*, Springer Singapore, Singapore, 2018: pp. 223–254. https://doi.org/10.1007/978-981-13-1840-5_10.
- [4] C. Pasparakis, A.J. Esbaugh, W. Burggren, M. Grosell, Impacts of deepwater horizon oil on fish, *Comp. Biochem. Physiol. Part - C Toxicol. Pharmacol.* 224 (2019) 108558. <https://doi.org/10.1016/j.cbpc.2019.06.002>.
- [5] J.T. Magnuson, N.M. Bautista, J. Lucero, A.K. Lund, E.G. Xu, D. Schlenk, W.W. Burggren, A.P. Roberts, Exposure to Crude Oil Induces Retinal Apoptosis and Impairs Visual Function in Fish, *Environ. Sci. Technol.* 54 (2020) 2843–2850. <https://doi.org/10.1021/acs.est.9b07658>.
- [6] O. Idowu, K.T. Semple, K. Ramadass, W. O’Connor, P. Hansbro, P. Thavamani, Beyond the obvious: Environmental health implications of polar polycyclic aromatic hydrocarbons, *Environ. Int.* 123 (2019) 543–557. <https://doi.org/10.1016/j.envint.2018.12.051>.
- [7] J. van Dorst, S.D. Siciliano, T. Winsley, I. Snape, B.C. Ferrari, Bacterial targets as potential indicators of diesel fuel toxicity in subantarctic soils, *Appl. Environ. Microbiol.* 80 (2014) 4021–4033. <https://doi.org/10.1128/AEM.03939-13>.
- [8] S.J. Varjani, Microbial degradation of petroleum hydrocarbons, *Bioresour. Technol.* 223 (2017) 277–286. <https://doi.org/10.1016/j.biortech.2016.10.037>.
- [9] L. Meng, W. Li, M. Bao, P. Sun, Promoting the treatment of crude oil alkane pollution through the study of enzyme activity, *Int. J. Biol. Macromol.* 119 (2018) 708–716. <https://doi.org/10.1016/j.ijbiomac.2018.07.160>.
- [10] J. V. Headley, K.M. Peru, M.P. Barrow, Advances in mass spectrometric characterization of naphthenic acids fraction compounds in oil sands environmental samples and crude oil-A review, *Mass Spectrom. Rev.* 35 (2016) 311–328. <https://doi.org/10.1002/mas.21472>.
- [11] A. V Callaghan, Metabolomic investigations of anaerobic hydrocarbon-impacted environments, *Curr. Opin. Biotechnol.* 24 (2013) 506–515. <https://doi.org/10.1016/j.copbio.2012.08.012>.
- [12] E. Overton, T. Wade, J. Radovic, B. Meyer, M.S. Miles, S. Larter, Chemical Composition of Macondo and Other Crude Oils and Compositional Alterations During Oil Spills, *Oceanography*. 29 (2016) 50–63. <https://doi.org/10.5670/oceanog.2016.62>.
- [13] R.M. Hlihor, M. Gavrilesco, T. Tavares, L. Favier, G. Olivieri, Bioremediation: An Overview on Current Practices, Advances, and New Perspectives in Environmental Pollution Treatment, *Biomed Res. Int.* 2017 (2017) 1–2. <https://doi.org/10.1155/2017/6327610>.

- [14] I. V. Chernushevich, A. V. Loboda, B.A. Thomson, An introduction to quadrupole-time-of-flight mass spectrometry, *J. Mass Spectrom.* 36 (2001) 849–865. <https://doi.org/10.1002/jms.207>.
- [15] M. Wei Lim, E. Von Lau, P. Eong Poh, A comprehensive guide of remediation technologies for oil contaminated soil-Present works and future directions, (2016). <https://doi.org/10.1016/j.marpolbul.2016.04.023>.
- [16] N. Das, P. Chandran, Microbial Degradation of Petroleum Hydrocarbon Contaminants: An Overview, *Biotechnol. Res. Int.* 2011 (2011) 1–13. <https://doi.org/10.4061/2011/941810>.
- [17] F.M. Olajuyigbe, K.I. Ehiosun, Assessment of crude oil degradation efficiency of newly isolated actinobacteria reveals untapped bioremediation potentials, *Bioremediat. J.* 20 (2016) 133–143. <https://doi.org/10.1080/10889868.2015.1113926>.
- [18] H.P. Bacosa, K. Suto, C. Inoue, Bacterial community dynamics during the preferential degradation of aromatic hydrocarbons by a microbial consortium, *Int. Biodeterior. Biodegrad.* 74 (2012) 109–115. <https://doi.org/10.1016/j.ibiod.2012.04.022>.
- [19] S. Maitra, IN SITU BIOREMEDIATION-AN OVERVIEW, (2018). <https://doi.org/10.26479/2018.0406.45>.
- [20] M. Megharaj, B. Ramakrishnan, K. Venkateswarlu, N. Sethunathan, R. Naidu, Bioremediation approaches for organic pollutants: A critical perspective, (2011). <https://doi.org/10.1016/j.envint.2011.06.003>.
- [21] I. Declercq, V. Cappuyns, Y. Duclos, Monitored natural attenuation (MNA) of contaminated soils: State of the art in Europe-A critical evaluation, *Sci. Total Environ.* 426 (2012) 393–405. <https://doi.org/10.1016/j.scitotenv.2012.03.040>.
- [22] A. Dzionek, D. Wojcieszńska, U. Guzik, Natural carriers in bioremediation: A review, *Electron. J. Biotechnol.* 23 (2016) 28–36. <https://doi.org/10.1016/j.ejbt.2016.07.003>.
- [23] M. Wu, J. Wu, X. Zhang, X. Ye, Effect of bioaugmentation and biostimulation on hydrocarbon degradation and microbial community composition in petroleum-contaminated loessal soil, *Chemosphere.* 237 (2019) 124456. <https://doi.org/10.1016/j.chemosphere.2019.124456>.
- [24] C.C. Azubuiké, C.B. Chikere, G.C. Okpokwasili, Bioremediation techniques—classification based on site of application: principles, advantages, limitations and prospects, *World J. Microbiol. Biotechnol.* 32 (2016) 180. <https://doi.org/10.1007/s11274-016-2137-x>.
- [25] D. Ghosal, S. Ghosh, T.K. Dutta, Y. Ahn, Current state of knowledge in microbial degradation of polycyclic aromatic hydrocarbons (PAHs): A review, *Front. Microbiol.* 7 (2016). <https://doi.org/10.3389/fmicb.2016.01369>.
- [26] J.-Q. Sun, L. Xu, X.-Y. Liu, G.-F. Zhao, H. Cai, Y. Nie, X.-L. Wu, Functional Genetic Diversity and Culturability of Petroleum-Degrading Bacteria Isolated From Oil-Contaminated Soils, *Front. Microbiol.* 9 (2018). <https://doi.org/10.3389/fmicb.2018.01332>.
- [27] P. Sarkar, A. Roy, S. Pal, B. Mohapatra, S.K. Kazy, M.K. Maiti, P. Sar, Enrichment and characterization of hydrocarbon-degrading bacteria from petroleum refinery waste as potent bioaugmentation agent for in situ bioremediation, *Bioresour. Technol.* 242 (2017) 15–27. <https://doi.org/10.1016/j.biortech.2017.05.010>.
- [28] F. Abbasian, T. Palanisami, M. Megharaj, R. Naidu, R. Lockington, K. Ramadass,

- Microbial diversity and hydrocarbon degrading gene capacity of a crude oil field soil as determined by metagenomics analysis, *Biotechnol. Prog.* 32 (2016) 638–648. <https://doi.org/10.1002/btpr.2249>.
- [29] T.L. Ataikiru, B.F. Okorhi-damisa, J.I. Akpaiboh, Microbial community structure of an oil polluted site in Effurun, Nigeria, *Int. Res. J. Public Environ. Heal.* 4 (2017) 41–47. <https://doi.org/10.15739/irjpeh.17.006>.
- [30] C.B. Chikere, I.J. Mordi, B.O. Chikere, R. Selvarajan, T.O. Ashafa, C.C. Obieze, Comparative metagenomics and functional profiling of crude oil-polluted soils in Bodo West Community, Ogoni, with other sites of varying pollution history, *Ann. Microbiol.* 69 (2019) 495–513. <https://doi.org/10.1007/s13213-019-1438-3>.
- [31] S. Fuentes, B. Barra, J. Gregory Caporaso, M. Seeger, From rare to dominant: A fine-tuned soil bacterial bloom during petroleum hydrocarbon bioremediation, *Appl. Environ. Microbiol.* 82 (2016) 888–896. <https://doi.org/10.1128/AEM.02625-15>.
- [32] S. Pal, A. Roy, S.K. Kazy, Exploring Microbial Diversity and Function in Petroleum Hydrocarbon Associated Environments Through Omics Approaches, in: S. Das, H.R. Dash (Eds.), *Microb. Divers. Genomic Era*, Elsevier, 2019: pp. 171–194. <https://doi.org/10.1016/b978-0-12-814849-5.00011-3>.
- [33] A.P. Napp, J.E.S. Pereira, J.S. Oliveira, R.C.B. Silva-Portela, L.F. Agnez-Lima, M.C.R. Peralba, F.M. Bento, L.M.P. Passaglia, C.E. Thompson, M.H. Vainstein, Comparative metagenomics reveals different hydrocarbon degradative abilities from enriched oil-drilling waste, *Chemosphere.* 209 (2018) 7–16. <https://doi.org/10.1016/j.chemosphere.2018.06.068>.
- [34] A.B. Patel, T. Manvar, K.R. Jain, C. Desai, D. Madamwar, Metagenomic insights into bacterial communities' structures in polycyclic aromatic hydrocarbons degrading consortia, *J. Environ. Chem. Eng.* 9 (2021) 106578. <https://doi.org/10.1016/j.jece.2021.106578>.
- [35] H. Chandran, M. Meena, K. Sharma, Microbial Biodiversity and Bioremediation Assessment Through Omics Approaches, *Front. Environ. Chem.* 1 (2020). <https://doi.org/10.3389/FENVC.2020.570326/FULL>.
- [36] M. Barbato, F. Mapelli, E. Crotti, D. Daffonchio, S. Borin, Cultivable hydrocarbon degrading bacteria have low phylogenetic diversity but highly versatile functional potential, *Int. Biodeterior. Biodegradation.* 142 (2019) 43–51. <https://doi.org/10.1016/j.ibiod.2019.04.012>.
- [37] F.O.P. Stefani, T.H. Bell, C. Marchand, I.E. De La Providencia, A. El Yassimi, M. St-Arnaud, M. Hijri, Culture-dependent and -independent methods capture different microbial community fractions in hydrocarbon-contaminated soils, *PLoS One.* 10 (2015) 1–16. <https://doi.org/10.1371/journal.pone.0128272>.
- [38] D. Ribicic, R. Netzer, A. Winkler, O.G. Brakstad, Comparison of microbial community dynamics induced by distinct crude oil dispersions reveals compositional differences, *J. Sea Res.* 141 (2018) 112–118. <https://doi.org/10.1016/j.seares.2018.09.001>.
- [39] W. Sun, Y. Dong, P. Gao, M. Fu, K. Ta, J. Li, Microbial communities inhabiting oil-contaminated soils from two major oilfields in Northern China: Implications for active petroleum-degrading capacity, *J. Microbiol.* 53 (2015) 371–378. <https://doi.org/10.1007/s12275-015-5023-6>.
- [40] Y. Wang, Q. Wang, L. Liu, Crude oil degrading fingerprint and the overexpression of

- oxidase and invasive genes for n-hexadecane and crude oil degradation in the acinetobacter pittii H9-3 strain, *Int. J. Environ. Res. Public Health*. 16 (2019). <https://doi.org/10.3390/ijerph16020188>.
- [41] Y. Pan, Y. Liao, Q. Shi, Variations of Acidic Compounds in Crude Oil during Simulated Aerobic Biodegradation: Monitored by Semiquantitative Negative-Ion ESI FT-ICR MS, *Energy & Fuels*. 31 (2017) 1126–1135. <https://doi.org/10.1021/acs.energyfuels.6b02167>.
- [42] S. Muthukamalam, S. Sivagangavathi, D. Dhrishya, S. Sudha Rani, Characterization of dioxygenases and biosurfactants produced by crude oil degrading soil bacteria, *Brazilian J. Microbiol.* 48 (2017) 637–647. <https://doi.org/10.1016/j.bjm.2017.02.007>.
- [43] S.S. Varma, M.B. Lakshmi, P. Rajagopal, M. Velan, Degradation of total petroleum hydrocarbon(TPH) in contaminated soil using *Bacillus pumilus* MVSV3, *Biocontrol Sci.* 22 (2017) 17–23. <https://doi.org/10.4265/bio.22.17>.
- [44] H. Sowani, A. Deshpande, V. Gupta, M. Kulkarni, S. Zinjarde, Biodegradation of squalene and n-hexadecane by *Gordonia amicalis* HS-11 with concomitant formation of biosurfactant and carotenoids, *Int. Biodeterior. Biodegrad.* 142 (2019) 172–181. <https://doi.org/10.1016/j.ibiod.2019.05.005>.
- [45] W. Tao, J. Lin, W. Wang, H. Huang, S. Li, Biodegradation of aliphatic and polycyclic aromatic hydrocarbons by the thermophilic bioemulsifier-producing *Aeribacillus pallidus* strain SL-1, *Ecotoxicol. Environ. Saf.* 189 (2020) 109994. <https://doi.org/10.1016/j.ecoenv.2019.109994>.
- [46] Y. Liu, Y.Y. Wan, C. Wang, Z. Ma, X. Liu, S. Li, Biodegradation of n-alkanes in crude oil by three identified bacterial strains, *Fuel*. 275 (2020) 117897. <https://doi.org/10.1016/j.fuel.2020.117897>.
- [47] D. Wang, J. Lin, J. Lin, W. Wang, S. Li, Biodegradation of Petroleum Hydrocarbons by *Bacillus subtilis* BL-27, a Strain with Weak Hydrophobicity, *Molecules*. 24 (2019) 3021. <https://doi.org/10.3390/molecules24173021>.
- [48] C. Li, Z.X. Zhou, X.Q. Jia, Y. Chen, J. Liu, J.P. Wen, Biodegradation of crude oil by a newly isolated strain *rhodococcus* sp. JZX-01, *Appl. Biochem. Biotechnol.* 171 (2013) 1715–1725. <https://doi.org/10.1007/s12010-013-0451-4>.
- [49] X. Jia, Y. He, L. Huang, D. Jiang, W. Lu, n-Hexadecane and pyrene biodegradation and metabolization by *Rhodococcus* sp. T1 isolated from oil contaminated soil ☆, (2018). <https://doi.org/10.1016/j.cjche.2018.03.034>.
- [50] V.B. Ferrari, A. Cesar, R. Cayô, R.B. Choueri, D.N. Okamoto, J.G. Freitas, M. Favero, A.C. Gales, C. V Niero, F.T. Saia, S.P. de Vasconcellos, Hexadecane biodegradation of high efficiency by bacterial isolates from Santos Basin sediments, *Mar. Pollut. Bull.* 142 (2019) 309–314. <https://doi.org/10.1016/j.marpolbul.2019.03.050>.
- [51] P. Elumalai, P. Parthipan, O.P. Karthikeyan, A. Rajasekar, Enzyme-mediated biodegradation of long-chain n-alkanes (C32 and C40) by thermophilic bacteria, *3 Biotech.* 7 (2017) 116. <https://doi.org/10.1007/s13205-017-0773-y>.
- [52] J. Trögl, C. Esuola, S. Kříženecká, P. Kuráň, L. Seidlová, P. Veronesi-Dáňová, J. Popelka, O. Babalola, P. Hrabák, M. Czinnerová, E. Kakosová, A. Ševců, D. Tischler, Biodegradation of High Concentrations of Aliphatic Hydrocarbons in Soil from a Petroleum Refinery: Implications for Applicability of New Actinobacterial Strains, *Appl.*

- Sci. 8 (2018) 1855. <https://doi.org/10.3390/app8101855>.
- [53] A. Ganesh Kumar, N. Nivedha Rajan, R. Kirubakaran, G. Dharani, Biodegradation of crude oil using self-immobilized hydrocarbonoclastic deep sea bacterial consortium, *Mar. Pollut. Bull.* 146 (2019) 741–750. <https://doi.org/10.1016/j.marpolbul.2019.07.006>.
- [54] M. Lin, X. Hu, W. Chen, H. Wang, C. Wang, Biodegradation of phenanthrene by *Pseudomonas* sp: BZ-3, isolated from crude oil contaminated soil, *Int. Biodeterior. Biodegrad.* 94 (2014) 176–181. <https://doi.org/10.1016/j.ibiod.2014.07.011>.
- [55] C. Balachandran, V. Duraipandiyar, K. Balakrishna, S. Ignacimuthu, Petroleum and polycyclic aromatic hydrocarbons (PAHs) degradation and naphthalene metabolism in *Streptomyces* sp. (ERI-CPDA-1) isolated from oil contaminated soil, *Bioresour. Technol.* 112 (2012) 83–90. <https://doi.org/10.1016/j.biortech.2012.02.059>.
- [56] J. Wang, J. Wang, Z. Zhang, Y. Li, B. Zhang, Z. Zhang, G. Zhang, Cold-adapted bacteria for bioremediation of crude oil-contaminated soil, *J. Chem. Technol. Biotechnol.* 91 (2016) 2286–2297. <https://doi.org/10.1002/jctb.4814>.
- [57] G.T. Mehetre, S.G. Dastager, M.S. Dharne, Biodegradation of mixed polycyclic aromatic hydrocarbons by pure and mixed cultures of biosurfactant producing thermophilic and thermo-tolerant bacteria, *Sci. Total Environ.* 679 (2019) 52–60. <https://doi.org/10.1016/j.scitotenv.2019.04.376>.
- [58] S. Mallick, Biodegradation of acenaphthene by *Sphingobacterium* sp. strain RTSB involving trans-3-carboxy-2-hydroxybenzylidenepyruvic acid as a metabolite, *Chemosphere.* 219 (2019) 748–755. <https://doi.org/10.1016/j.chemosphere.2018.12.046>.
- [59] Y. Lyu, W. Zheng, T. Zheng, Y. Tian, Biodegradation of Polycyclic Aromatic Hydrocarbons by *Novosphingobium pentaromativorans* US6-1, *PLoS One.* 9 (2014) 101438. <https://doi.org/10.1371/journal.pone.0101438>.
- [60] I. Ghosh, J. Jasmine, S. Mukherji, Biodegradation of pyrene by a *Pseudomonas aeruginosa* strain RS1 isolated from refinery sludge, (2014). <https://doi.org/10.1016/j.biortech.2014.05.074>.
- [61] D.A. Al Farraj, R.M. Alkufeidy, N.A. Alkubaisi, M.K. Alshammari, Polynuclear aromatic anthracene biodegradation by psychrophilic *Sphingomonas* sp., cultivated with tween-80, *Chemosphere.* 263 (2021) 128115. <https://doi.org/10.1016/j.chemosphere.2020.128115>.
- [62] A. Wongbunmak, S. Khiawjan, M. Suphantharika, T. Pongtharangkul, BTEX biodegradation by *Bacillus amyloliquefaciens* subsp. *plantarum* W1 and its proposed BTEX biodegradation pathways, *Sci. Rep.* 10 (2020) 17408. <https://doi.org/10.1038/s41598-020-74570-3>.
- [63] H. Gao, J. Zhang, H. Lai, Q. Xue, Degradation of asphaltenes by two *Pseudomonas aeruginosa* strains and their effects on physicochemical properties of crude oil, *Int. Biodeterior. Biodegrad.* 122 (2017) 12–22. <https://doi.org/10.1016/j.ibiod.2017.04.010>.
- [64] Y. Shahebrahimi, A. Fazlali, H. Motamedi, S. Kord, Experimental and Modeling Study on Precipitated Asphaltene Biodegradation Process Using Isolated Indigenous Bacteria, *Ind. Eng. Chem. Res.* 57 (2018) 17064–17075. <https://doi.org/10.1021/acs.iecr.8b04661>.
- [65] Y. Liu, Y.Y. Wan, Y. Zhu, C. Fei, Z. Shen, Y. Ying, Impact of Biodegradation on Polar Compounds in Crude Oil: Comparative Simulation of Biodegradation from Two Aerobic

- Bacteria Using Ultrahigh-Resolution Mass Spectrometry, *Energy & Fuels*. 34 (2020) 5553–5565. <https://doi.org/10.1021/acs.energyfuels.0c00030>.
- [66] M. Mahjoubi, S. Cappello, Y. Souissi, A. Jaouani, A. Cherif, Microbial Bioremediation of Petroleum Hydrocarbon– Contaminated Marine Environments, in: *Recent Insights Pet. Sci. Eng., InTech*, 2018: p. 13. <https://doi.org/10.5772/intechopen.72207>.
- [67] H. Harms, K.E.C. Smith, L.Y. Wick, Introduction: Problems of Hydrophobicity/Bioavailability, in: *Handb. Hydrocarb. Lipid Microbiol.*, Springer Berlin Heidelberg, Berlin, Heidelberg, 2010: pp. 1437–1450. https://doi.org/10.1007/978-3-540-77587-4_98.
- [68] S. Kuppusamy, N.R. Maddela, M. Megharaj, K. Venkateswarlu, Bioavailability of Total Petroleum Hydrocarbons, *Total Pet. Hydrocarb.* (2020) 79–94. https://doi.org/10.1007/978-3-030-24035-6_4.
- [69] H. Harms, K.E.C. Smith, L.Y. Wick, Problems of Hydrophobicity/Bioavailability: An Introduction, in: *Cell. Ecophysiol. Microbe*, Springer International Publishing, Cham, 2017: pp. 1–13. https://doi.org/10.1007/978-3-319-20796-4_38-1.
- [70] A.P. Karlapudi, T.C. Venkateswarulu, J. Tammineedi, L. Kanumuri, B.K. Ravuru, V. ramu Dirisala, V.P. Kodali, Role of biosurfactants in bioremediation of oil pollution-a review, *Petroleum*. 4 (2018) 241–249. <https://doi.org/10.1016/j.petlm.2018.03.007>.
- [71] K. Gupta, Biosurfactant-based bioremediation of soil and aquatic contaminants, Elsevier Inc., 2021. <https://doi.org/10.1016/b978-0-12-822696-4.00002-4>.
- [72] A. Ebadi, M. Olamaee, N.A. Khoshkholgh Sima, R. Ghorbani Nasrabadi, M. Hashemi, Isolation and Characterization of Biosurfactant Producing and Crude Oil Degrading Bacteria from Oil Contaminated Soils, Iran. *J. Sci. Technol. Trans. A Sci.* 42 (2018) 1149–1156. <https://doi.org/10.1007/s40995-017-0162-8>.
- [73] W. Sun, W. Cao, M. Jiang, G. Saren, J. Liu, J. Cao, I. Ali, X. Yu, C. Peng, I. Naz, Isolation and characterization of biosurfactant-producing and diesel oil degrading *Pseudomonas* sp. CQ2 from Changqing oil field, China, *RSC Adv.* 8 (2018) 39710–39720. <https://doi.org/10.1039/C8RA07721E>.
- [74] L. Domdi, A.K. Lakra, K. Mohan, Y.M. Tilwani, N. Jha, V. Arul, Microbial degradation of n-hexadecane using *Pseudomonas aeruginosa* PU1 isolated from transformer-oil contaminated soil, *Biocatal. Agric. Biotechnol.* 38 (2021) 102213. <https://doi.org/10.1016/j.bcab.2021.102213>.
- [75] E.C. Souza, T.C. Vessoni-Penna, R.P. de Souza Oliveira, Biosurfactant-enhanced hydrocarbon bioremediation: An overview, *Int. Biodeterior. Biodegradation.* 89 (2014) 88–94. <https://doi.org/10.1016/j.ibiod.2014.01.007>.
- [76] O. Marchut-Mikolajczyk, P. Drozdzyński, D. Pietrzyk, T. Antczak, Biosurfactant production and hydrocarbon degradation activity of endophytic bacteria isolated from *Chelidonium majus* L. 06 Biological Sciences 0605 Microbiology 06 Biological Sciences 0607 Plant Biology 09 Engineering 0907 Environmental Engineering, *Microb. Cell Fact.* 17 (2018) 171. <https://doi.org/10.1186/s12934-018-1017-5>.
- [77] Y. Wu, M. Xu, J. Xue, K. Shi, M. Gu, Characterization and Enhanced Degradation Potentials of Biosurfactant-Producing Bacteria Isolated from a Marine Environment, *ACS Omega.* 4 (2019) 1645–1651. <https://doi.org/10.1021/acsomega.8b02653>.

- [78] F.A. Bezza, E.M. Nkhambayausi Chirwa, Biosurfactant-enhanced bioremediation of aged polycyclic aromatic hydrocarbons (PAHs) in creosote contaminated soil, *Chemosphere*. 144 (2016) 635–644. <https://doi.org/10.1016/j.chemosphere.2015.08.027>.
- [79] D.W. Lee, H. Lee, B.O. Kwon, J.S. Khim, U.H. Yim, B.S. Kim, J.J. Kim, Biosurfactant-assisted bioremediation of crude oil by indigenous bacteria isolated from Taean beach sediment, *Environ. Pollut.* 241 (2018) 254–264. <https://doi.org/10.1016/j.envpol.2018.05.070>.
- [80] S. Joy, P.K.S.M. Rahman, S. Sharma, Biosurfactant production and concomitant hydrocarbon degradation potentials of bacteria isolated from extreme and hydrocarbon contaminated environments, *Chem. Eng. J.* 317 (2017) 232–241. <https://doi.org/10.1016/j.cej.2017.02.054>.
- [81] B. Tuleva, N. Christova, R. Cohen, D. Antonova, T. Todorov, I. Stoineva, Isolation and characterization of trehalose tetraester biosurfactants from a soil strain *Micrococcus luteus* BN56, *Process Biochem.* 44 (2009) 135–141. <https://doi.org/10.1016/j.procbio.2008.09.016>.
- [82] A. Franzetti, P. Caredda, P. La Colla, M. Pintus, E. Tamburini, M. Papacchini, G. Bestetti, Cultural factors affecting biosurfactant production by *Gordonia* sp. BS29, *Int. Biodeterior. Biodegradation*. 63 (2009) 943–947. <https://doi.org/10.1016/j.ibiod.2009.06.001>.
- [83] A. Medić, M. Lješević, H. Inui, V. Beškoski, I. Kojić, K. Stojanović, I. Karadžić, Efficient biodegradation of petroleum: N -alkanes and polycyclic aromatic hydrocarbons by polyextremophilic *Pseudomonas aeruginosa* strain ai with multidegradative capacity, *RSC Adv.* 10 (2020) 14060–14070. <https://doi.org/10.1039/c9ra10371f>.
- [84] A.M. Abdel-Mawgoud, M.M. Aboulwafa, N.A.-H. Hassouna, Optimization of Surfactin Production by *Bacillus subtilis* Isolate BS5, *Appl. Biochem. Biotechnol.* 150 (2008) 305–325. <https://doi.org/10.1007/s12010-008-8155-x>.
- [85] R. Thavasi, V.R.M. Subramanyam Nambaru, S. Jayalakshmi, T. Balasubramanian, I.M. Banat, Biosurfactant Production by *Azotobacter chroococcum* Isolated from the Marine Environment, *Mar. Biotechnol.* 11 (2009) 551–556. <https://doi.org/10.1007/s10126-008-9162-1>.
- [86] F. Peng, Y. Wang, F. Sun, Z. Liu, Q. Lai, Z. Shao, A novel lipopeptide produced by a Pacific Ocean deep-sea bacterium, *Rhodococcus* sp. TW53, *J. Appl. Microbiol.* 105 (2008) 698–705. <https://doi.org/10.1111/j.1365-2672.2008.03816.x>.
- [87] P. Parthipan, E. Preetham, L.L. Machuca, P.K.S.M. Rahman, K. Murugan, A. Rajasekar, Biosurfactant and degradative enzymes mediated crude oil degradation by bacterium *Bacillus subtilis* A1, *Front. Microbiol.* 8 (2017) 1–14. <https://doi.org/10.3389/fmicb.2017.00193>.
- [88] P. Parthipan, P. Elumalai, K. Sathishkumar, D. Sabarinathan, K. Murugan, G. Benelli, A. Rajasekar, Biosurfactant and enzyme mediated crude oil degradation by *Pseudomonas stutzeri* NA3 and *Acinetobacter baumannii* MN3, *3 Biotech.* 7 (2017). <https://doi.org/10.1007/s13205-017-0902-7>.
- [89] H. Amani, H. Kariminezhad, Study on emulsification of crude oil in water using emulsan biosurfactant for pipeline transportation, *Pet. Sci. Technol.* 34 (2016) 216–222. <https://doi.org/10.1080/10916466.2015.1118500>.

- [90] M. Rosenberg, E.A. Bayer, J. Delarea, E. Rosenberg, Role of Thin Fimbriae in Adherence and Growth of *Acinetobacter calcoaceticus* RAG-1 on Hexadecane, *Appl. Environ. Microbiol.* 44 (1982) 929–937. <https://doi.org/10.1128/aem.44.4.929-937.1982>.
- [91] E. Gayathiri, P. Prakash, N. Karmegam, S. Varjani, M.K. Awasthi, B. Ravindran, Biosurfactants: Potential and Eco-Friendly Material for Sustainable Agriculture and Environmental Safety—A Review, *Agronomy.* 12 (2022) 662. <https://doi.org/10.3390/agronomy12030662>.
- [92] J.J. Ortega-Calvo, Strategies to Increase Bioavailability and Uptake of Hydrocarbons, *Cell. Ecophysiol. Microbe.* (2017) 1–12. https://doi.org/10.1007/978-3-319-20796-4_10-1.
- [93] H.-C. Flemming, J. Wingender, U. Szewzyk, P. Steinberg, S.A. Rice, S. Kjelleberg, Biofilms: an emergent form of bacterial life, *Nat. Rev. Microbiol.* 14 (2016) 563–575. <https://doi.org/10.1038/nrmicro.2016.94>.
- [94] D. Dasgupta, R. Ghosh, T.K. Sengupta, Biofilm-Mediated Enhanced Crude Oil Degradation by Newly Isolated *Pseudomonas* Species, *ISRN Biotechnol.* 2013 (2013) 1–13. <https://doi.org/10.5402/2013/250749>.
- [95] S.K. Shukla, N. Mangwani, T.S. Rao, S. Das, Biofilm-Mediated Bioremediation of Polycyclic Aromatic Hydrocarbons, in: S. Das (Ed.), *Microb. Biodegrad. Bioremediation*, Elsevier, 2014: pp. 203–232. <https://doi.org/10.1016/B978-0-12-800021-2.00008-X>.
- [96] P. Sivadon, C. Barnier, L. Urios, R. Grimaud, Biofilm formation as a microbial strategy to assimilate particulate substrates, *Environ. Microbiol. Rep.* 11 (2019) 749–764. <https://doi.org/10.1111/1758-2229.12785>.
- [97] N. Mangwani, S. Kumari, S. Das, Bacterial biofilms and quorum sensing: fidelity in bioremediation technology, *Biotechnol. Genet. Eng. Rev.* 32 (2017) 43–73. <https://doi.org/10.1080/02648725.2016.1196554>.
- [98] N. Mangwani, S.K. Shukla, S. Kumari, T.S. Rao, S. Das, Characterization of *Stenotrophomonas acidaminiphila* NCW-702 biofilm for implication in the degradation of polycyclic aromatic hydrocarbons, *J. Appl. Microbiol.* 117 (2014) 1012–1024. <https://doi.org/10.1111/jam.12602>.
- [99] M. Naeimi, M. Shavandi, E. Alaie, Determining the impact of biofilm in the bioaugmentation process of benzene-contaminated resources, *J. Environ. Chem. Eng.* 9 (2021) 104976. <https://doi.org/10.1016/j.jece.2020.104976>.
- [100] G. O’Toole, H.B. Kaplan, R. Kolter, Biofilm Formation as Microbial Development, *Annu. Rev. Microbiol.* 54 (2000) 49–79. <https://doi.org/10.1146/annurev.micro.54.1.49>.
- [101] K.U. Mahto, S. Kumari, S. Das, Unraveling the complex regulatory networks in biofilm formation in bacteria and relevance of biofilms in environmental remediation, *Crit. Rev. Biochem. Mol. Biol.* 57 (2022) 305–332. <https://doi.org/10.1080/10409238.2021.2015747>.
- [102] M.H. Muhammad, A.L. Idris, X. Fan, Y. Guo, Y. Yu, X. Jin, J. Qiu, X. Guan, T. Huang, Beyond Risk: Bacterial Biofilms and Their Regulating Approaches, *Front. Microbiol.* 11 (2020). <https://doi.org/10.3389/fmicb.2020.00928>.
- [103] M. Krsmanovic, D. Biswas, H. Ali, A. Kumar, R. Ghosh, A.K. Dickerson, Hydrodynamics and surface properties influence biofilm proliferation, *Adv. Colloid Interface Sci.* 288 (2021). <https://doi.org/10.1016/J.CIS.2020.102336>.

- [104] M.H. Muhammad, A.L. Idris, X. Fan, Y. Guo, Y. Yu, X. Jin, J. Qiu, X. Guan, T. Huang, Beyond Risk: Bacterial Biofilms and Their Regulating Approaches, *Front. Microbiol.* 11 (2020). <https://doi.org/10.3389/fmicb.2020.00928>.
- [105] L. Meng, H. Li, M. Bao, P. Sun, Metabolic pathway for a new strain *Pseudomonas synxantha* LSH-7': from chemotaxis to uptake of n-hexadecane, *Sci. Rep.* 7 (2017) 39068. <https://doi.org/10.1038/srep39068>.
- [106] Ł. Ławniczak, M. Woźniak-Karczewska, A.P. Loibner, H.J. Heipieper, Ł. Chrzanowski, Microbial degradation of hydrocarbons—basic principles for bioremediation: A review, *Molecules.* 25 (2020) 1–19. <https://doi.org/10.3390/molecules25040856>.
- [107] V. Carniello, B.W. Peterson, H.C. van der Mei, H.J. Busscher, Physico-chemistry from initial bacterial adhesion to surface-programmed biofilm growth, *Adv. Colloid Interface Sci.* 261 (2018) 1–14. <https://doi.org/10.1016/J.CIS.2018.10.005>.
- [108] H. Abbasnezhad, M. Gray, J.M. Foght, Influence of adhesion on aerobic biodegradation and bioremediation of liquid hydrocarbons, *Appl. Microbiol. Biotechnol.* 92 (2011) 653–675. <https://doi.org/10.1007/s00253-011-3589-4>.
- [109] M. Bouchez-Naïtali, D. Blanchet, V. Bardin, J.P. Vandecasteele, Evidence for interfacial uptake in hexadecane degradation by *Rhodococcus equi*: The importance of cell flocculation, *Microbiology.* 147 (2001) 2537–2543. <https://doi.org/10.1099/00221287-147-9-2537/CITE/REFWORKS>.
- [110] M. Cappelletti, S. Fedi, D. Zannoni, Degradation of Alkanes in *Rhodococcus*, in: Springer, Cham, 2019: pp. 137–171. https://doi.org/10.1007/978-3-030-11461-9_6.
- [111] M. Rosenberg, D. Gutnick, E. Rosenberg, Adherence of bacteria to hydrocarbons: A simple method for measuring cell-surface hydrophobicity, *FEMS Microbiol. Lett.* 9 (1980) 29–33. <https://doi.org/10.1111/j.1574-6968.1980.tb05599.x>.
- [112] G. Subbiahdoss, E. Reimhult, Biofilm formation at oil-water interfaces is not a simple function of bacterial hydrophobicity, *Colloids Surfaces B Biointerfaces.* 194 (2020) 111163. <https://doi.org/10.1016/j.colsurfb.2020.111163>.
- [113] L. Vaccari, M. Molaei, T.H.R. Niepa, D. Lee, R.L. Leheny, K.J. Stebe, Films of bacteria at interfaces, *Adv. Colloid Interface Sci.* 247 (2017) 561–572. <https://doi.org/10.1016/j.cis.2017.07.016>.
- [114] T.H.R. Niepa, L. Vaccari, R.L. Leheny, M. Goulian, D. Lee, K.J. Stebe, Films of Bacteria at Interfaces (FBI): Remodeling of Fluid Interfaces by *Pseudomonas aeruginosa*, *Sci. Rep.* 7 (2017) 17864. <https://doi.org/10.1038/s41598-017-17721-3>.
- [115] M. Moormann, U. Zähringer, H. Moll, R. Kaufmann, R. Schmid, K. Altendorf, A New Glycosylated Lipopeptide Incorporated into the Cell Wall of a Smooth Variant of *Gordonia hydrophobica*, *J. Biol. Chem.* 272 (1997) 10729–10738. <https://doi.org/10.1074/jbc.272.16.10729>.
- [116] A. Franzetti, G. Bestetti, P. Caredda, P. La Colla, E. Tamburini, Surface-active compounds and their role in the access to hydrocarbons in *Gordonia* strains, *FEMS Microbiol. Ecol.* 63 (2008) 238–248. <https://doi.org/10.1111/j.1574-6941.2007.00406.x>.
- [117] N.K. Dewangan, J.C. Conrad, Bacterial motility enhances adhesion to oil droplets, *Soft Matter.* 16 (2020) 8237–8244. <https://doi.org/10.1039/D0SM00944J>.

- [118] A. Jain, Y. Gupta, R. Agrawal, S. Jain, P. Khare, Biofilms-A Microbial Life Perspective: A Critical Review, *Crit. Rev. Ther. Drug Carr. Syst.* 24 (2007) 393–443. <https://doi.org/10.1615/CritRevTherDrugCarrierSyst.v24.i5.10>.
- [119] S. Mishra, Y. Huang, J. Li, X. Wu, Z. Zhou, Q. Lei, P. Bhatt, S. Chen, Biofilm-mediated bioremediation is a powerful tool for the removal of environmental pollutants, *Chemosphere*. 294 (2022) 133609. <https://doi.org/10.1016/j.chemosphere.2022.133609>.
- [120] M. Omarova, L.T. Swientoniewski, I.K. Mkam Tsengam, D.A. Blake, V. John, A. McCormick, G.D. Bothun, S.R. Raghavan, A. Bose, Biofilm Formation by Hydrocarbon-Degrading Marine Bacteria and Its Effects on Oil Dispersion, *ACS Sustain. Chem. Eng.* 7 (2019) 14490–14499. <https://doi.org/10.1021/acssuschemeng.9b01923>.
- [121] K. Brindhadevi, F. LewisOscar, E. Mylonakis, S. Shanmugam, T.N. Verma, A. Pugazhendhi, Biofilm and Quorum sensing mediated pathogenicity in *Pseudomonas aeruginosa*, *Process Biochem.* 96 (2020) 49–57. <https://doi.org/10.1016/j.procbio.2020.06.001>.
- [122] H. Ennouri, P. D’Abzac, F. Hakil, P. Branchu, M. Naïtali, A.M. Lomenech, R. Oueslati, J. Desbrières, P. Sivadon, R. Grimaud, The extracellular matrix of the oleolytic biofilms of *Marinobacter hydrocarbonoclasticus* comprises cytoplasmic proteins and T2SS effectors that promote growth on hydrocarbons and lipids, *Environ. Microbiol.* 19 (2017) 159–173. <https://doi.org/10.1111/1462-2920.13547>.
- [123] T. Abee, Á.T. Kovács, O.P. Kuipers, S. van der Veen, Biofilm formation and dispersal in Gram-positive bacteria, *Curr. Opin. Biotechnol.* 22 (2011) 172–179. <https://doi.org/10.1016/J.COPBIO.2010.10.016>.
- [124] D. An, S.M. Caffrey, J. Soh, A. Agrawal, D. Brown, K. Budwill, X. Dong, P.F. Dunfield, J. Foght, L.M. Gieg, S.J. Hallam, N.W. Hanson, Z. He, T.R. Jack, J. Klassen, K.M. Konwar, E. Kuatsjah, C. Li, S. Larter, V. Leopatra, C.L. Nesbø, T. Oldenburg, A.P. Pagé, E. Ramos-Padron, F.F. Rochman, A. Saidi-Mehrabad, C.W. Sensen, P. Sipahimalani, Y.C. Song, S. Wilson, G. Wolbring, M.L. Wong, G. Voordouw, Metagenomics of hydrocarbon resource environments indicates aerobic taxa and genes to be unexpectedly common, *Environ. Sci. Technol.* 47 (2013) 10708–10717. <https://doi.org/10.1021/es4020184>.
- [125] F. Révész, P.A. Figueroa-Gonzalez, A.J. Probst, B. Kriszt, S. Banerjee, S. Szoboszlay, G. Maróti, A. Tánicsics, Microaerobic conditions caused the overwhelming dominance of *Acinetobacter* spp. and the marginalization of *Rhodococcus* spp. in diesel fuel/crude oil mixture-amended enrichment cultures, *Arch. Microbiol.* 202 (2020) 329–342. <https://doi.org/10.1007/s00203-019-01749-2>.
- [126] A. Gruner, R. Jarling, A. Vieth-Hillebrand, K. Mangelsdorf, C. Janka, G.M. van der Kraan, T. Köhler, B.E.L. Morris, H. Wilkes, Tracing microbial hydrocarbon transformation processes in a high temperature petroleum reservoir using signature metabolites, *Org. Geochem.* 108 (2017) 82–93. <https://doi.org/10.1016/j.orggeochem.2017.03.003>.
- [127] F. Abbasian, R. Lockington, M. Mallavarapu, R. Naidu, A Comprehensive Review of Aliphatic Hydrocarbon Biodegradation by Bacteria, *Appl. Biochem. Biotechnol.* 176 (2015) 670–699. <https://doi.org/10.1007/s12010-015-1603-5>.
- [128] J.H. Ji, Y.F. Liu, L. Zhou, S.M. Mbadanga, P. Pan, J. Chen, J.F. Liu, S.Z. Yang, W. Sand, J.D. Gu, B.Z. Mu, Methanogenic degradation of long n-alkanes requires fumarate-dependent activation, *Appl. Environ. Microbiol.* 85 (2019).

- <https://doi.org/10.1128/AEM.00985-19>.
- [129] Y. Ji, G. Mao, Y. Wang, M. Bartlam, Structural insights into diversity and n-alkane biodegradation mechanisms of alkane hydroxylases, *Front. Microbiol.* 4 (2013). <https://doi.org/10.3389/fmicb.2013.00058>.
- [130] A. Agrawal, L.M. Gieg, In situ detection of anaerobic alkane metabolites in subsurface environments, *Front. Microbiol.* 4 (2013). <https://doi.org/10.3389/fmicb.2013.00140>.
- [131] L. Cabral, P. Giovanella, E.P. Pellizzer, E.H. Teramoto, C.H. Kiang, L.D. Sette, Microbial communities in petroleum-contaminated sites: Structure and metabolisms, *Chemosphere.* 286 (2022) 131752. <https://doi.org/10.1016/j.chemosphere.2021.131752>.
- [132] G. Kharey, G. Scheffer, L.M. Gieg, Combined Use of Diagnostic Fumarate Addition Metabolites and Genes Provides Evidence for Anaerobic Hydrocarbon Biodegradation in Contaminated Groundwater, *Microorganisms.* 8 (2020) 1532. <https://doi.org/10.3390/microorganisms8101532>.
- [133] R.E. Mohler, K.T. O'Reilly, D.A. Zemo, A.K. Tiwary, R.I. Magaw, K.A. Synowiec, Non-targeted analysis of petroleum metabolites in groundwater using GC×GC-TOFMS, *Environ. Sci. Technol.* 47 (2013) 10471–10476. <https://doi.org/10.1021/es401706m>.
- [134] A. Mikolasch, A. Omirbekova, P. Schumann, A. Reinhard, H. Sheikhany, R. Berzhanova, T. Mukasheva, F. Schauer, Enrichment of aliphatic, alicyclic and aromatic acids by oil-degrading bacteria isolated from the rhizosphere of plants growing in oil-contaminated soil from Kazakhstan, *Appl. Microbiol. Biotechnol.* 99 (2015) 4071–4084. <https://doi.org/10.1007/s00253-014-6320-4>.
- [135] C.M. So, C.D. Phelps, L.Y. Young, Anaerobic transformation of alkanes to fatty acids by a sulfate-reducing bacterium, strain Hxd3, *Appl. Environ. Microbiol.* 69 (2003) 3892–3900. <https://doi.org/10.1128/AEM.69.7.3892-3900.2003>.
- [136] M. Cai, J. Yao, H. Yang, R. Wang, K. Masakorala, Aerobic biodegradation process of petroleum and pathway of main compounds in water flooding well of Dagang oil field, *Bioresour. Technol.* 144 (2013) 100–106. <https://doi.org/10.1016/j.biortech.2013.06.082>.
- [137] L.M. Gieg, C.R.A. Toth, Signature Metabolite Analysis to Determine In Situ Anaerobic Hydrocarbon Biodegradation, in: *Anaerob. Util. Hydrocarb. Oils, Lipids*, Springer International Publishing, Cham, 2017: pp. 1–30. https://doi.org/10.1007/978-3-319-33598-8_19-1.
- [138] X.Y. Bian, S.M. Mbadinga, Y.F. Liu, S.Z. Yang, J.F. Liu, R.Q. Ye, J.D. Gu, B.Z. Mu, Insights into the anaerobic biodegradation pathway of n-Alkanes in oil reservoirs by detection of signature metabolites, *Sci. Rep.* 5 (2015) 9801. <https://doi.org/10.1038/srep09801>.
- [139] H.R. Beller, Analysis of Benzylsuccinates in Groundwater by Liquid Chromatography/Tandem Mass Spectrometry and Its Use for Monitoring In Situ BTEX Biodegradation, *Environ. Sci. Technol.* 36 (2002) 2724–2728. <https://doi.org/10.1021/es025527l>.
- [140] L.M. Gieg, J.M. Suflita, Detection of anaerobic metabolites of saturated and aromatic hydrocarbons in petroleum-contaminated aquifers, *Environ. Sci. Technol.* 36 (2002) 3755–3762. <https://doi.org/10.1021/es0205333>.

- [141] L.Y. Young, C.D. Phelps, Metabolic Biomarkers for Monitoring in Situ Anaerobic Hydrocarbon Degradation, *Environ. Health Perspect.* 113 (2005) 62–67. <https://doi.org/10.1289/ehp.6940>.
- [142] R.U. Meckenstock, M. Safinowski, C. Griebler, Anaerobic degradation of polycyclic aromatic hydrocarbons, *FEMS Microbiol. Ecol.* 49 (2004) 27–36. <https://doi.org/10.1016/j.femsec.2004.02.019>.
- [143] C.M. Aitken, D.M. Jones, S.R. Larter, Anaerobic hydrocarbon biodegradation in deep subsurface oil reservoirs, *Nature*. 431 (2004) 291–294. <https://doi.org/10.1038/nature02922>.
- [144] S. Kim, L.A. Stanford, R.P. Rodgers, A.G. Marshall, C.C. Walters, K. Qian, L.M. Wenger, P. Mankiewicz, Microbial alteration of the acidic and neutral polar NSO compounds revealed by Fourier transform ion cyclotron resonance mass spectrometry, *Org. Geochem.* 36 (2005) 1117–1134. <https://doi.org/10.1016/j.orggeochem.2005.03.010>.
- [145] S. Zan, J. Wang, F. Wang, Z. Li, M. Du, Y. Cai, A novel degradation mechanism of naphthenic acids by marine *Pseudoalteromonas* sp., *J. Hazard. Mater.* 424 (2022) 127534. <https://doi.org/10.1016/j.jhazmat.2021.127534>.
- [146] J. Zhong, L. Luo, B. Chen, S. Sha, Q. Qing, N.F.Y. Tam, Y. Zhang, T. Luan, Degradation pathways of 1-methylphenanthrene in bacterial *Sphingobium* sp. MP9-4 isolated from petroleum-contaminated soil, *Mar. Pollut. Bull.* 114 (2017) 926–933. <https://doi.org/10.1016/j.marpolbul.2016.11.020>.
- [147] D.C. Palacio Lozano, R. Gavard, J.P. Arenas-Diaz, M.J. Thomas, D.D. Stranz, E. Mejía-Ospino, A. Guzman, S.E.F. Spencer, D. Rossell, M.P. Barrow, Pushing the analytical limits: New insights into complex mixtures using mass spectra segments of constant ultrahigh resolving power, *Chem. Sci.* 10 (2019) 6966–6978. <https://doi.org/10.1039/c9sc02903f>.
- [148] S. Alves, E. Rathahao-Paris, J.C. Tabet, Potential of Fourier Transform Mass Spectrometry for High-Throughput Metabolomics Analysis, in: *Metabolomics Coming Age with Its Technol. Divers.*, 2013: pp. 219–302. <https://doi.org/10.1016/B978-0-12-397922-3.00005-8>.
- [149] E. Rathahao-Paris, S. Alves, C. Junot, J.C. Tabet, High resolution mass spectrometry for structural identification of metabolites in metabolomics, *Metabolomics*. 12 (2016) 1–15. <https://doi.org/10.1007/s11306-015-0882-8>.
- [150] S. Gutiérrez Sama, C. Barrère-Mangote, B. Bouyssière, P. Giusti, R. Lobinski, Recent trends in element speciation analysis of crude oils and heavy petroleum fractions, *TrAC - Trends Anal. Chem.* 104 (2018) 69–76. <https://doi.org/10.1016/j.trac.2017.10.014>.
- [151] S. Rezaee, M. Tavakkoli, R. Doherty, F.M. Vargas, A new experimental method for a fast and reliable quantification of saturates, aromatics, resins, and asphaltenes in crude oils, *Pet. Sci. Technol.* 38 (2020) 955–961. <https://doi.org/10.1080/10916466.2020.1790598>.
- [152] D. Petras, I. Koester, R. Da Silva, B.M. Stephens, A.F. Haas, C.E. Nelson, L.W. Kelly, L.I. Aluwihare, P.C. Dorrestein, High-Resolution Liquid Chromatography Tandem Mass Spectrometry Enables Large Scale Molecular Characterization of Dissolved Organic Matter, *Front. Mar. Sci.* 4 (2017) 405. <https://doi.org/10.3389/fmars.2017.00405>.
- [153] A.R. Oka, C.D. Phelps, X. Zhu, D.L. Saber, L.Y. Young, Dual Biomarkers of Anaerobic Hydrocarbon Degradation in Historically Contaminated Groundwater, *Environ. Sci.*

- Technol. 45 (2011) 3407–3414. <https://doi.org/10.1021/es103859t>.
- [154] B.G. Vaz, R.C. Silva, C.F. Klitzke, R.C. Simas, H.D. Lopes Nascimento, R.C.L. Pereira, D.F. Garcia, M.N. Eberlin, D.A. Azevedo, Assessing biodegradation in the llanos orientales crude oils by electrospray ionization ultrahigh resolution and accuracy fourier transform mass spectrometry and chemometric analysis, *Energy and Fuels*. 27 (2013) 1277–1284. <https://doi.org/10.1021/ef301766r>.
- [155] J.S. Watson, D.M. Jones, R.P.J. Swannell, A.C.T. Van Duin, Formation of carboxylic acids during aerobic biodegradation of crude oil and evidence of microbial oxidation of hopanes, *Org. Geochem.* 33 (2002) 1153–1169. [https://doi.org/10.1016/S0146-6380\(02\)00086-4](https://doi.org/10.1016/S0146-6380(02)00086-4).
- [156] L.K. Oberding, L.M. Gieg, Methanogenic Paraffin Biodegradation: Alkylsuccinate Synthase Gene Quantification and Dicarboxylic Acid Production, *Appl. Environ. Microbiol.* 84 (2017) 1–14. <https://doi.org/10.1128/AEM.01773-17>.
- [157] S. Godin, P. Kubica, A. Ranchou-Peyruse, I. Le Hecho, D. Patriarche, G. Caumette, J. Szpunar, R. Lobinski, An LC-MS/MS Method for a Comprehensive Determination of Metabolites of BTEX Anaerobic Degradation in Bacterial Cultures and Groundwater, *Water*. 12 (2020) 1869. <https://doi.org/10.3390/w12071869>.
- [158] A.M. Mckenna, H. Chen, C.R. Weisbrod, G.T. Blakney, Molecular Comparison of Solid-Phase Extraction and Liquid/Liquid Extraction of Water-Soluble Petroleum Compounds Produced through Photodegradation and Biodegradation by FT-ICR Mass Spectrometry, *Cite This Anal. Chem.* 93 (2021) 4611–4618. <https://doi.org/10.1021/acs.analchem.0c05230>.
- [159] D.R. Van Stempvoort, K. Millar, J.R. Lawrence, Accumulation of short-chain fatty acids in an aquitard linked to anaerobic biodegradation of petroleum hydrocarbons, *Appl. Geochemistry*. 24 (2008) 77–85. <https://doi.org/10.1016/j.apgeochem.2008.11.004>.
- [160] C. Griebler, M. Safinowski, A. Vieth, H.H. Richnow, R.U. Meckenstock, Combined Application of Stable Carbon Isotope Analysis and Specific Metabolites Determination for Assessing In Situ Degradation of Aromatic Hydrocarbons in a Tar Oil-Contaminated Aquifer, *Environ. Sci. Technol.* 38 (2004) 617–631. <https://doi.org/10.1021/es0344516>.
- [161] J. Vila, Z. López, J. Sabaté, C. Minguillón, A.M. Solanas, M. Grifoll, Identification of a Novel Metabolite in the Degradation of Pyrene by *Mycobacterium* sp. Strain AP1: Actions of the Isolate on Two- and Three-Ring Polycyclic Aromatic Hydrocarbons, *Appl. Environ. Microbiol.* 67 (2001) 5497–5505. <https://doi.org/10.1128/AEM.67.12.5497-5505.2001>.
- [162] A.L. Lotte Ask Reitzel, P.L. Bjerg, Quantitative determination of toluene, ethylbenzene, and xylene degradation products in contaminated groundwater by solid-phase extraction and in-vial derivatization, *Int. J. Environ. Anal. Chem.* 85 (2005) 1075–1087. <https://doi.org/10.1080/03067310500194920>.
- [163] J. Guevara-Luna, P. Alvarez-Fitz, E. Ríos-Leal, M. Acevedo-Quiroz, S. Encarnación-Guevara, · Ma, E. Moreno-Godinez, M. Castellanos-Escamilla, J. Toribio-Jiménez, Y. Romero-Ramírez, Biotransformation of benzo[a]pyrene by the thermophilic bacterium *Bacillus licheniformis* M2-7, *World J. Microbiol. Biotechnol.* 34 (2018) 88. <https://doi.org/10.1007/s11274-018-2469-9>.
- [164] L. Cheng, S. Shi, L. Yang, Y. Zhang, J. Dolfing, Y. Sun, L. Liu, Q. Li, B. Tu, L. Dai, Q. Shi, H. Zhang, Preferential degradation of long-chain alkyl substituted hydrocarbons in

- heavy oil under methanogenic conditions, *Org. Geochem.* 138 (2019) 103927. <https://doi.org/10.1016/j.orggeochem.2019.103927>.
- [165] A. Vetere, W. Schrader, Mass Spectrometric Coverage of Complex Mixtures: Exploring the Carbon Space of Crude Oil, *ChemistrySelect.* 2 (2017) 849–853. <https://doi.org/10.1002/slct.201601083>.
- [166] J.-H. Ji, L. Zhou, S.M. Mbadinga, M. Irfan, Y.-F. Liu, P. Pan, Z.-Z. Qi, J. Chen, J.-F. Liu, S.-Z. Yang, J.-D. Gu, B.-Z. Mu, Methanogenic biodegradation of C₉ to C_{12n}-alkanes initiated by *Smithella* via fumarate addition mechanism, *AMB Express.* 10 (2020) 23. <https://doi.org/10.1186/s13568-020-0956-5>.
- [167] C. Jobelius, B. Ruth, C. Griebler, R.U. Meckenstock, J. Hollender, A. Reineke, F.H. Frimmel, C. Zwiener, Metabolites indicate hot spots of biodegradation and biogeochemical gradients in a high-resolution monitoring well, *Environ. Sci. Technol.* 45 (2011) 474–481. <https://doi.org/10.1021/es1030867>.
- [168] A. Imam, S.K. Suman, D. Ghosh, P.K. Kanaujia, Analytical approaches used in monitoring the bioremediation of hydrocarbons in petroleum-contaminated soil and sludge, *TrAC - Trends Anal. Chem.* 118 (2019) 50–64. <https://doi.org/10.1016/j.trac.2019.05.023>.
- [169] U. Jaekel, J. Zedelius, H. Wilkes, F. Musat, Anaerobic degradation of cyclohexane by sulfate-reducing bacteria from hydrocarbon-contaminated marine sediments, *Front. Microbiol.* 6 (2015). <https://doi.org/10.3389/fmicb.2015.00116>.
- [170] D. Schemeth, N.J. Nielsen, J.H. Christensen, SPE-LC-MS investigations for the isolation and fractionation of acidic oil degradation products, *Anal. Chim. Acta.* 1038 (2018) 182–190. <https://doi.org/10.1016/j.aca.2018.06.074>.
- [171] C.M. Aitken, I.M. Head, D.M. Jones, S.J. Rowland, A.G. Scarlett, C.E. West, Comprehensive two-dimensional gas chromatography-mass spectrometry of complex mixtures of anaerobic bacterial metabolites of petroleum hydrocarbons, *J. Chromatogr. A.* 1536 (2018) 96–109. <https://doi.org/10.1016/j.chroma.2017.06.027>.
- [172] A.M. McKenna, R.K. Nelson, C.M. Reddy, J.J. Savory, N.K. Kaiser, J.E. Fitzsimmons, A.G. Marshall, R.P. Rodgers, Expansion of the analytical window for oil spill characterization by ultrahigh resolution mass spectrometry: Beyond gas chromatography, *Environ. Sci. Technol.* 47 (2013) 7530–7539. <https://doi.org/10.1021/es305284t>.
- [173] Y. Cho, A. Ahmed, A. Islam, S. Kim, Developments in FT-ICR MS instrumentation, ionization techniques, and data interpretation methods for petroleomics, *Mass Spectrom. Rev.* 34 (2015) 248–263. <https://doi.org/10.1002/mas.21438>.
- [174] W. Liu, Y. Liao, Y. Pan, B. Jiang, Q. Zeng, Q. Shi, C.S. Hsu, Use of ESI FT-ICR MS to investigate molecular transformation in simulated aerobic biodegradation of a sulfur-rich crude oil, *Org. Geochem.* 123 (2018) 17–26. <https://doi.org/10.1016/j.orggeochem.2018.06.003>.
- [175] R.P. Rodgers, M.M. Mapolelo, W.K. Robbins, M.L. Chacón-Patiño, J.C. Putman, S.F. Niles, S.M. Rowland, A.G. Marshall, Combating selective ionization in the high resolution mass spectral characterization of complex mixtures, *Faraday Discuss.* 218 (2019) 29–51. <https://doi.org/10.1039/c9fd00005d>.
- [176] R.S. Borisov, L.N. Kulikova, V.G. Zaikin, Mass Spectrometry in Petroleum Chemistry (Petroleomics) (Review), *Pet. Chem.* 59 (2019) 1055–1076.

- <https://doi.org/10.1134/S0965544119100025>.
- [177] X. Zhang, Z. Chen, X. Huo, J. Kang, S. Zhao, Y. Peng, F. Deng, J. Shen, W. Chu, Application of Fourier transform ion cyclotron resonance mass spectrometry in deciphering molecular composition of soil organic matter: A review, *Sci. Total Environ.* 756 (2021) 144140. <https://doi.org/10.1016/j.scitotenv.2020.144140>.
- [178] R.E. Mohler, S. Ahn, K. O'Reilly, D.A. Zemo, C. Espino Devine, R. Magaw, N. Sihota, Towards comprehensive analysis of oxygen containing organic compounds in groundwater at a crude oil spill site using GC×GC-TOFMS and Orbitrap ESI-MS, *Chemosphere.* 244 (2020) 125504. <https://doi.org/10.1016/j.chemosphere.2019.125504>.
- [179] S. Kim, R.W. Kramer, P.G. Hatcher, Graphical Method for Analysis of Ultrahigh-Resolution Broadband Mass Spectra of Natural Organic Matter, the Van Krevelen Diagram, *Anal. Chem.* 75 (2003) 5336–5344. <https://doi.org/10.1021/ac034415p>.
- [180] M.S.S. Amaral, Y. Nolvachai, P.J. Marriott, Comprehensive Two-Dimensional Gas Chromatography Advances in Technology and Applications: Biennial Update, *Anal. Chem.* 92 (2020) 85–104. <https://doi.org/10.1021/acs.analchem.9b05412>.
- [181] H. Van De Weghe, G. Vanermen, J. Gemoets, R. Lookman, D. Bertels, Application of comprehensive two-dimensional gas chromatography for the assessment of oil contaminated soils, *J. Chromatogr. A.* 1137 (2006) 91–100. <https://doi.org/10.1016/j.chroma.2006.10.014>.
- [182] S.E. Prebihalo, K.L. Berrier, C.E. Freye, H.D. Bahaghighat, N.R. Moore, D.K. Pinkerton, R.E. Synovec, Multidimensional Gas Chromatography: Advances in Instrumentation, Chemometrics, and Applications, *Anal. Chem.* 90 (2018) 505–532. <https://doi.org/10.1021/acs.analchem.7b04226>.
- [183] H. Chen, A. Hou, Y.E. Corilo, Q. Lin, J. Lu, I.A. Mendelssohn, R. Zhang, R.P. Rodgers, A.M. McKenna, 4 Years after the Deepwater Horizon Spill: Molecular Transformation of Macondo Well Oil in Louisiana Salt Marsh Sediments Revealed by FT-ICR Mass Spectrometry, *Environ. Sci. Technol.* 50 (2016) 9061–9069. <https://doi.org/10.1021/acs.est.6b01156>.
- [184] M. Vinaixa, E.L. Schymanski, S. Neumann, M. Navarro, R.M. Salek, O. Yanes, Mass spectral databases for LC/MS- and GC/MS-based metabolomics: State of the field and future prospects, *TrAC - Trends Anal. Chem.* 78 (2016) 23–35. <https://doi.org/10.1016/j.trac.2015.09.005>.
- [185] X. Bian, S.M. Mbadanga, S. Yang, J. Gu, R. Ye, B. Mu, Synthesis of Anaerobic Degradation Biomarkers Alkyl-, Aryl- and Cycloalkylsuccinic Acids and Their Mass Spectral Characteristics, *Eur. J. Mass Spectrom.* 20 (2014) 287–297. <https://doi.org/10.1255/ejms.1280>.
- [186] D.X. Li, L. Gan, A. Bronja, O.J. Schmitz, Gas chromatography coupled to atmospheric pressure ionization mass spectrometry (GC-API-MS): Review, *Anal. Chim. Acta.* 891 (2015) 43–61. <https://doi.org/10.1016/j.aca.2015.08.002>.
- [187] M.P. Barrow, K.M. Peru, J. V. Headley, An added dimension: GC atmospheric pressure chemical ionization FTICR MS and the athabasca oil sands, *Anal. Chem.* 86 (2014) 8281–8288. <https://doi.org/10.1021/ac501710y>.
- [188] T. Schwemer, C.P. Rüger, M. Sklorz, R. Zimmermann, Gas Chromatography Coupled to

- Atmospheric Pressure Chemical Ionization FT-ICR Mass Spectrometry for Improvement of Data Reliability, *Anal. Chem.* 87 (2015) 11957–11961.
https://doi.org/10.1021/ACS.ANALCHEM.5B02114/SUPPL_FILE/AC5B02114_SI_001.PDF.
- [189] T.M. Gröger, U. Käfer, R. Zimmermann, Gas chromatography in combination with fast high-resolution time-of-flight mass spectrometry: Technical overview and perspectives for data visualization, *TrAC - Trends Anal. Chem.* 122 (2020).
<https://doi.org/10.1016/j.trac.2019.115677>.
- [190] G.A. Theodoridis, H.G. Gika, E.J. Want, I.D. Wilson, Liquid chromatography-mass spectrometry based global metabolite profiling: A review, *Anal. Chim. Acta.* 711 (2012) 7–16. <https://doi.org/10.1016/j.aca.2011.09.042>.
- [191] A. Daverey, K. Dutta, A. Sarkar, An overview of analytical methodologies for environmental monitoring, in: A. Daverey, K. Dutta, A. Sarkar (Eds.), *Tools, Tech. Protoc. Monit. Environ. Contam.*, Elsevier Inc., 2019: pp. 3–17. <https://doi.org/10.1016/B978-0-12-814679-8.00001-7>.
- [192] R.A. Zubarev, A. Makarov, Orbitrap mass spectrometry, *Anal. Chem.* 85 (2013) 5288–5296. <https://doi.org/10.1021/ac4001223>.
- [193] Y. Liu, H.K. White, R.L. Simister, D. Waite, S.L. Lyons, E.B. Kujawinski, Probing the Chemical Transformation of Seawater-Soluble Crude Oil Components during Microbial Oxidation, *ACS Earth Sp. Chem.* 4 (2020) 690–701.
<https://doi.org/10.1021/acsearthspacechem.9b00316>.
- [194] E.L. Schymanski, J. Jeon, R. Gulde, K. Fenner, M. Ruff, H.P. Singer, J. Hollender, Identifying Small Molecules via High Resolution Mass Spectrometry: Communicating Confidence, *Environ. Sci. Technol.* 48 (2014) 2097–2098.
<https://doi.org/10.1021/es5002105>.
- [195] M.T. Jamal, A. Pugazhendi, Isolation and characterization of halophilic bacterial consortium from seagrass, Jeddah coast, for the degradation of petroleum hydrocarbons and treatment of hydrocarbons-contaminated boat fuel station wastewater, *Clean Technol. Environ. Policy.* 23 (2021) 77–88. <https://doi.org/10.1007/s10098-020-01957-1>.
- [196] S.S. Meena, R.S. Sharma, P. Gupta, S. Karmakar, K.K. Aggarwal, Isolation and identification of *Bacillus megaterium* YB3 from an effluent contaminated site efficiently degrades pyrene, *J. Basic Microbiol.* 56 (2016) 369–378.
<https://doi.org/10.1002/jobm.201500533>.
- [197] C.M. Aitken, D.M. Jones, M.J. Maguire, N.D. Gray, A. Sherry, B.F.J. Bowler, A.K. Ditchfield, S.R. Larter, I.M. Head, Evidence that crude oil alkane activation proceeds by different mechanisms under sulfate-reducing and methanogenic conditions, *Geochim. Cosmochim. Acta.* 109 (2013) 162–174. <https://doi.org/10.1016/j.gca.2013.01.031>.
- [198] L. Goswami, N.A. Manikandan, B. Dolman, K. Pakshirajan, G. Pugazhenth, Biological treatment of wastewater containing a mixture of polycyclic aromatic hydrocarbons using the oleaginous bacterium *Rhodococcus opacus*, *J. Clean. Prod.* 196 (2018) 1282–1291.
<https://doi.org/10.1016/j.jclepro.2018.06.070>.
- [199] D.I. Little, K. Holtzmann, E.R. Gundlach, Y. Galperin, Sediment hydrocarbons in former mangrove areas, southern ogoniland, eastern niger delta, nigeria, *Coast. Res. Libr.* 25

- (2018) 323–342. https://doi.org/10.1007/978-3-319-73016-5_14.
- [200] H. Li, Y. Zhang, D. Li, H. Xu, G. Chen, C. Zhang, Comparisons of different hypervariable regions of rrs genes for fingerprinting of microbial communities in paddy soils, *Soil Biol. Biochem.* 41 (2009) 954–968. <https://doi.org/10.1016/j.soilbio.2008.10.030>.
- [201] ASTM, Standard Test Method for Separation of Asphalt into Four Fractions. ASTM D4124-09, Annu. B. ASTM Stand. 09 (2018) 3–10. <https://doi.org/10.1520/D4124-09R18.2>.
- [202] J. Mounier, A. Camus, I. Mitteau, P.-J. Vaysse, P. Goulas, R. Grimaud, P. Sivadon, The marine bacterium *Marinobacter hydrocarbonoclasticus* SP17 degrades a wide range of lipids and hydrocarbons through the formation of oleolytic biofilms with distinct gene expression profiles, *FEMS Microbiol. Ecol.* 90 (2014) 816–831. <https://doi.org/10.1111/1574-6941.12439>.
- [203] M. Rosenberg, Bacterial adherence to hydrocarbons: a useful technique for studying cell surface hydrophobicity, *FEMS Microbiol. Lett.* 22 (1984) 289–295. <https://doi.org/10.1111/j.1574-6968.1984.tb00743.x>.
- [204] M. Vorregaard, Comstat2-a modern 3D image analysis environment for biofilms, echnical University of Denmark, DTU, 2008. www.imm.dtu.dk (accessed March 1, 2022).
- [205] A. Heydorn, A.T. Nielsen, M. Hentzer, C. Sternberg, M. Givskov, B.K. Ersboll, S. Molin, Quantification of biofilm structures by the novel computer program COMSTAT, *Microbiology.* 146 (2000) 2395–2407. <https://doi.org/10.1099/00221287-146-10-2395>.
- [206] P. Datta, P. Tiwari, L.M. Pandey, Isolation and characterization of biosurfactant producing and oil degrading *Bacillus subtilis* MG495086 from formation water of Assam oil reservoir and its suitability for enhanced oil recovery, *Bioresour. Technol.* 270 (2018) 439–448. <https://doi.org/10.1016/j.biortech.2018.09.047>.
- [207] J. Benjamins, A. Cagna, E.H. Lucassen-Reynders, Viscoelastic properties of triacylglycerol/water interfaces covered by proteins, *Colloids Surfaces A Physicochem. Eng. Asp.* 114 (1996) 245–254. [https://doi.org/10.1016/0927-7757\(96\)03533-9](https://doi.org/10.1016/0927-7757(96)03533-9).
- [208] M. Xia, Y. Liu, A.A. Taylor, D. Fu, A.R. Khan, N. Terry, Crude oil depletion by bacterial strains isolated from a petroleum hydrocarbon impacted solid waste management site in California, *Int. Biodeterior. Biodegrad.* 123 (2017) 70–77. <https://doi.org/10.1016/j.ibiod.2017.06.003>.
- [209] X. Xu, W. Liu, S. Tian, W. Wang, Q. Qi, P. Jiang, X. Gao, F. Li, H. Li, H. Yu, Petroleum Hydrocarbon-Degrading Bacteria for the Remediation of Oil Pollution Under Aerobic Conditions: A Perspective Analysis, *Front. Microbiol.* 9 (2018). <https://doi.org/10.3389/fmicb.2018.02885>.
- [210] S.J. Varjani, V.N. Upasani, A new look on factors affecting microbial degradation of petroleum hydrocarbon pollutants, *Int. Biodeterior. Biodegrad.* 120 (2017) 71–83. <https://doi.org/10.1016/j.ibiod.2017.02.006>.
- [211] R. Yang, G. Zhang, S. Li, F. Moazeni, Y. Li, Y. Wu, W. Zhang, T. Chen, G. Liu, B. Zhang, X. Wu, Degradation of crude oil by mixed cultures of bacteria isolated from the Qinghai-Tibet plateau and comparative analysis of metabolic mechanisms, *Environ. Sci. Pollut. Res.* 26 (2019) 1834–1847. <https://doi.org/10.1007/s11356-018-3718-z>.

- [212] A. Janbandhu, M.H. Fulekar, Biodegradation of phenanthrene using adapted microbial consortium isolated from petrochemical contaminated environment, *J. Hazard. Mater.* 187 (2011) 333–340. <https://doi.org/10.1016/j.jhazmat.2011.01.034>.
- [213] A. Moreno-Ulloa, V. Sicairos Diaz, J.A. Tejada-Mora, M.I. Macias Contreras, F.D. Castillo, A. Guerrero, R. Gonzalez Sanchez, O. Mendoza-Porras, R. Vazquez Duhalt, A. Licea-Navarro, Chemical Profiling Provides Insights into the Metabolic Machinery of Hydrocarbon-Degrading Deep-Sea Microbes, *MSystems*. 5 (2020) 1–19. <https://doi.org/10.1128/mSystems.00824-20>.
- [214] F. Pinu, S. Villas-Boas, Extracellular Microbial Metabolomics: The State of the Art, *Metabolites*. 7 (2017) 43. <https://doi.org/10.3390/metabo7030043>.
- [215] S. Heyen, B.M. Scholz-Böttcher, R. Rabus, H. Wilkes, Release of carboxylic acids into the exometabolome during anaerobic growth of a denitrifying bacterium with single substrates or crude oil, *Org. Geochem.* 154 (2021) 104179. <https://doi.org/10.1016/J.ORGGEOCHEM.2020.104179>.
- [216] M.T. Bidja Abena, G. Chen, Z. Chen, X. Zheng, S. Li, T. Li, W. Zhong, Microbial diversity changes and enrichment of potential petroleum hydrocarbon degraders in crude oil-, diesel-, and gasoline-contaminated soil, *3 Biotech.* 10 (2020) 42. <https://doi.org/10.1007/s13205-019-2027-7>.
- [217] Y. Liao, W.L. Wu, F.Q. Meng, P. Smith, R. Lal, Increase in soil organic carbon by agricultural intensification in northern China, *Biogeosciences*. 12 (2015) 1403–1413. <https://doi.org/10.5194/bg-12-1403-2015>.
- [218] H. Kim, K. Dong, J. Kim, S. Lee, Characteristics of crude oil-degrading bacteria *Gordonia iterans* isolated from marine coastal in Taean sediment, *Microbiologyopen*. 8 (2019) 1–10. <https://doi.org/10.1002/mbo3.754>.
- [219] Y.-B. Qi, C.-Y. Wang, C.-Y. Lv, Z.-M. Lun, C.-G. Zheng, Removal Capacities of Polycyclic Aromatic Hydrocarbons (PAHs) by a Newly Isolated Strain from Oilfield Produced Water, *Int. J. Environ. Res. Public Health*. 14 (2017) 215. <https://doi.org/10.3390/ijerph14020215>.
- [220] Y. Xue, X. Sun, P. Zhou, R. Liu, F. Liang, Y. Ma, *Gordonia paraffinivorans* sp. nov., a hydrocarbon-degrading actinomycete isolated from an oil-producing well, *Int. J. Syst. Evol. Microbiol.* 53 (2003) 1643–1646. <https://doi.org/10.1099/ijes.0.02605-0>.
- [221] C. Kummer, P. Schumann, E. Stackebrandt, *Gordonia alkanivorans* sp. nov., isolated from tar-contaminated soil, *Int. J. Syst. Evol. Microbiol.* 49 (1999) 1513–1522. <https://doi.org/10.1099/00207713-49-4-1513>.
- [222] M.A. Kertesz, A. Kawasaki, Hydrocarbon-Degrading Sphingomonads: *Sphingomonas*, *Sphingobium*, *Novosphingobium*, and *Sphingopyxis*, in: *Handb. Hydrocarb. Lipid Microbiol.*, Springer Berlin Heidelberg, Berlin, Heidelberg, 2010: pp. 1693–1705. https://doi.org/10.1007/978-3-540-77587-4_119.
- [223] B. Chettri, A.K. Singh, Kinetics of hydrocarbon degradation by a newly isolated heavy metal tolerant bacterium *Novosphingobium panipatense* P5:ABC, *Bioresour. Technol.* 294 (2019) 122190. <https://doi.org/10.1016/j.biortech.2019.122190>.
- [224] N.M. Silva, A.M.S.A. de Oliveira, S. Pegorin, C.E. Giusti, V.B. Ferrari, D. Barbosa, L.F. Martins, C. Morais, J.C. Setubal, S.P. Vasconcellos, A.M. da Silva, J.C.F. de Oliveira, R.C.

- Pascon, C. Viana-Niero, Characterization of novel hydrocarbon-degrading *Gordonia* paraffinivorans and *Gordonia* sihwensis strains isolated from composting, *PLoS One*. 14 (2019) e0215396. <https://doi.org/10.1371/journal.pone.0215396>.
- [225] B. Klein, V. Grossi, P. Bouriat, P. Goulas, R. Grimaud, Cytoplasmic wax ester accumulation during biofilm-driven substrate assimilation at the alkane–water interface by *Marinobacter hydrocarbonoclasticus* SP17, *Res. Microbiol.* 159 (2008) 137–144. <https://doi.org/10.1016/j.resmic.2007.11.013>.
- [226] I.P. Solyanikova, L.A. Golovleva, Hexadecane and Hexadecane-Degrading Bacteria: Mechanisms of Interaction, *Microbiology*. 88 (2019) 15–26. <https://doi.org/10.1134/S0026261718060152>.
- [227] H. Sowani, M. Kulkarni, S. Zinjarde, Harnessing the catabolic versatility of *Gordonia* species for detoxifying pollutants, *Biotechnol. Adv.* 37 (2019) 382–402. <https://doi.org/10.1016/j.biotechadv.2019.02.004>.
- [228] M. Klausen, A. Heydorn, P. Ragas, L. Lambertsen, A. Aaes-Jørgensen, S. Molin, T. Tolker-Nielsen, Biofilm formation by *Pseudomonas aeruginosa* wild type, flagella and type IV pili mutants, *Mol. Microbiol.* 48 (2003) 1511–1524. <https://doi.org/10.1046/j.1365-2958.2003.03525.x>.
- [229] E.M. Rodrigues, D.E. Cesar, R. Santos de Oliveira, T. de Paula Siqueira, M.R. Tótola, Hydrocarbonoclastic bacterial species growing on hexadecane: Implications for bioaugmentation in marine ecosystems, *Environ. Pollut.* 267 (2020) 115579. <https://doi.org/10.1016/j.envpol.2020.115579>.
- [230] K. Erstad, I. V Hvidsten, K.M. Askvik, T. Barth, Changes in Crude Oil Composition during Laboratory Biodegradation: Acids and Oil–Water, Oil–Hydrate Interfacial Properties, *Energy & Fuels*. 23 (2009) 4068–4076. <https://doi.org/10.1021/ef900038z>.
- [231] L.K. Oberding, L.M. Gieg, Methanogenic Paraffin Biodegradation: Alkylsuccinate Synthase Gene Quantification and Dicarboxylic Acid Production, *Appl. Environ. Microbiol.* 84 (2018). <https://doi.org/10.1128/AEM.01773-17>.
- [232] S.. Singh, B. Kumari, S. Mishra, *Microbial Degradation of Xenobiotics*, Springer Berlin Heidelberg, Berlin, Heidelberg, 2012. <https://doi.org/10.1007/978-3-642-23789-8>.
- [233] J. Tanzadeh, M.F. Ghasemi, M. Anvari, K. Issazadeh, Biological removal of crude oil with the use of native bacterial consortia isolated from the shorelines of the Caspian Sea, *Biotechnol. Equip.* 34 (2020) 361–374. <https://doi.org/10.1080/13102818.2020.1756408>.
- [234] W. Chen, J. Li, X. Sun, J. Min, X. Hu, High efficiency degradation of alkanes and crude oil by a salt-tolerant bacterium *Dietzia* species CN-3, *Int. Biodeterior. Biodegrad.* 118 (2017) 110–118. <https://doi.org/10.1016/j.ibiod.2017.01.029>.
- [235] V.P. Beškoski, S. Miletić, M. Ilić, G. Gojgić-Cvijović, P. Papić, N. Marić, T. Šolević-Knudsen, B.S. Jovančićević, T. Nakano, M.M. Vrvic, Biodegradation of Isoprenoids, Steranes, Terpanes, and Phenanthrenes During In Situ Bioremediation of Petroleum-Contaminated Groundwater, *CLEAN - Soil, Air, Water*. 45 (2017) 1600023. <https://doi.org/10.1002/clen.201600023>.
- [236] B. Jovančićević, M. Antić, I. Pavlović, M. Vrvic, V. Beškoski, A. Kronimus, J. Schwarzbauer, Transformation of Petroleum Saturated Hydrocarbons during Soil

- Bioremediation Experiments, *Water. Air. Soil Pollut.* 190 (2008) 299–307.
<https://doi.org/10.1007/s11270-007-9601-z>.
- [237] R. Gurav, H. Lyu, J. Ma, J. Tang, Q. Liu, H. Zhang, Degradation of n-alkanes and PAHs from the heavy crude oil using salt-tolerant bacterial consortia and analysis of their catabolic genes, *Environ. Sci. Pollut. Res.* 24 (2017) 11392–11403.
<https://doi.org/10.1007/s11356-017-8446-2>.

UNIVERSITE DE PAU ET DES PAYS DE L'ADOUR
ÉCOLE DOCTORALE DES SCIENCES EXACTES ET DE LEURS APPLICATIONS
(ED 211)

LABORATOIRE :

Institut des Sciences Analytiques et de Physico-Chimie pour l'Environnement et les Matériaux
(IPREM)